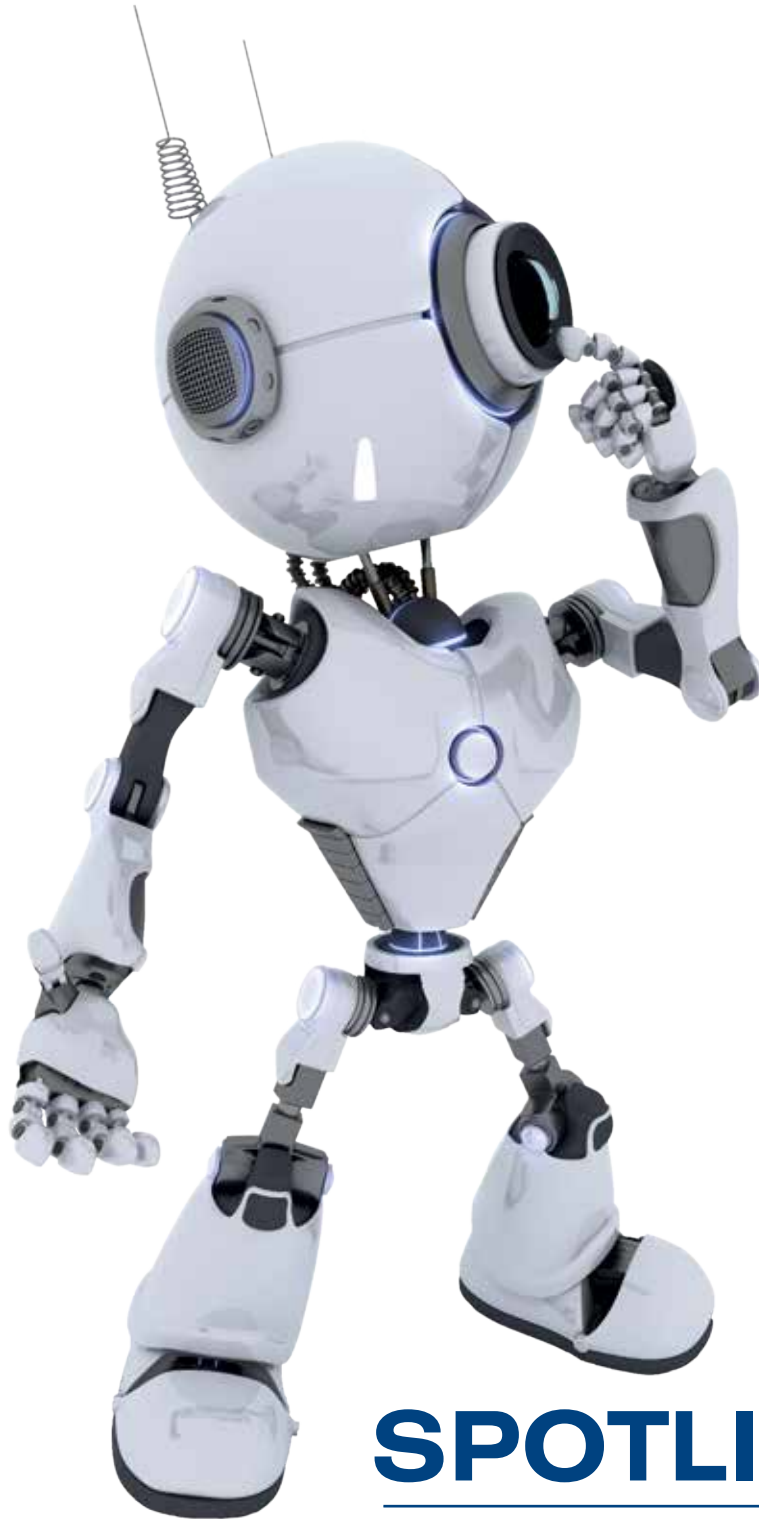


futurities

The Simulation Based Engineering & Sciences Magazine

Year 20
01
Spring
2023



SPOTLIGHT

Robots and cobots

ON SITE & ONLINE



automotive
CAE
GRAND
CHALLENGE

April 25 – 26, 2023
Congress Park Hanau
Germany

// ARTIFICIAL INTELLIGENCE, MACHINE LEARNING, BIG DATA: MASSIVE DATA EXPLORATION OF SIMULATION AND TEST RESULTS

// BODY STIFFNESS & STRENGTH: STRUCTURAL PROPERTIES OF BATTERY PACKS

// CAE PROCESS & QUALITY ASSURANCE: CAE IN ADVANCED VEHICLE DEVELOPMENT (PRE-CAD)

// FULL VEHICLE SIMULATION: VIRTUAL TESTING OF AUTONOMOUS VEHICLES

// MODELING ISSUES CRASH ANALYSIS: MODELING CRASH BEHAVIOR OF BATTERY PACKS

// OCCUPANT SAFETY: VIRTUAL TESTING WITH DUMMIES UND HBMS

// OPTIMIZATION & ROBUSTNESS: ROBUST DESIGN – CREATING AND VERIFYING ROBUST DESIGNS

- Editor's Note

The first issue of Futurities for 2023 places the **Spotlight** on robots and cobots (collaborative robots) positing that they represent the meeting point for collaboration and innovation. Articles in this section include a look at robotic assistants in the operating theatre where they are being used to assist surgeons with joint replacement operations, while other robots are being developed to assist with highly complex procedures at the microscopic scale. In another article we look at progress that is being made in developing robots to assist children with special needs to learn at school, AI-powered chatbots to provide psychologically supportive homebased care around the clock for people with mental health conditions, and home assistant robots with camera vision to assist adults with cognitive decline to perform everyday tasks.

In the agricultural sector, scientists are studying the use of miniature robots combined with AI and Machine Learning technologies to foster the wellbeing of queen bees in the hopes of stimulating better and more widespread pollination of crops and plants for stronger ecosystems, while other scientists are using robotics to learn more about the symbiosis between fungi and plant roots with a view to learning how to protect and support these processes to maintain healthy ecosystems and lock up carbon to limit global warming. At a more immediately practical level, AI-assisted robots are also being used to execute the laborious, time-intensive, back-breaking and mind-numbing task of weeding, or for disease detection in order to limit the use of herbicides and pesticides and address, or to prune vines and help address the persistent problem of the shortage of farmhands.

The section also includes a case study concerning an optimization process to develop and improve the design of a legged robot to achieve greater physical ability, versatility, and robustness – all of which are essential if robots are to substitute or assist humans in either daily or dangerous tasks. The key objective is to harness all the electrical and mechanical components to guarantee optimal and safe performance at a low production cost.

In our **Technology Transfer** section, there is a Particleworks case study from the University of Michigan comparing finite volume and particle CFD simulation methods for understanding lubrication in automotive transmissions and axles while our **Know-how** section has an industrial use case for Digital Image Correlation from Eikosim, and a thermo-fluid dynamics analysis of a hot water distribution network in a paint shop. The **Research & Innovation** section includes a paper concerning the development of a decision-support system for smart cities to assess and manage terrorist threats and an overview of some of the success stories from the EU's FF4EuroHPC initiative to promote the uptake of advanced HPC technologies and services by funding business-oriented experiments for European SMBs. Our **Product Peeks** this month look in greater detail at the latest releases of Cetol 6σ, Multiscale.Sim and Ansys Twin Builder.

I wish you an interesting and informative read.

Stefano Odorizzi

Editor in chief



Traditional industrial robotics is learning from cobot development and taking advantage of advances in AI-assisted programming.



Futurities

Year 20 n°1 - Spring 2023

To receive a free copy of the next magazine, please contact our Marketing office at: marketing@enginsoft.com

All pictures are protected by copyright. Any reproduction of these pictures in any media and by any means is forbidden unless written authorization by EnginSoft has been obtained beforehand. ©Copyright EnginSoft.

EnginSoft S.p.A.

24126 BERGAMO c/o Parco Scientifico Tecnologico
Kilometro Rosso - Edificio A1, Via Stezzano 87 • Tel. +39 035 368711
50127 FIRENZE Via Panciattichi, 40 • Tel. +39 055 4376113
35129 PADOVA Via Giambellino, 7 • Tel. +39 049 7705311
72023 MESAGNE (BRINDISI) Via A. Murri, 2 - Z.I. • Tel. +39 0831 730194
38123 TRENTO fraz. Mattarello - Via della Stazione, 27 • Tel. +39 0461 915391
10133 TORINO Corso Marconi, 20 • Tel. +39 011 6525211

www.enginsoft.com

e-mail: info@enginsoft.com

Futurities is a quarterly magazine published by EnginSoft SpA

COMPANY INTERESTS

EnginSoft GmbH - Germany
EnginSoft UK - United Kingdom
EnginSoft Turkey - Turkey
EnginSoft USA
Particleworks Europe
www.enginsoft.com

CONSORZIO TCN www.consorziotcn.it • www.improve.it
M3E Mathematical Methods and Models for Engineering www.m3eweb.it
AnteMotion antemotion.com

ASSOCIAZIONE INTERESTS

NAFEMS International www.nafems.it • www.nafems.org
TechNet Alliance www.technet-alliance.com

ADVERTISING

For advertising opportunities, please contact our Marketing office at: marketing@enginsoft.com

RESPONSIBLE DIRECTOR

Stefano Odorizzi

PRINTING

Grafiche Dalpiaz - Trento

Autorizzazione del Tribunale di Trento
n° 1353 RS di data 2/4/2008

The *Futurities* editions contain references to the following products which are trademarks or registered trademarks of their respective owners:

Ansys, **Ansys Workbench**, **AUTODYN**, **CFX**, **Fluent**, **Forte**, **SpaceClaim** and any and all Ansys, Inc. brand, product, service and feature names, logos and slogans are registered trademarks or trademarks of Ansys, Inc. or its subsidiaries in the United States or other countries. [ICEM CFD is a trademark used by Ansys, Inc. under license] (www.ansys.com) - **modeFRONTIER** is a trademark of ESTECO Spa (www.esteco.com) - **Flownex** is a registered trademark of M-Tech Industrial - South Africa (www.flownex.com) - **MAGMASOFT** is a trademark of MAGMA GmbH (www.magmasoft.de) - **FORGE**, **COLDFORM**, **FORGE Nxt** and **SIMHEAT** are trademarks of Transvalor S.A. (www.transvalor.com) - **LS-DYNA** is a trademark of LSTC (www.lstc.com) - **Cetol 6** is a trademark of Sigmatrix L.L.C. (www.sigmatrix.com) - **RecurDyn™** and **MBD for Ansys** is a registered trademark of FunctionBay, Inc. (www.functionbay.org) - **Maplesoft** is a trademark of Maplesoft™, a subsidiary of Cybernet Systems Co. Ltd. in Japan (www.maplesoft.com) - **Particleworks** is a trademark of Prometech Software, Inc. (www.prometechsoftware.com). **Multiscale.Sim** is an add-in tool developed by CYBERNET SYSTEMS CO.,LTD., Japan for the Ansys Workbench environment - **Rocky** is a trademark of ESSS (www.esss.co) - **industrialPhysics** is a trademark of Machineering GmbH (www.machineering.com) - **SIMUL8** is a trademark of SIMUL8 Corporation (www.simul8.com) - **ViveLab Ergo** is a trademark of ViveLab Ergo Ltd. (www.vivelab.cloud) - **True-Load** is a trademark of Wolf Star Technologies (www.wolfstartech.com)

Contents

TECHNOLOGY TRANSFER



- 24 Comparing finite volume and particle CFD simulation methods for understanding lubrication in automotive transmissions and axles
by Western Michigan University

KNOW-HOW



- 30 Analysis of the thermo-fluid dynamics of a paint shop's hot water distribution network
by SimulHub



- 33 Digital image correlation (DIC) for vibration analysis
by EikoSim

RESEARCH & INNOVATION



- 36 FF4EuroHPC continues inspiring SMEs to unleash their innovation potential with cutting-edge technologies
by Bettair Cities and Barcelona Supercomputing Centre

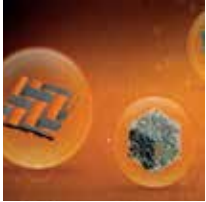


- 39 Multiphysics and multiscale modelling of aeronautical components
by CETMA and MANTA Group

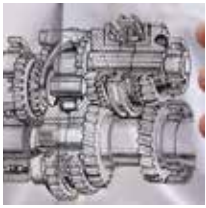


- 42 Decision-support system for smart cities to assess and manage terrorist threats
by Universidad de la Cantabria

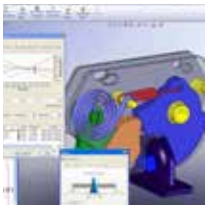
PRODUCT PEEKS



49 Identifying unknown material properties using reverse engineering by combining materials databases and artificial intelligence
by CYBERNET SYSTEMS



52 Understanding tolerance stacking: Using CETOL 6 σ to improve production quality
by Tae Sung S&E



54 What is new in CETOL 6 σ ver. 11.3.1
by EnginSoft



56 Teaching AI “brains” using digital twins with Microsoft Project Bonsai
by Ansys

NEWS & TRENDS



59 SPACE - Scalable Parallel Astrophysical Codes for Exascale – launches in Turin

SPOTLIGHT



6 **Robots and cobots:**
When collaboration and innovation combine



7 Designing versatile and athletic robots with CAE
by Istituto Italiano di Tecnologia

12 New robots in Europe can be workers' best friends
by Gareth Willmer

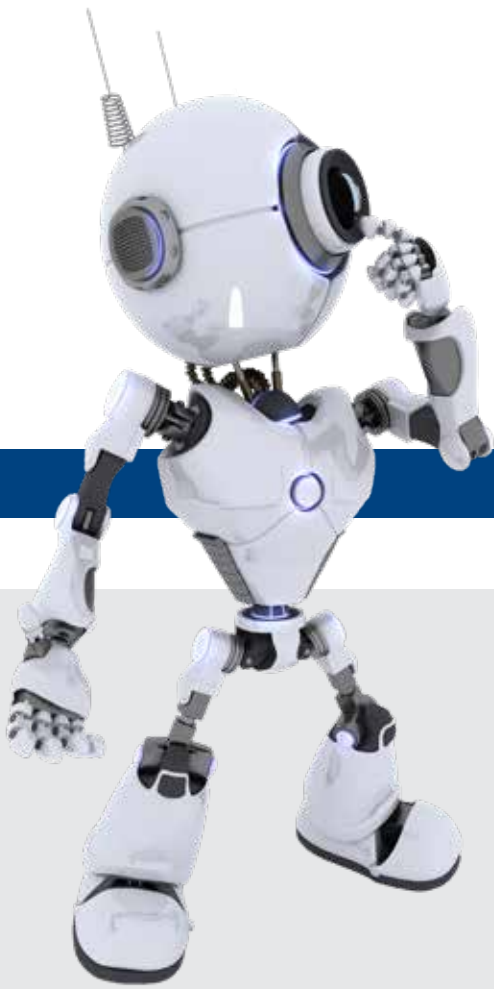
14 Futuristic fields: Europe's farm industry on cusp of robotic revolution
by Sofia Strodt

16 Robotic bees and roots offer hope of healthier environment and sufficient food
by Gareth Willmer

18 Robot dogs take a walk on the wired side
by Tom Cassauwers

20 Education and healthcare are set for a high-tech boost
by Caleb Davies

22 Robot assistants in the operating room promise safer surgery
by Gareth Willmer



SPOTLIGHT

Robots and cobots

When collaboration and innovation combine

While some parts of manufacturing continue to make use of traditional robots – installations in 2021 increased by a record 31% over 2020 (IFR World Robotics Report) – the collaborative robot (cobot) industry is growing rapidly and is expected to reach \$2.2 billion by 2026 (Interact Analysis, Collaborative Robot Market 2022 Report). This growth is largely fuelled by their greater affordability, manoeuvrability, versatility and adaptability; easier programmability and deployment; and the fact that they are safer to use around people.

Cobots are being developed to make robotic-assisted work safer for humans; easier to use without the need for specialized programming skills and therefore more affordable even for small companies; and to render the robots themselves more versatile and intuitive so that human-machine collaboration is more fluid and natural, reducing the need for human physical labour and freeing precious human resources to be applied to activities where they can add greater value. The humans in “cobotized” production lines are then able to tackle a wider variety of tasks rendering their jobs more interesting and hence more attractive.

With their greater strength, indefatigability, speed and accuracy, cobots are already impacting activities such as welding, assembly, picking, packing and palletizing, but their advantages mean they are highly attractive to all manufacturers or assemblers wishing to increase automation, error-reduction, and modularity in their production lines. Advances in AI and machine learning are making robotic programming simpler and easier, enabling customization even by non-experts and in small

and medium-sized companies. As a result, cobots represent a straightforward solution to the worldwide shortages of skills and labour.

Furthermore, the rapid advances in AI-supported machine learning are allowing cobot owners to adapt their production or assembly lines cost-effectively and rapidly to the variability and modularity required for mass customization. Digital twins play a fundamental role here allowing different options that integrate cobots and other equipment to be explored and tested risk-free after which processes can be optimized and fine-tuned using real-time feedback and monitoring from sensors in the actual production line to ensure the best performance and uptime while also predicting and planning for maintenance. Combined with AI-powered cobots, digital twins enable manufacturers of any size to adapt quickly to market demands.

Traditional industrial robotics is learning from cobot development and taking advantage of advances in AI-assisted programming together with the use of sensors to render large industrial robots more collaborative and adaptable to allow existing implementations to be leveraged and achieve the twin benefits of robust yet precise performance with greater versatility.

Allied with the progress towards the industrial internet of things and the evolutions in cloud computing, big data analytics and 5G mobile networks, the cable-free smart factory is daily becoming a more tangible reality.



Designing versatile and athletic robots with CAE

by Antonios E. Gkikakis¹, Federico Allione^{1,3}, Roy Featherstone²

1. Istituto Italiano di Tecnologia, Advanced Robotics - 2. Formerly Istituto Italiano di Tecnologia - 3. DIBRIS, University of Genoa

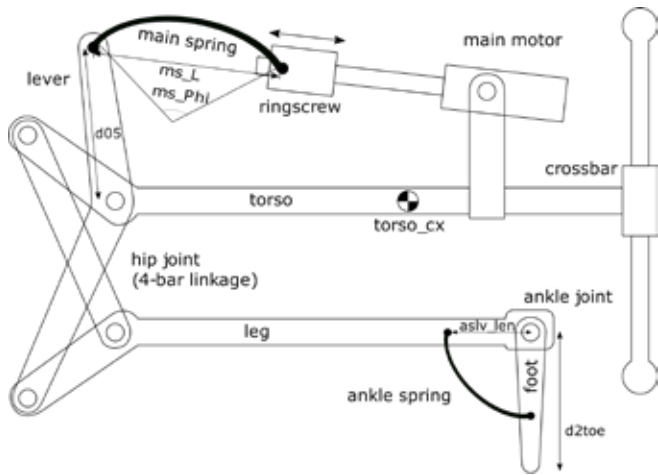
Despite recent technological advances in Artificial Intelligence and engineering, general purpose robots are still not a part of our everyday lives. Robots consist of multiple electrical and mechanical components and must possess great physical ability, versatility, and robustness to substitute or assist humans in either daily or dangerous tasks.

To create and deliver these types of products to market requires realistic models and Computer Aided Engineering (CAE) approaches to guarantee optimal and safe performance with a low production cost. This article presents an example of a proposed design optimization approach with a case study.

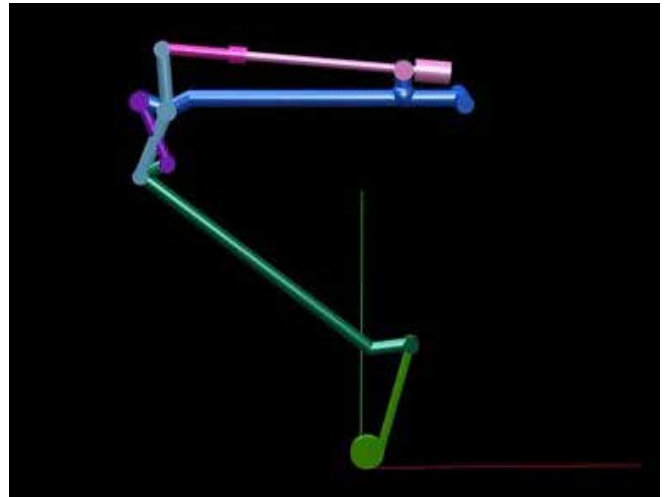
Robots are already extensively used in various sectors of industry and have recently found several new applications, for instance in medicine and for inspection scenarios. Today's technology offers light, powerful, and precise actuators, sophisticated sensors, and a variety of materials with amazing mechanical properties. These

available technologies mean robots can be made more versatile, faster, and more robust than they currently are. However, the complexity of the individual components, and their limits and capabilities, as well as the intended use for the robot make robot design highly challenging.

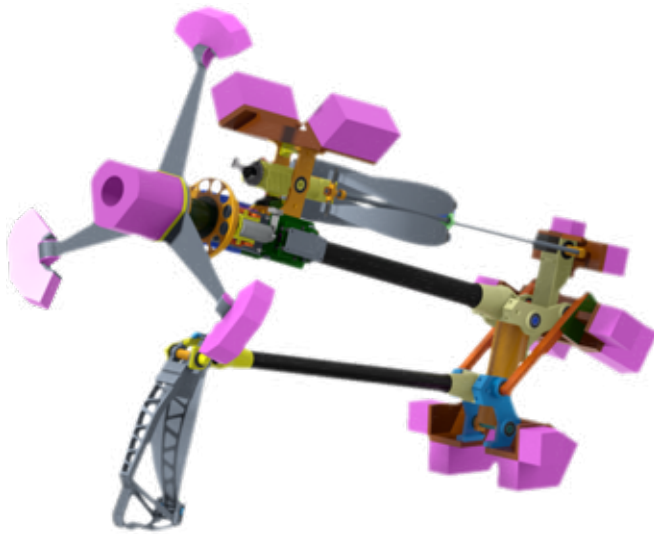
It is therefore essential to define systematic and scientifically-based approaches to design, test, and produce robots, similarly to what is done with other high-tech products such as satellites. This article presents a CAE-based design approach that considers the requirements, specifications, available resources, and the constraints in the production line (i.e. manufacturability) together with uncertainties in the real world (e.g. mechanical imperfections). Achieving this requires the creation of realistic computational models and simulations so that CAE techniques can be effectively applied. This can lead to new or improved robots and faster prototyping with fewer design iterations resulting in lower production costs. The proposed approach is applied to the case study of an athletic one-legged robot that can balance and hop, which has been designed to explore the physical performance of today's robotic technology.



STEP 1 - Concept



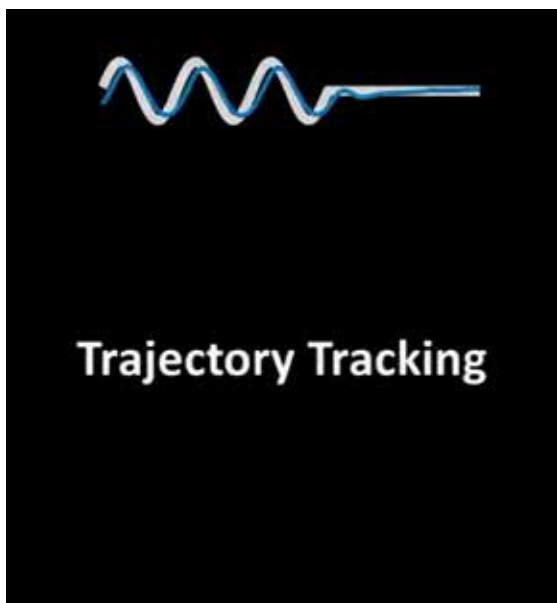
STEP 2 - Simulation & proof of concept



STEP 3 - CAD



STEP 4 - Prototyping



STEP 5 - Experimental results

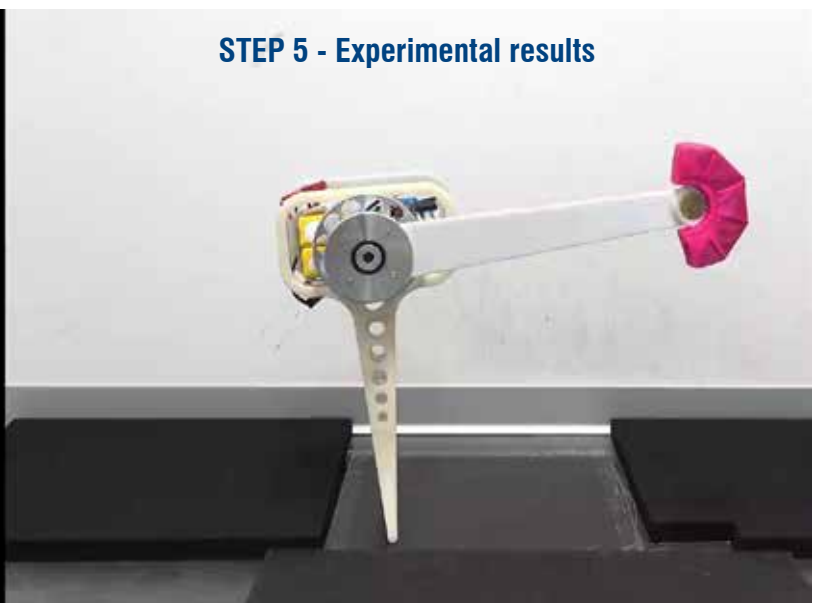


Fig. 1. Overview of robot design process.

The robot design process

Fig. 1 presents an overview of the proposed robot design process, which can be summarized as follows:

- Concept and requirements.
- Specifications, modelling, and simulation.
- Design and behaviour co-optimization (not shown).
- CAD, manufacturing, and assembly.
- Prototyping.
- Experimental results.

Concept and requirements

We now define the overall mechanical structure; actuation, sensing and control technologies; what the robot must be able to do; and how well it should do it.

- The one-legged robot presented in this article was not designed for a specific application but rather to achieve unprecedented performance in a variety of athletic tasks in order to demonstrate the importance of a systematic approach to its design.
- The robot consists of a torso, a leg, a foot, and a crossbar that rotates out of the plane and serves to balance and steer the robot in 3D (see image 1 of Fig. 1). The leg is connected to the torso via a hip joint implemented as a crossed 4-bar linkage. The hip joint is actuated via a linear drive mechanism called a ring screw [1] and a set of fibreglass leaf springs. Finally, the foot is connected to the leg via a spring-loaded ankle joint.
- We wanted to push the mechanism to its limits in order to explore the potential of this approach. We thus decided that the robot should meet the following requirements: a) achieve high vertical hops, b) acrobatics, c) fast travelling hops, d) balancing, and e) surviving a crash-landing undamaged.

Specifications, modelling, and simulation

The simulations serve as a feasibility study with the objective of finding out whether the conceptual design really can achieve all that we want, and how well. The conceptual design can be changed at this or the following stages in response to findings.

The model of the robot was implemented in MATLAB and the simulations were performed in Simulink. This study examines movements in the 2D plane in which only the hip is actuated. The robot and its actions can be accurately described by means of 104 parameters of which:

- 76 are design parameters, and
- 28 are behaviour parameters.

The design parameters provide a description of the complete robot and include information about its mechanism (e.g. kinematics, dynamics); actuators (e.g. electromechanical, and thermal models); sensors (e.g. saturation limits); and more. The behavioural parameters define a virtual environment to simulate all the actions and limitations experienced by the robot during operation. The simulation input is a set of initial conditions and

a feed-forward voltage profile to control the brushed DC motor of the hip. After a series of preliminary experiments, we defined the following specifications:

- vertical hops: up to 3m;
- acrobatics: triple backflip;
- travelling: continuous travelling hops at 2.5m per hop; and
- balancing on a very narrow toe at the bottom of the foot

which push the robot to its limits (i.e. the robot reaches current, voltage and/or speed saturation to achieve many of them). To safely reach the maximum physical capabilities of the robot we included individual component limits, such as motor current saturation, speed, and kinematic limits. Then, we mapped the specifications to a multi-objective optimization problem consisting of 13 objectives and 12 behaviour constraints. The objectives are defined as the difference between the desired and the achieved performance, e.g. hop height, and are conflicting in nature, making it a challenging problem.

Design approach

The design approach is divided into two parts: a framework and a methodology. The first is a conceptual structure for the design study, and the second is a series of steps where CAE methods are used to discover optimal outcomes. The following steps are implemented in modeFRONTIER, and a thorough discussion of the approach and the case study is presented in [2].

Optimization framework

Similar to the way a cheetah's body enables it to run at high speeds but is not good for climbing trees, whereas a chimpanzee's body is good for climbing trees but cannot run very fast, this framework was developed based on the premise that a design and its behaviours have an inextricable relationship that can lead to better performance in certain tasks because of physical traits and the behaviours that evolve to exploit them. Fig. 2 presents the two-layer optimization framework. In the first layer a global

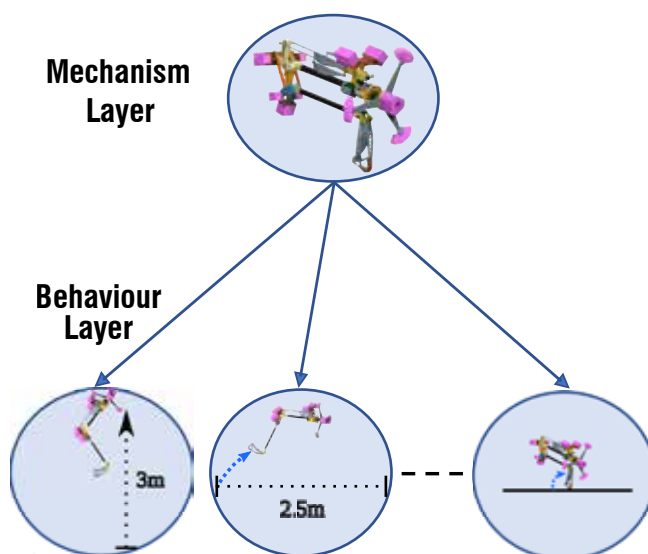


Fig. 2. Design approach, optimization framework.

optimization algorithm (MOGA-II) generates new robot designs by selecting the parametric values for the model. The new design then moves to the second layer where it undergoes a series of physical tests to determine its physical capabilities.

Each test is itself an optimization experiment (MOGA-II) in which optimal behaviours are sought to achieve the best performance. Finally, the best behaviours and associated performance scores (e.g. running speed) are sent back to the first layer to be evaluated and for new designs to be generated.

Optimization methodology

Fig. 3 shows an intuitive representation of the optimization methodology (does not include sensitivity analysis), which consists of five main steps:

- A DOE (Design of Experiments) is performed before each experiment and can lead to faster convergence of the algorithms, requiring fewer computing resources, efficient exploitation of prior knowledge, and a higher probability of finding the best solutions.
- A sensitivity analysis provides a deeper understanding of the problem being investigated to guide early design decisions and select the most important parameters to be optimized. As a result, the computational cost can be reduced and the manufacturing accuracy can be decided based on a component's sensitivity, which can potentially reduce the production cost.
- A rough optimization using global search algorithms generates a Pareto front of designs and their optimal behaviours. Depending on the application or requirements, the designer selects the design with the best trade-offs.
- The Pareto set is refined using local optimization algorithms to improve its quality and achieve maximum theoretical performance.
- A robustness analysis helps unveil the most robust designs given expected uncertainties (manufacturing errors, initial conditions, sensor accuracy and noise, etc.). This can reduce the simulation-to-reality gap and improve the consistency of performance among the same robot designs.

Sensitivity analysis

Thirteen mechanism parameters were selected for this study and tested for their sensitivity in all 13 objectives. The SS-ANOVA approach was used to estimate the interaction effects, and a two-level reduced factorial algorithm was used to generate 1,024 designs.

The parameters selected are spring model parameters, a dynamic parameter, and six kinematic parameters. The outcome is that eight out of 13 parameters have a significant impact on the robot's overall performance across all objectives. The remaining five parameters were set at constant values, which allowed us to proceed with manufacturing and ordering most of the robot components while performing optimization studies.

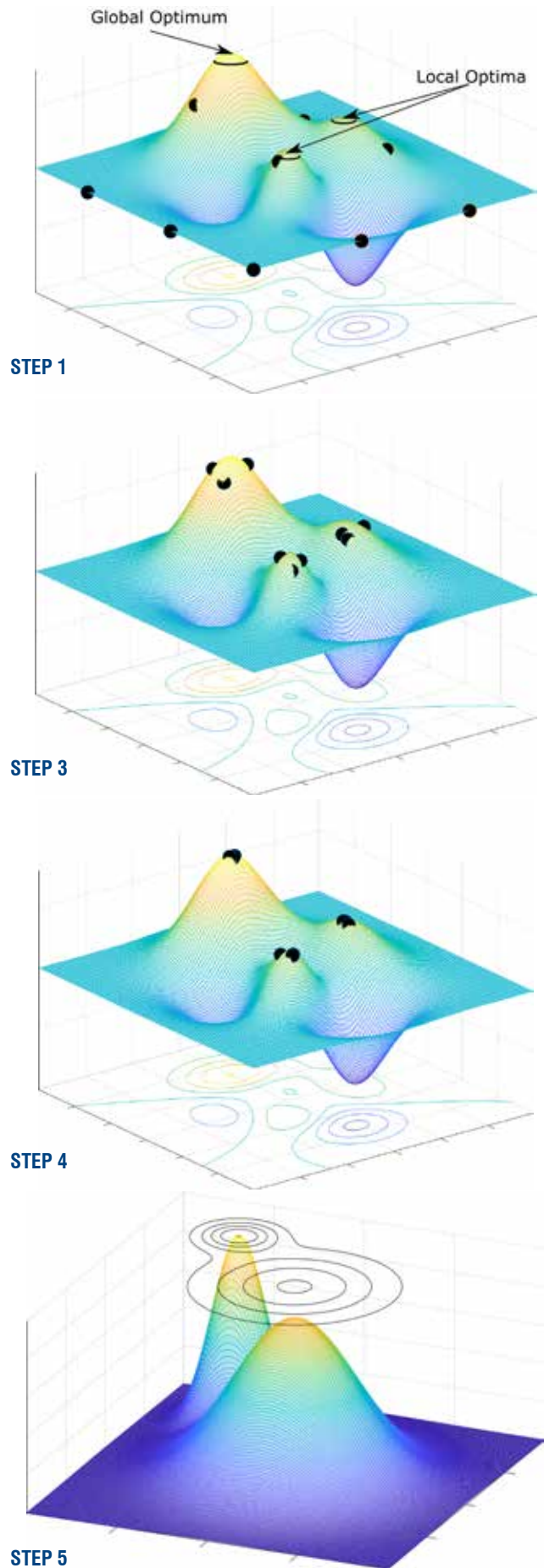


Fig. 3. Design approach, steps 1, 3, 4 and 5 of optimization methodology (sensitivity analysis is not shown).

Rough optimization

In this part, hundreds of designs were generated in the first layer and tested in the second layer. Among the resulting 34 designs that met the performance requirements and did not violate any constraints, we selected five Pareto optimal designs, which were the best: a) vertical hopper, b) acrobat, c) runner, d) balancer, and e) the design with the best overall performance.

To give an idea of the trade-off between the performance of these designs, the best running design expends 11% less energy (drawn from the battery) on running at the same speed as the design with the best overall performance; however, it underperforms in balancing and acrobatics. These results are discussed extensively in [2].

In another study with the same approach, we discovered skilled one-legged runners that can achieve running speeds of up to 22km/h; however, they had very poor performance in the other tasks.

Refinement optimization

An additional round of optimization was then performed to discover the maximum theoretical performance of the designs. The result was increased performance in most objectives. For example, the best runner increased its maximum hop height by 5%.

Robustness analysis

In this study, we examine the robustness of the designs discovered for the 13

objectives with respect to expected variations in 15 design parameters. Using modeFRONTIER's robust design optimization tool we generated 50 new designs for each design in the Pareto front. We did this using multimodal distributions to model the uncertainty and then sample them. For instance, fibreglass springs were measured to have a difference in their maximum stiffness of up to 3% when tested on a tensile strength machine.

The results showed that even for slight variations in the robot mechanism, significant discrepancies can be observed between the best and average performance.

For example, the best acrobat, which has a maximum hop height of 3m, was found to have an average performance of 2.8m, which is 7% lower than expected. The results indicate that this method can help bridge the gap between simulation and reality, justify inconsistencies in performance, and can be used as an additional evaluation criterion for design selection [4].

Experimental results and prototyping

Physical prototypes must be built and tested because no simulation or mathematical model can capture every detail of physical reality, so prototypes are needed to serve as "ground truth".

The first complete prototype is presented in image 4 in Fig. 1. It has a length of 1.4m with the hip fully extended and has a mass

of ~5.3kg. Image 5 also shows a frame from the experimental results for balancing for the first incomplete version, published in [3].

Conclusion

The results of this case study show that versatile robotic systems can be governed by complex trade-offs, which may depend on many factors including the system components, their combined behaviours and limitations, and the tasks for which they are designed.

Moreover, in complex and highly dynamic electromechanical systems, typical optimization approaches tend to over-optimize the model, which results in theoretical performance that is unfeasible in practice. In conclusion, building robots that are efficient physical actors is not an easy task, and designing them for widespread commercial use renders imperative the need for more systematic and scientifically grounded approaches during their design process.

For more information:

Antonios Emmanouil Gkikakis - IIT
antonios.gkikakis@gmail.com

References

- [1] R. Featherstone, "Ring screw project webpage". royfeatherstone.org/ringscrew, accessed Mar. 2023
- [2] A. E. Gkikakis, *Mechanism and Behaviour Co-optimisation of High Performance Mobile Robots*, PhD thesis, 2021. doi: 10.15167/gkikakisantoniosemmanouil_phd2021-04-21
- [3] F. Allione, A. E. Gkikakis and R. Featherstone, "Experimental Demonstration of a General Balancing Controller on an Untethered Planar Inverted Double Pendulum", 2022 IEEE/RSJ International Conference on Intelligent Robots and Systems (IROS), Kyoto, Japan, 2022, pp. 8292-8297, doi: 10.1109/IROS47612.2022.9981380
- [4] A. E. Gkikakis and R. Featherstone, "Robust Analysis for Mechanism and Behavior Co-optimization of High-performance Legged Robots", 2022 IEEE-RAS 21st International Conference on Humanoid Robots (Humanoids), Ginowan, Japan, 2022, pp. 752-758, doi: 10.1109/Humanoids53995.2022.9999745.

About Istituto Italiano di Tecnologia (IIT)

The Istituto Italiano di Tecnologia (IIT), based in Genoa in Italy, is a state-funded foundation to conduct scientific research in the public interest for the purpose of technological development. IIT aims to promote excellence in basic and applied research and to foster the development of the national economy.

As of February 2023, IIT has produced about 18,000 publications, participated in more than 380 European projects and more than 880 commercial projects, created more than 1,290 active patents, formed 33 established start-ups, and has more than 50 under due diligence. It has a network of five hubs in Genoa that form its Central Research Laboratories, 11 other research centres around Italy, and two outstations located in the US at MIT and Harvard.



©BigBlueStudio, Shutterstock

New robots in Europe can be workers' best friends

More sophisticated robots are on the way, accelerating a drive to ensure they help workers rather than take their places.

by Gareth Willmer

Researchers are ushering in a new way of thinking about robots in the workplace based on the idea of robots and workers as teammates rather than competitors.

For decades, the arrival of robots in the workplace has been a source of public anxiety over fears that they will replace workers and create unemployment. Now that more sophisticated and humanoid robots are actually emerging, the picture is changing, with some seeing robots as promising teammates rather than unwelcome competitors.

"Cobot" colleagues

Take Italian industrial-automation company Comau. It has developed a robot that can collaborate with – and enhance the safety of – workers in strict cleanroom settings in the pharmaceutical, cosmetics, electronics, food and beverage industries. The innovation is

known as a “collaborative robot”, or “cobot”. Comau’s arm-like cobot, which is designed for handling and assembly tasks, can automatically switch from an industrial to a slower speed when a person enters the work area. This new feature allows one robot to be used instead of two, maximizing productivity and protecting workers.

“It has advanced things by allowing a dual mode of operation,” says Dr Sotiris Makris, a roboticist at the University of Patras in Greece. “You can either use it as a conventional robot or, when it is in collaborative mode, the worker can grab it and move it around as an assisting device.”

Makris was coordinator of the just-completed EU-funded SHERLOCK project, which explored new methods for safely combining human and robotic capabilities from what it regarded as an often-overlooked research angle: psychological and social well-being.

Creative and inclusive

Robotics can help society by carrying out repetitive, tedious tasks, freeing up workers to engage in more creative activities. And robotic technologies that can collaborate effectively with workers could make workplaces more inclusive, such as by aiding people with disabilities.

These opportunities are important to seize as the structure and the age profile of the

“There is increasing competition around the globe, with new advances in robotics.

Dr Sotiris Makris,
SHERLOCK

“You find interesting differences in how much the machine and how much the person should do.

Prof Giulio Jacucci
CO-ADAPT

European workforce changes. For example, the proportion of 55-to-64-year-olds increased from 12.5% of the EU's employees in 2009 to 19% in 2021.

Alongside the social dimension, there is also economic benefit from greater industrial efficiency, showing that neither necessarily needs to come at the expense of the other.

“There is increasing competition around the globe, with new advances in robotics,” says Makris, “That is calling for actions and continuous improvement in Europe.”

Makris cites the humanoid robots being developed by Elon Musk-led car manufacturer, Tesla. Wearable robotics, bionic limbs and exoskeleton suits are also being developed that promise to enhance people's capabilities in the workplace.

Still, the rapidly advancing wave of robotics poses big challenges when it comes to ensuring they are effectively integrated into the workplace and that people's individual needs are met when working with them.

Case for SHERLOCK

SHERLOCK also examined the potential for smart exoskeletons to support workers in carrying and handling heavy parts in places such as workshops, warehouses or assembly sites. Wearable sensors and AI were used to monitor and track human movements.

With this feedback, the idea is that the exoskeleton can then adapt to the needs of the specific task while helping workers retain an ergonomic posture to avoid injury. “Using sensors to collect data from how the

exoskeleton performs allowed us to see and better understand the human condition,” says Dr Makris. “This allowed us to have prototypes on how exoskeletons need to be further redesigned and developed in the future, depending on different user profiles and different countries.”

SHERLOCK, which has just ended after four years, brought together 18 European organizations in multiple countries from Greece to Italy and the UK working on different areas of robotics.

The range of participants enabled the project to harness a wide variety of perspectives, which Dr Makris says was also beneficial in the light of differing national rules on integrating robotics technology.

As a result of the interaction of these robotic systems with people, the software is advanced enough to give direction to “future developments on the types of features to have and how the workplace should be designed,” says Dr Makris.

Old hands, new tools

Another EU-funded project that ended this year, CO-ADAPT, used cobots to help older people navigate the digitalized workplace. The project team developed a cobot-equipped adaptive workstation to aid people in assembly tasks, such as making a phone, car or toy – or indeed combining any set of individual components into a finished product during manufacturing. The station can adapt workbench height and lighting to a person's physical characteristics and visual abilities. It also includes features like eye-tracking glasses to gather information on mental workload.

That brings more insight into what all kinds of people need, says Professor Giulio Jacucci, coordinator of CO-ADAPT and a computer scientist at the University of Helsinki in Finland.

“You find interesting differences in how much the machine and how much the person should do, as well as how much the machine should try to give guidance and how,” Jacucci says, “This is important work that goes down to the nuts and bolts of making this work.”

However cobot-equipped workplaces that can fully tap into and respond to people's mental states in real-life settings could still be a number of years away, he says.

“It is so complex because there is the whole mechanical part, plus trying to understand people's status from their psychophysiological states,” says Prof. Jacucci.

Meanwhile, because new technologies can be used in much simpler ways to improve the workplace, CO-ADAPT also explored digitalization more broadly.

Smart shifts

One area was software that enables “smart-shift scheduling”, which arranges duty periods for workers based on their personal circumstances. The approach has been shown to reduce sick leave, stress and sleep disorders among social welfare and health care workers.

“It is a fantastic example of how workability improves because we use evidence-based knowledge of how to have well-being-informed schedules,” says Prof. Jacucci.

Focusing on the individual is key to the future of well-integrated digital tools and robotics, he says. “Let's say you have to collaborate with some robot in an assembly task,” he says, “The question is: should the robot be aware of my cognitive and other abilities? And how should we divide the task between the two?”

The basic message from the project is that plenty of room exists to improve and broaden working environments. “It shows how much untapped potential there is,” says Prof. Jacucci.



Research in this article was funded by the EU.

This article was originally published in *Horizon, the EU Research and Innovation magazine*.

ec.europa.eu/research-and-innovation/en/horizon-magazine/new-robots-europe-can-be-workers-best-friends



©baranozdemir, iStock

Futuristic fields: Europe's farm industry on cusp of robotic revolution

From oxen to horses to tractors to robots: the European farm industry is poised to undergo another innovative disruption - this time brought about by artificial intelligence.

by **Sofia Strodt**

Artificial intelligence is set to revolutionise agriculture by helping farmers meet field-hand needs and identify diseased plants.

In the Dutch province of Zeeland, a robot moves swiftly through a field of crops including sunflowers, shallots and onions. The machine weeds autonomously – and tirelessly – day in, day out.

“Farmdroid” has made life a lot easier for Mark Buijze, who runs a biological farm with 50 cows and 15 hectares of land. Buijze is one of the very few owners of robots in European agriculture.

Robots to the rescue

His electronic field worker uses GPS and is multifunctional, switching between weeding

and seeding. With the push of a button, all Buijze has to do is enter coordinates and Farmdroid takes it from there.

“With the robot, the weeding can be finished within one to two days – a task that would normally take weeks and roughly four to five workers if done by hand,” he says. “By using GPS, the machine can identify the exact location of where it has to go in the field.”

About 12,000 years ago, the end of foraging and start of agriculture heralded big improvements in people's quality of life. Few sectors have a history as rich as that of farming, which has evolved over the centuries in step with technological advancements.

In the current era, however, agriculture has been slower than other industries to follow one

tech trend: artificial intelligence (AI). While already commonly used in forms ranging from automated chatbots and face recognition to car braking and warehouse controls, AI for agriculture is still in the early stages of development. Now, advances in research are spurring farmers to embrace robots by showing

“Labour is one of the biggest obstacles in agriculture.

Fritz van Evert,
ROBS4CROPS

“With this robot everything is done in the field.”

Francisco Javier Nieto De Santos
FLEXIGROBOTS

how they can do everything from meeting field-hand needs to detecting crop diseases early.

Lean and green

For French agronomist Bertrand Pinel, farming in Europe will require far greater use of robots to be productive, competitive and green – three top EU goals for a sector whose output is worth around €190 billion a year.

One reason for using robots is the need to forgo the use of herbicides by eliminating weeds the old-fashioned way: mechanical weeding, a task that is not just mundane but also arduous and time consuming.

Another is the frequent shortage of workers to prune grapevines. “In both cases, robots would help,” says Pinel, who is research and development project manager at France-based Terrena Innovation. “That is our idea of the future for European agriculture.”

Pinel is part of the EU-funded ROBS4CROPS project. With some 50 experts and 16 institutional partners involved, it is pioneering a robot technology on participating farms in the Netherlands, Greece, Spain and France. “This initiative is quite innovative,” says Frits van Evert, coordinator of the project. “It has not been done before.”

In the weeds

AI in agriculture looks promising for tasks that need to be repeated throughout the year such as weeding, according to van Evert, a senior researcher in precision agriculture at Wageningen University in the Netherlands.

“If you grow a crop like potatoes, typically you plant the crop once per year in the spring and

you harvest in the fall, but the weeding has to be done somewhere between six and 10 times per year,” he says.

Plus, there is the question of speed. Often machines work faster than any human being can. Francisco Javier Nieto De Santos, coordinator of the EU-funded FLEXIGROBOTS project, is particularly impressed by a model robot that takes soil samples. When done by hand, this practice requires special care to avoid contamination, delivery to a laboratory and days of analysis.

“With this robot everything is done in the field,” De Santos says. “It can take several samples per hour, providing results within a matter of minutes.” Eventually, he says, the benefits of such technologies will extend beyond the farm industry to reach the general public by increasing the overall supply of food.

Unloved labour

Meanwhile, agricultural robots may be in demand not because they can work faster than any person but simply because no people are available for the job.

Even before inflation rates and fertiliser prices began to surge in 2021 amid an energy squeeze made worse by Russia’s invasion of Ukraine, farmers across Europe were struggling on another front: finding enough field hands including seasonal workers. “Labour is one of the biggest obstacles in agriculture,” says van Evert. “It is costly and hard to get these days because fewer and fewer people are willing to work in agriculture. We think that robots, such as self-driving tractors, can take away this obstacle.”

The idea behind ROBS4CROPS is to create a robotic system where existing agricultural machinery is upgraded so it can work in tandem with farm robots. For the system to work, raw data such as images or videos must first be labelled by researchers in ways that can later be read by the AI.

Driverless tractors

The system then uses these large amounts of information to make “smart” decisions as well as predictions – think about the autocorrect feature on laptop computers and mobile phones, for example.

A farming controller comparable to the “brain” of the whole operation decides what needs to happen next or how much work remains to be done and where – based on information from maps or instructions provided by the farmer.

The machinery – self-driving tractors and smart implements like weeders equipped with sensors and cameras – gathers and stores more information as it works, becoming “smarter”.

Crop protection

FLEXIGROBOTS, based in Spain, aims to help farmers use existing robots for multiple tasks including disease detection. Take drones, for example. Because they can spot a diseased plant from the air, drones can help farmers detect sick crops early and prevent a wider infestation.

“If you can’t detect diseases in an early stage, you may lose the produce of an entire field, the production of an entire year,” says De Santos. “The only option is to remove the infected plant.”

For example, there is no treatment for the fungus known as mildew, so identifying and removing diseased plants early on is crucial. Pooling information is key to making the whole system smarter, De Santos says. Sharing data gathered by drones with robots or feeding the information into models expands the “intelligence” of the machines.

Although agronomist Pinel does not believe that agriculture will ever be solely reliant on robotics, he’s certain about their revolutionary impact. “In the future, we hope that the farmers can just put a couple of small robots in the field and let them work all day,” he says.



Research in this article was funded by the EU.

This article was originally published in *Horizon, the EU Research and Innovation magazine*.

ec.europa.eu/research-and-innovation/en/horizon-magazine/futuristic-fields-europes-farm-industry-cusp-robot-revolution



©Lorenzo Bernini, Shutterstock.com

Robotic bees and roots offer hope of healthier environment and sufficient food

Miniature robots that mimic living organisms are being developed to explore and support real-life ecosystems.

By Gareth Willmer

Robotics and AI can help build healthier bee colonies, benefitting biodiversity and food supply.

The robotic bee replicants home in on the unsuspecting queen of a hive. But unlike the rebellious replicants in the 1982 sci-fi thriller *Blade Runner*, these ones are here to work. Combining miniature robotics, artificial intelligence (AI) and machine learning, the plan is for the robotic bees to stimulate egg laying in the queen by, for example, feeding her the right foods at the right time.

Survive and thrive

“We plan to affect a whole ecosystem by interacting with only one single animal, the queen,” says Dr Farshad Arvin, a roboticist and computer scientist at the University of Durham in the UK. “If we can keep activities like egg laying happening at the right time, we are expecting to have healthier broods and more active and healthy colonies. This will then improve pollination.”

While that goes on above the surface, shape-morphing robot roots that can adapt and

interact with real plants and fungi are hard at work underground. There, plants and their fungal partners form vast networks.

These robotic bees and roots are being developed by two EU-funded projects. Both initiatives are looking into how artificial versions of living things central to maintaining ecosystems can help real-life organisms and their environment survive and thrive – while ensuring food for people remains plentiful. That could be crucial to the planet’s long-term future, particularly with many species currently facing steep population declines as a result of threats that include habitat loss, pollution and climate change.

One of those at risk is the honeybee, a keystone species in insect pollination required for 75% of crops grown for human food globally.

Fit for a queen

The RoboRoyale project that Arvin leads combines micro-robotic, biological and machine-learning technologies to nurture the queen honeybee’s well-being. The project is

funded by the European Innovation Council's Pathfinder programme.

A unique aspect of RoboRoyale is its sole focus on the queen rather than the entire colony, according to Arvin. He says the idea is to demonstrate how supporting a single key organism can stimulate production in the whole environment, potentially affecting hundreds of millions of organisms.

The multi-robot system, which the team hopes to start testing in the coming months,

“If we can keep activities like egg laying happening at the right time, we are expecting to have healthier broods.”

Dr Farshad Arvin,
RoboRoyale

“Biomimicry in robotics and technology will have a fundamental role in saving our planet.

Dr Barbara Mazzolai,
I-Wood

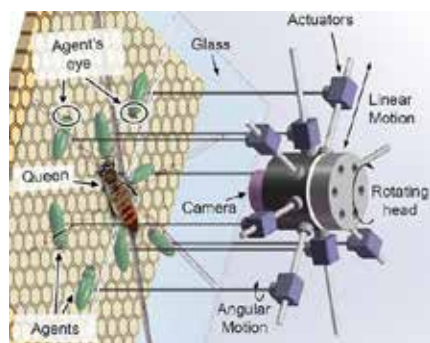
will learn over time how to groom the queen to optimize her egg laying and production of pheromones – chemical scents that influence the behaviour of the hive.

The system is being deployed in artificial glass observation hives in Austria and Turkey, with the bee replicants designed to replace the so-called court bees that normally interact with the queen.

Foods for broods

One aim is that the robot bees can potentially stimulate egg laying by providing the queen with specific protein-rich foods at just the right time to boost this activity. In turn, an expected benefit is that a resulting increase in bees and foraging flights would mean stronger pollination of the surrounding ecosystem to support plant growth and animals.

The system enables six to eight robotic court bees, some equipped with microcameras, to be steered inside an observation hive by a controller attached to them from outside. The end goal is to make the robot bees fully autonomous.



The concept design of RoboRoyale robotic controller.
©Farshad Arvin, 2023

Prior to this, the RoboRoyale team observed queen bees in several hives using high-resolution cameras and image-analysis software to get more insight into their behaviour. The team captured more than 150 million samples of the queens' trajectories inside the hive and detailed footage of their social interactions with other bees. It is now analysing the data.

Once the full robotic system is sufficiently tested the RoboRoyale researchers hope it will foster understanding of the potential for bio-hybrid technology not only in bees but also in other organisms. “It might lead to a novel type of sustainable technology that positively impacts surrounding ecosystems,” says Arvin.

Wood Wide Web

The other project, I-Wood, is exploring a very different type of social network – one that is underground.

Scientists at the Italian Institute of Technology (IIT) in Genoa are studying what they call the Wood Wide Web. It consists of plant roots connected to each other through a symbiotic network of fungi that provide them with nutrients and help them to share resources and communicate.

To understand these networks better and find ways to stimulate their growth, I-Wood is developing soft, shape-changing robotic roots that can adapt and interact with real plants and fungi. The idea is for a robotic plant root to use a miniaturized 3D printer in its tip to enable it to grow and branch out, layer by layer, in response to environmental factors such as temperature, humidity and available nutrients.

“These technologies will help to increase knowledge about the relationship between symbionts and hosts,” says Dr Barbara Mazzolai, an IIT roboticist who leads the project. Mazzolai's team has a greenhouse where it grows rice plants inoculated with fungi. So far, the researchers have separately examined the growth of roots and fungi. Soon they plan to merge their findings to see how, when and where the interaction between the two occurs and what molecules it involves.

The findings can later be used by I-Wood's robots to help the natural symbiosis between fungi and roots work as effectively as possible. The team hopes to start experimenting with robots in the greenhouse by the end of this year.

The robotic roots can be programmed to move autonomously, helped by sensors in their tips, according to Mazzolai. Like the way real roots or earthworms move underground, they will also seek passages that are easier to move through due to softer or less compact soil.

Tweaks of the trade

But there are challenges in combining robotics with nature. For example, bees are sensitive to alien objects in their hive and may remove them or coat them in wax. This makes it tricky to use items like tracking tags.

The bees have, however, become more accepting after the team tweaked elements of the tags such as their coating, materials and smell, according to Arvin of RoboRoyale.

Despite these challenges, Arvin and Mazzolai believe robotics and artificial intelligence could play a key part in sustaining ecosystems and the environment in the long term. For Mazzolai the appeal lies in the technologies' potential to offer deeper analysis of little-understood interactions among plants, animals and the environment.

For instance, with the underground web of plant roots and fungi believed to be crucial to maintaining healthy ecosystems and limiting global warming by locking up carbon, the project's robotic roots can help shed light on how we can protect and support these natural processes. “Biomimicry in robotics and technology will have a fundamental role in saving our planet,” Mazzolai says.

This article was originally published in *Horizon, the EU Research and Innovation magazine*.

ec.europa.eu/research-and-innovation/en/horizon-magazine/robotic-bees-and-roots-offer-hope-healthier-environment-and-sufficient-food



©ETH Zurich

Robot dogs take a walk on the wired side

The LeMo project's dog-like robot is one of the first to have learned to walk through reinforcement learning.

By Tom Cassauwers

Robots are learning to walk and work. While robot dogs are not yet man's best friend, real autonomy and reasoning will make them useful companions in industry, search and rescue, and even space exploration. But you must walk before you can run and machines are learning lessons from biology for better walking robots.

The first chords of the 1960s Motown song Do You Love Me by the Contours sound on the speakers as the robots start to dance. Several models, including a bipedal humanoid version and a four-legged dog-like contraption are seen dancing with each other. They shuffle, do pirouettes, and swing.

Released by the US robotics company Boston Dynamics the viral video of robots with legs dancing created a stir at the end of 2020. Reactions ranged from people suggesting it was made using CGI (computer generated imagery) to fear that the robots were going to take over the world. Yet for all the impressive engineering the video also showed the limitations that legged robots face. Whereas

for humans dancing is quite easy, for robots it is incredibly hard, and the three-minute video meant that every movement of the robots had to be manually scripted in detail.

"Today robots are still relatively stupid," says Marco Hutter, professor at ETH Zurich and expert in robotics. "A lot of the Boston Dynamics videos are hand-crafted movements for specific environments. They need human supervision. In terms of real autonomy and reasoning, we are still far away from humans, animals or what we expect from science-fiction."

Yet these sorts of robots could be very helpful to humanity. They could help us when disasters strike, they could improve industrial operations and logistics, and they could even help us explore outer space. But for that to happen we need to make legged robots better at basic tasks like walking and teach them how to do so without supervision.

Virtual learning

The European Research Council (ERC) project LeMo is one of the investigations launched by European researchers to make robots move

more autonomously. Their core premise is that legged locomotion is not what it could be, and that machine learning techniques could improve it. LeMo is specifically focused on so-called reinforcement learning.

"Reinforcement learning uses a simulation to generate massive data for training a neural network control policy," explains Hutter, who is also the project leader of LeMo. "The better the robot walks in the simulation, the higher reward it gets. If the robot falls over, or slips, it gets punished." The robot they use in the project is a 50kg dog-like, four-legged robot. On top of it are several sensors and cameras

“In terms of real autonomy and reasoning, we're still far away from science-fiction.

Marco Hutter,
LeMo

that allow it to detect its environment. This part has become pretty standard for legged robots, yet the advancement LeMo produces lies in the software. Instead of using a model-based approach, where the researchers program rules into the system, like “when there is a rock on the ground, lift up your feet higher”, they “train” an AI-system in a simulation.

Here the robot's system walks over and over through a virtual terrain simulation, and every time it performs well it receives a reward. Every time it fails it receives a punishment. By repeating this process millions of times, the robot learns how to walk through trial-and-error.

“LeMo is one of the first times reinforcement learning has been used on legged robots,” says Hutter, “Because of this, the robot can now walk across challenging terrain, like slippery ground and inclined steps. We practically never fall anymore.” Using this technology, the ETH Zurich team recently won a \$2-million Defense Advanced Research Projects Agency (DARPA) contest in which teams were challenged to deploy a fleet of robots to explore challenging underground areas by themselves.

“Legged robots are already used for industrial inspections and other observation tasks,” says Hutter, “but there are also applications like search and rescue and even space exploration where we need better locomotion. Using

techniques like reinforcement learning we can accomplish this.”

Natural inspiration

Another ERC project called M-Runners is working on how to build legged robots that work in outer space. Today when we launch robots to places like the moon or Mars, they are generally wheeled robots. These need to land, and ride on, relatively flat pieces of terrain.

“But the interesting things for geologists are not generally located in the flatlands,” says professor Alin Albu-Schäffer of the TU Munich and the German Aerospace Centre, “they are found in places like canyons, where rovers cannot easily go.”

This is why there is a strong interest in sending legged robots up into space. But before we can do that, more research needs to be done on making them work better. M-Runner takes inspiration from nature.

“Our hypothesis is that biology is more energy efficient,” says Albu-Schäffer, “our muscles and tendons have some elasticity. Animals, like a horse galloping, use this elasticity to store and release energy. Traditional robots on the other hand are rigid and do not do that.”

This means that legged robots are not as efficient as they could be. But really understanding these processes and transferring them to robots is quite a challenge. It requires a deep understanding of biology, but also of the mathematics behind how movements are

made and repeated. The complex system of the limb with a high number of interdependent parts like muscles, tendons, and bones works together very closely to repeat movements like walking or running. “Modelling this mathematically is a scientifically unsolved question,” says Albu-Schäffer.

This is what the M-Runner project is trying to solve and transfer to robots, a quest that is heavily interdisciplinary. “We work on biomechanics and biological systems,” says Albu-Schäffer, “but also neuroscience, mathematics, and physics. In turn we build tools that apply this to the actual robots.”

So far the project has already built a prototype robot, a dog-sized variant, on which the researchers are testing different types of running and gaits. The eventual goal is to apply this theoretical research into a role such as space exploration. “We also think about low gravity in simulations,” says Albu-Schäffer, “the robot here can do more spectacular jumps and stride farther.” Beyond this research, legged robots are already becoming integrated into our economy and society today. “These machines are already in use,” says Hutter, “it is not a household item yet. But in industrial contexts it is getting more popular, and in China even household use-cases are being investigated.”

But their mass market appeal relies on these robots becoming better at walking and acting in the real world. Which is why more research is needed. “Legged robots aren't just about Boston Dynamics,” says Albu-Schäffer, “In Europe cutting edge-research is also being done, and we're seeing real advances in the technology.”



Research in this article was funded by the EU.

This article was originally published in *Horizon, the EU Research and Innovation magazine*.

ec.europa.eu/research-and-innovation/en/horizon-magazine/robot-dogs-take-walk-wired-side



Robots with improved locomotive abilities can help in search and rescue operations and space exploration. © ETH Zurich



©Elnur, Shutterstock

Education and healthcare are set for a high-tech boost

The enhancement of human-machine interaction is expected to bring big improvements in support for learning and access to healthcare.

By Caleb Davies

Robotics and AI are poised to fundamentally change the future of healthcare.

In a Swiss classroom, two children are engrossed in navigating an intricate maze with the help of a small, rather cute, robot. The interaction is easy and playful – it is also providing researchers with valuable information on how children learn and the conditions in which information is most effectively absorbed.

Rapid improvements in intuitive human-machine interactions (HMI) are poised to kick off big changes in society. In particular,

two European research projects give a sense of how these trends could influence two core areas: education and healthcare.

Child learning

In EU-funded ANIMATAS, a cross-border network of universities and industrial partners is exploring if, and how, robots and artificial intelligence (AI) can help us learn more effectively. One idea is around making mistakes: children can learn by spotting and correcting others' errors – and having a robot make them might be useful.

“A teacher can’t make mistakes,” says project coordinator Professor Mohamed

Chetouani of the Sorbonne University in Paris, France. “But robots? They could. And mistakes are very useful in education.”

“Mistakes are very useful in education.”

Professor Mohamed Chetouani
ANIMATAS



Healthcare can be 24/7.

Aki Härmä
PhilHumans

According to Prof. Chetouani, it is simplistic to ask questions like “can robots help children learn better?” because learning is such a complex concept.

He says that, for example, any automatic assumption that pupils who concentrate on lessons are learning more isn't necessarily true. That's why, from the start, the project set out to ask smarter, more specific questions that would help identify just how robots could be useful in classrooms.

ANIMATAS is made up of sub-projects each led by an early-stage researcher. One of the sub-project goals was to better understand the learning process in children and analyse what types of interaction best help them to retain information.

Robot roles

An experiment set up to investigate this question invited children to team up with the aptly named QTRobot to find the most efficient route around a map.

During the exercise, the robot reacts interactively with the children to offer tips and suggestions. It is also carefully measuring various indicators in the children's body language such as eye contact and direction, tone of voice and facial expression.

As hoped, researchers did indeed find that certain patterns of interaction corresponded with improved learning. With this information, they will be better able to evaluate how well children are engaging with educational material and, in the longer term, develop strategies to maximize such engagement – thereby boosting learning potential.

Future steps will include looking at how to adapt this robot-enhanced learning to children with special educational needs.

Help at hand

Aki Härmä, a researcher at Philips Research Eindhoven in the Netherlands, believes that robotics and AI are going to fundamentally change healthcare.

In the EU-funded PhilHumans project that he is coordinating, early-stage researchers from five universities across Europe work with two commercial partners – R2M Solution in Spain and Philips Electronics in the Netherlands – to learn how innovative technologies can improve people's health.

AI makes new services possible and “it means healthcare can be 24/7,” Härmä says. He points to the vast potential for technology to help people manage their own health from home: apps able to track a person's mental and physical state and spot problems early on, chatbots that can give advice and propose diagnoses, and algorithms for robots to navigate safely around abodes.

Empathetic bots

The project, which started in 2019 and will run until late 2023, is made up of eight sub-projects, each led by a doctoral student. One sub-project, supervised by Phillips researcher Rim Helaoui, is looking at how the specific skills of mental-health practitioners – such as empathy and open-ended questioning – may be encoded into an AI-powered chatbot. This could mean that people with mental-health conditions would be able to access relevant support from home, potentially at a lower cost.

The team quickly realized that replicating the full range of psychotherapeutic skills in a chatbot would involve challenges that could not be solved all at once. It focused instead on one key challenge: how to generate a bot that displayed empathy. “This is the essential first step to get people to feel they can open up and share,” says Helaoui.

As a starting point, the team produced an algorithm able to respond with the appropriate tone and content to convey empathy. The

technology has yet to be converted into an app or product, but provides a building block that could be used in many different applications.

Rapid advances

PhilHumans is also exploring other possibilities for the application of AI in healthcare. An algorithm is being developed that can use “camera vision” to understand the tasks that a person is trying to carry out and analyse the surrounding environment.

The ultimate goal would be to use this algorithm in a home-assistant robot to help people with cognitive decline complete everyday tasks successfully.

One thing that has helped the project overall, says Härmä, is the speed with which other organizations have been developing natural language processors with impressive capabilities, like GPT-3 from OpenAI. The project expects to be able to harness the unexpectedly rapid improvements in these and other areas to advance faster.

Both ANIMATAS and PhilHumans are actively working on expanding the limits of intuitive HMI. In doing so they have provided a valuable training ground for young researchers and given them important exposure to the commercial world. Overall, the two projects are ensuring that a new generation of highly skilled researchers is equipped to lead the way forward in HMI and its potential applications.



Research in this article was funded via the EU's Marie Skłodowska-Curie Actions (MSCA).

This article was originally published in *Horizon, the EU Research and Innovation magazine*.

ec.europa.eu/research-and-innovation/en/horizon-magazine/education-and-healthcare-are-set-high-tech-boost



©Microsure BV, 2022

Robot assistants in the operating room promise safer surgery

With extreme precision needed for certain medical operations, state-of-the-art robots offer a way to make surgery easier, safer and more successful.

By Gareth Willmer

Advanced robotics can help surgeons carry out procedures where there is little margin for error.

In a surgery in India, a robot scans a patient's knee to figure out how best to carry out a joint replacement. Meanwhile, in an operating room in the Netherlands, another robot is performing highly challenging microsurgery under the control of a doctor using joysticks.

Such scenarios look set to become more common. At present, some manual operations are so difficult they can be performed by only a small number of surgeons worldwide, while others are invasive and depend on a surgeon's specific skill.

Advanced robotics are providing tools that have the potential to enable more surgeons to carry out such operations and do so with a higher rate of success. "We're entering the next revolution in medicine," says Sophie Cahen, chief executive officer and co-founder of Ganymed Robotics in Paris.

New knees

Cahen leads the EU-funded Ganymed project, which is developing a compact robot to make joint-replacement operations more precise, less invasive and – by extension – safer.

The initial focus is on a type of surgery called total knee arthroplasty (TKA), though Ganymed is looking to expand to other joints including the shoulder, ankle and hip. Ageing populations and lifestyle changes are accelerating demand for such surgery, according to Cahen. Interest in Ganymed's robot has been expressed in many quarters, including distributors in emerging economies such as India. "Demand is super-high because arthroplasty is driven by the age and weight of patients, which is increasing all over the world," Cahen says.

Arm with eyes

Ganymed's robot will aim to perform two main functions: contactless localization of bones and collaboration with surgeons to support joint-replacement procedures.

It comprises an arm mounted with "eyes" that use advanced computer-vision-driven intelligence to examine the exact position and orientation of a patient's anatomical structure. This avoids the need to insert invasive rods and optical trackers into the body.

Surgeons can then perform operations using tools such as sagittal saws – used for orthopaedic procedures – in collaboration with the robotic arm. The "eyes" aid precision

“We're entering the next revolution in medicine.

Sophie Cahen
Ganymed

by providing so-called haptic feedback, which prevents the movement of instruments beyond predefined virtual boundaries. The robot also collects data that it can process in real time and use to hone procedures further. Ganymed has already carried out a clinical study on 100 patients of the bone-localization technology and Cahen says it achieved the desired precision.

Now the firm is performing studies on the TKA procedure with hopes that the robot will be fully available commercially by the end of 2025 and become a mainstream tool used globally. “We want to make it affordable and accessible, so as to democratize access to quality care and surgery,” says Cahen.

Microscopic matters

Robots are being explored not only for orthopaedics but also for highly complex surgery at the microscopic level.

The EU-funded MEETMUSA project has been further developing what it describes as the world’s first surgical robot for microsurgery certified under the EU’s “CE” regulatory regime. Called MUSA, the small lightweight robot is attached to a platform equipped with arms able to hold and manipulate microsurgical instruments with a high degree of precision. The platform is suspended above the patient during an operation and is controlled by the surgeon through specially adapted joysticks.

In a 2020 study, surgeons reported using MUSA to treat breast-cancer-related lymphedema – a chronic condition that commonly occurs as a side effect of cancer treatment and is

characterized by a swelling of body tissues as a result of a build-up of fluids.

To carry out the surgery, the robot successfully sutured – or connected – tiny lymph vessels measuring 0.3-0.8mm in diameter to nearby veins in the affected area.

“Lymphatic vessels are below 1mm in diameter so it requires a lot of skill to do this,” says Tom Konert who leads MEETMUSA and is a clinical field specialist at robot-assisted medical technology company Microsure in Eindhoven in the Netherlands, “But with robots, you can more easily do it. So far, with regard to the clinical outcomes, we see really nice results.”

Steady hands

When such delicate operations are conducted manually, they are affected by slight shaking in the hands, even with highly skilled surgeons, according to Konert. With the robot, this problem can be avoided. MUSA can also significantly scale down the surgeon’s general hand movements rather than simply repeating them one-to-one, allowing for even greater accuracy than with conventional surgery.

“When a signal is created with the joystick, we have an algorithm that will filter out the tremor,” says Konert, “It downscales the movement as well. This can be by a factor-10 or 20 difference and gives the surgeon a lot of precision.”

In addition to treating lymphedema, the current version of MUSA – the second, after a previous prototype – has been used for other procedures including nerve repair and soft-tissue reconstruction of the lower leg.

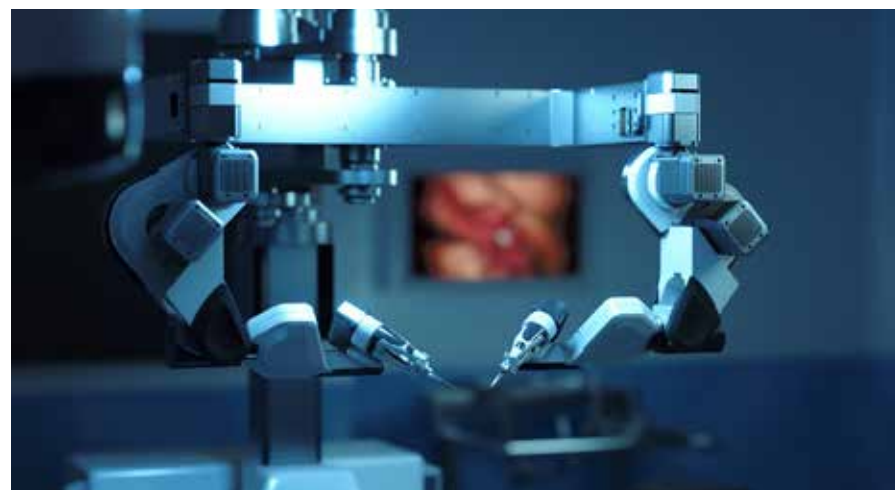
Next generation

Microsure is now developing a third version of the robot, MUSA-3, which Konert expects to become the first one available on a widespread commercial basis.

This new version will have various upgrades, such as better sensors to enhance precision and improved manoeuvrability of the robot’s arms. It will also be mounted on a cart with wheels rather than a fixed table to enable easy transport within and between operating theatres. Furthermore, the robots will be used with exoscopes – a novel high-definition digital camera system. This will allow the surgeon to view a three-dimensional screen through goggles in order to perform “heads-up microsurgery” rather than the less-comfortable process of looking through a microscope.

Konert is confident that MUSA-3 will be widely used across Europe and the US before a 2029 target date. “We are currently finalizing product development and preparing for clinical trials of MUSA-3,” he says, “These studies will start in 2024, with approvals and start of commercialization scheduled for 2025 to 2026.”

MEETMUSA is also looking into the potential of artificial intelligence (AI) to further enhance robots. However, Konert believes that the aim of AI solutions may be to guide surgeons towards their goals and support them in excelling rather than achieving completely autonomous surgery. “I think the surgeon will always be there in the feedback loop, but these tools will definitely help the surgeon perform at the highest level in the future,” he says.



MUSA’s robotic arms. Microsure BV, 2022



Research in this article was funded via the EU’s European Innovation Council (EIC).

This article was originally published in *Horizon, the EU Research and Innovation magazine*.

ec.europa.eu/research-and-innovation/en/horizon-magazine/robot-assistants-operating-room-promise-safer-surgery



Comparing finite volume and particle CFD simulation methods for understanding lubrication in automotive transmissions and axles

by Jin Xu^{1,2}, William W. Liou^{1,2}, and Yang Yang³

1. Department of Mechanical and Aerospace Engineering, Western Michigan University, USA

2. Computational Engineering Physics Lab, Western Michigan University, USA

3. Cook Research Incorporated, USA

Particleworks was 38.9 times faster than a finite volume approach. Particleworks ran on a quad-core PC with a GPU card and the finite-volume code ran on a 90-core CPU cluster.

Understanding the flow of oil lubrication in transmissions and axles is vital to improving their efficiency and reducing the wear of key components [1, 2]. Most geared transmissions and axles are splash lubricated, which means that lubrication of gears and bearings relies on complex flow patterns created by the gears churning the oil and the oil then deflecting off the walls of the gearbox housing. Appropriate levels of lubricant are required to keep all components lubricated [3, 4]. Lack of adequate lubrication where gears mesh and within the bearings will increase friction, leading to increased temperatures and premature failure of system components. Likewise, excessive lubrication can increase

churning losses and reduce efficiency. Gearboxes generally operate conservatively with an excess supply of oil to improve operational reliability and gear life, but at the cost of operational efficiency. The choice, and volume of lubricant, and the shape of the gearbox housing can all be optimized for the expected gear speeds, loads, and temperatures. For example, lubricant viscosity varies with temperature. A low viscosity can cause excessive metal-to-metal friction between the gears during engagement, while high-viscosity lubricants can significantly increase the shear stress acting on the gear surfaces thus increasing the churning losses.

Computational fluid dynamics (CFD) simulations are widely accepted in the automotive industry as a method to understand lubricant flow progression within gearboxes and to optimize lubrication [5, 6]. CFD simulations represent a systematic and

cost-effective method to study the performance of fluid-lubricated [7] or fluid-cooled devices under a wider range of operating conditions than could be tested using physical prototypes. CFD models based on finite volumes have been widely used to study gearbox lubrication and lubricant flow [8, 9]. Simulations focusing on lubricant flow give results that are in good agreement with experimental results [8, 10]. Currently, two main challenges limit the effectiveness of finite volume methods for simulating gearbox lubrication. First, the combination of the unsteady and turbulent nature of the flow and the need for some type of sliding or adaptive mesh to account for gear rotation can lead to computationally expensive simulations that may require prohibitively long simulation times on expensive hardware. Second, remeshing increases the technical skills a CFD engineer needs to achieve good results.

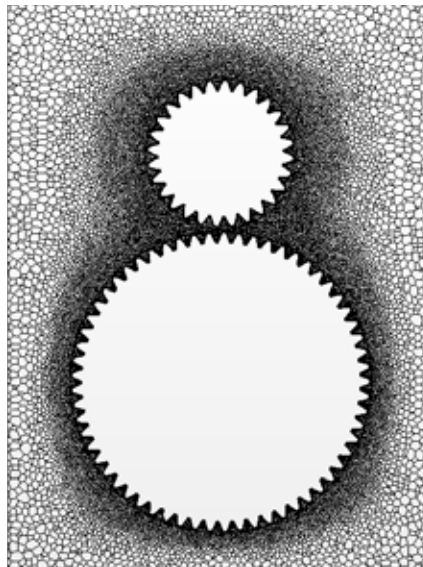


Fig. 1. Sliding mesh with 5.2M cells.

Particle-based CFD emerged in the 1970s in the form of smoothed-particle hydrodynamics [11] and later methods such as semi-implicit moving particle methods [12, 13]. The advantage of particle-based methods over finite-volume CFD methods [14, 15] is that remeshing is not required when free surfaces undergo drastic changes or when fluids coalesce or separate, which is commonly observed in lubrication flows.

The fluid mass represented by the particles can respond to moving boundaries as effectively as it does to stationary boundaries. Furthermore, CFD can be efficiently calculated on GPUs using meshfree particle methods. Modern advances in GPU technology allow CFD simulations with millions of particles to be calculated on a single GPU. This means that meshfree particle methods [16, 17] can handle complex gearbox geometries with the efficient use of computing resources. It has great potential for simulations involving free surfaces, such as lubricant oil flow simulations.

We compared CFD simulations using the finite volume (STAR-CCM+) and the meshfree particle (Particleworks) methods. The results show that both methods can be used to successfully understand lubrication and oil churning losses in the gearbox. However, in terms of calculation time, the Particleworks results are obtained much more efficiently.

Gearbox geometry and operating conditions

The internal dimensions of the example gearbox are 170mm (W) × 240mm (H) × 98mm (D). The larger of the two helical gears is the driving gear (or ring gear), which rotates clockwise (viewed from the front) at 3000rpm, as shown in Fig. 1. The driven gear (or pinion gear) has a corresponding rotational speed of 6535.7rpm.

The top-land-to-top-land lengths for both gears are 118mm and 58mm, respectively. The lubricant level is 41.7mm from the lowest point of the ring gear, which is 22.21mm above the bottom of the gearbox interior. In other words, the lubricant filling depth is 63.91mm and the oil volume is 957cc. The effect of the friction between the lubricant and the gears on the oil temperature is not considered and it is assumed that the lubricant temperature is constant at 37.5°C. The corresponding lubricant density is 836.8kg/m³ and the dynamic viscosity is 0.0281374Pa·s.

Simulation settings in STAR-CCM+

Finite volume-based simulations were performed using STAR-CCM+ [20] using the multiphase segregated flow solver and the

realizable k-ε turbulence model [21], implemented with a constant time step of 2.5 × 10⁻⁵s. A sinusoidal ramp-up period of 0.01s was used to simulate the speed increase. A sliding mesh was used where a rotating sliding mesh shifts the mesh vertices of a region during the transient analysis of the rotating mesh. To apply the sliding mesh method, the upper gear (i.e. the pinion) was pulled upward by 4mm so that the closest (vertical) distance between the two gears was 2.25mm. Fig. 1 shows a two-dimensional (2D) representation of the mesh used in our simulation with 2.324 million (M), 0.504M and 2.343M cell elements for the ring gear refinement region, the pinion gear refinement region, and the remainder of the computational domain, respectively.

The total number of cells was 5.171M. Grid-independence studies were performed by varying the total number of cells from 1.7M to 5.2M and comparing the average churning loss. The largest difference in predicting the mean loss from two adjacent cell counts was less than 5%. The surface tension model was found to be negligible and was thus not included in the model. The simulations were performed with CPU-based cluster computing.

Simulation settings in Particleworks

Particle-based simulations were performed using Particleworks [22]. The large eddy simulation (LES) model was used for turbulence and the wall model was used to compensate for the lack of resolution near the wall in the LES model. The time interval (Δt) varies during the run and is defined as the minimum value of the initial time interval (set to 10–5s),

$$\Delta t = \frac{(\text{Courant \#}) \times (\text{Particle size})}{\text{Maximum velocity of particles}}, \quad \frac{(\text{Diffusion \#}) \cdot (\text{Particle size})^2}{\text{Maximum kinematic viscosity}}$$

Smaller initial time intervals have been found to significantly increase the total number of time steps required for the simulation to reach a certain number of gear revolutions. The maximum peripheral speed of the gear was used to estimate the maximum particle velocity and was set to 30m/s. Particleworks simulations



were performed using two particle counts: 0.95M with 1mm particles, and 1.87M with 0.8mm particles. To validate the computational speedup of the particle-based method running on a GPU, two computing platforms were compared: a multi-CPU workstation and a single GPU workstation.

STAR-CCM+ simulation results

The images in Fig. 2 demonstrate the temporospatial progression of the lubricant's volume fraction (VF) in the gearbox at four different instants of time, from 0.1s to approximately 0.7s (approximately 10.9–70.3 revolutions of the driven gear). While panel (a) is a 3D visualization of the flow behaviour in which the front wall is not visible, panel (b) provides a plan view of the axial median plane of the gear or the centre of the front and rear walls of the gearbox.

As the ring gear rotated clockwise, a significant amount of lubricant travelled along the port wall (seen from the front) with considerable accumulation in the corners adjoining the top wall, with occasional build-up on other walls. As the lubricant initially travelled along the port wall, it began to fall back down by about 0.16s (~17.4 revolutions of the driven gear). Also, at 0.15s (~16.3 revolutions of the pinion), the lubricant appeared to have passed over the top wall and started dripping along the starboard wall.

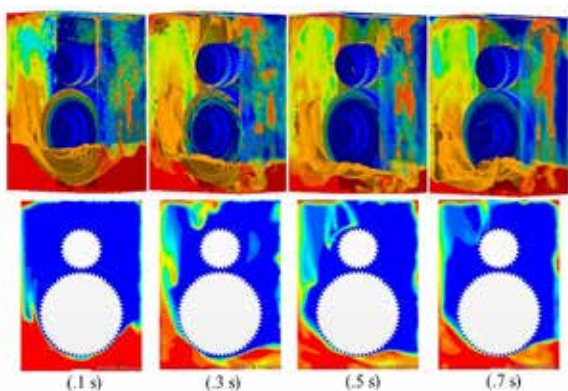


Fig. 2. Spatial progression of VF of lubricant predicted using STAR-CCM+.

Fig. 3 shows the temporal history of normalized churning loss. Viscous force and pressure were considered in the calculation of churning losses. Since the gears were set to rotate at the target speeds at the beginning of the simulations, an initial transient occurred as the flow was responding to the sudden rotation of the gears.

The normalization parameter was chosen based on the value of the power loss after the initial transition of the simulated flow subsided. STAR-CCM+ predicted that the ring gear contributed about 80% of the total churning loss. Approximately 40% of the ring gear surface area was initially immersed in the lubricant pool.

The results show that the ring gear contributes significantly to the churning loss. The (normalized) average values of the pinion gear churning torque due to pressure and viscous forces were 4.79% and 6.84%, respectively. Furthermore, the counterparts of the ring gear were 19.63% and 28.12% due to pressure and viscous forces, respectively. It is worth noting that the viscosity mechanism played a more important role than pressure in terms of losses. The solution process was halted when the mass loss of the lubricant, common in similar simulations, exceeded 5% of the initial mass.

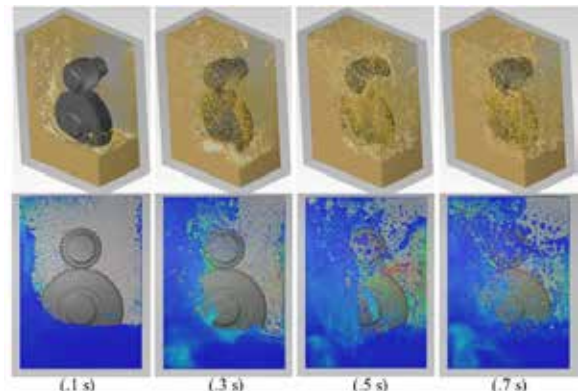


Fig. 4. Surface scene (top) and velocity scene (bottom) showing the lubricant progression predicted using Particleworks.

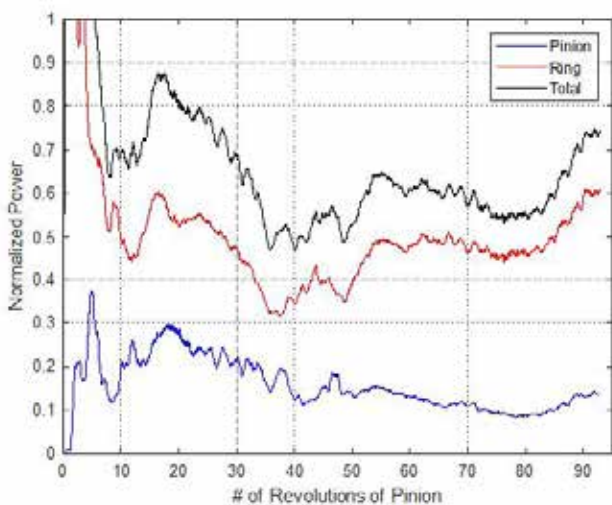


Fig. 3. Temporal history of churning losses for the two gears predicted using STAR-CCM+.

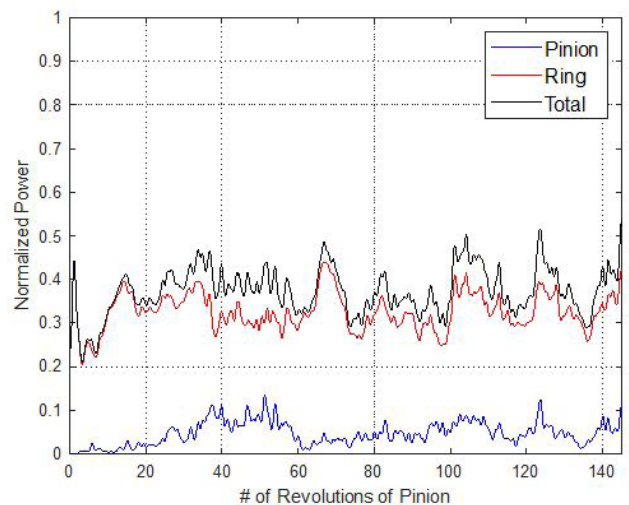


Fig. 5. Time history of predicted churning losses for the two gears using 1.87M particles.

Particleworks simulation results

Both a time-stepped velocity field and a surface formation were generated. Fig. 4 shows the simulation results for the same four moments as in Fig. 2 (0.1–0.7s and 10.9–70.3 pinion revolutions). While the maximum particle velocity may have exceeded the linear circumferential velocity (approximately 19m/s), the vast majority of particles moved far more slowly, justifying the use of an upper bound of 5m/s in the flow visualization. It would seem that the particle-based simulation was better able to capture cluster formation, fragmentation, and atomization.

Fig. 5 shows the time history of the churning losses calculated. Both viscous and pressure forces were taken into account. Similar to the STAR-CCM+ simulation results, the flow has an initial transient response to sudden gear rotation, and the contribution of the ring gear accounted for a considerable portion of the total churning loss.

Fig. 6 shows a breakdown of the contribution of pressure and viscous forces to the churning power loss on the ring gear and compares the results obtained using the two different particle counts (0.95M particles and 1.87M particles). The simulation ended at approximately 218 revolutions of the pinion gear i.e. 2s after the gears were moved. The trends in the evolution of power losses appear to be similar. The main contributor to the churning loss is the viscous force acting on the ring gear.

For the simulations of 0.95M and 1.87M particles, the values for the averaged total churning loss (sum of the viscous and pressure force contributions) are 0.353 and 0.341, respectively. Doubling the particle count resulted in a change of ~3.4% in the churning loss predicted, indicating that sufficient numerical accuracy was achieved with the use of 0.95M particles.

Calculation time result

It is interesting to evaluate the calculation time of the CFD simulations. While the simulations based on finite volumes were run

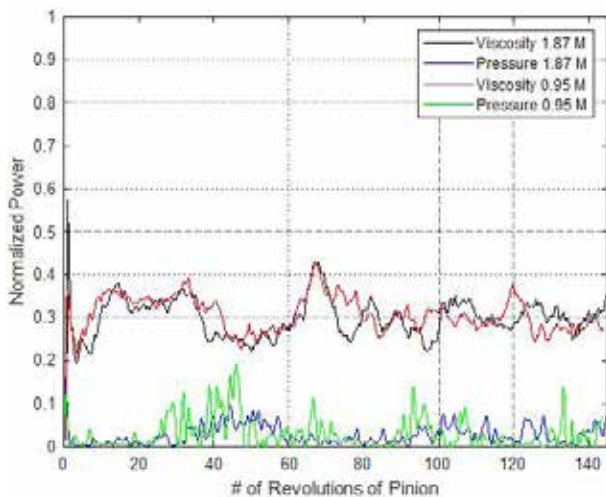


Fig. 6. Contribution to the ring gear power loss predicted using 0.95M and 1.87M particles.

Software	# of particles (million)	Particle size (mm)	Computing time/Physical time (normalized to PW on GPU)	Average time (s) per step
PW on GPU	1.87	0.8	1	1.4
PW on CPU	0.95	1	10.6	16.0
PW on CPU	1.87	0.8	22.6	35.9
STAR-CCM+	N/A	N/A	38.9	N/A

Table 1. Comparison of computation times.

on a computer cluster with a 90-core CPU, the particle-based solver was run on two different computers: an 8-core CPU workstation and a GPU workstation. Only four cores were used for the CPU calculation.

Table 1 lists the computing performance in terms of computation time per unit of physical time. In physical time, the three particle-based CFD simulations required less solver time than their finite volume-based counterparts. The results also show that the computation time of the particle-based approach is proportional to the number of particles used in the simulation. For the same number of particles (1.87M), the simulation speed using the GPU workstation was 22.6 times faster than that using the quad-core CPU workstation, indicating that the particle-based approach is significantly faster for GPU computing.

Discussion and conclusion

Overall, the two simulation methods show good agreement. Both methods show flow patterns that are immediately recognizable visually in the other. Furthermore, the volume fraction measurements taken at different positions in the gearbox were in significant agreement, with two exceptions. Firstly, Particleworks seemed to be able to capture the lubricant build-up more easily, and dripping was observed from the middle of the top wall (see Fig. 7). Specifically, at 0.38s (corresponding to ~41.4 pinion revolutions), the dripping liquid counteracted the rotation of the pinion and increased the overall power loss. Secondly, the two simulations predicted different flow behaviours just outside the ring gear, with Particleworks predicting that a larger proportion of the oil would spread out from the ring gear to the wall.

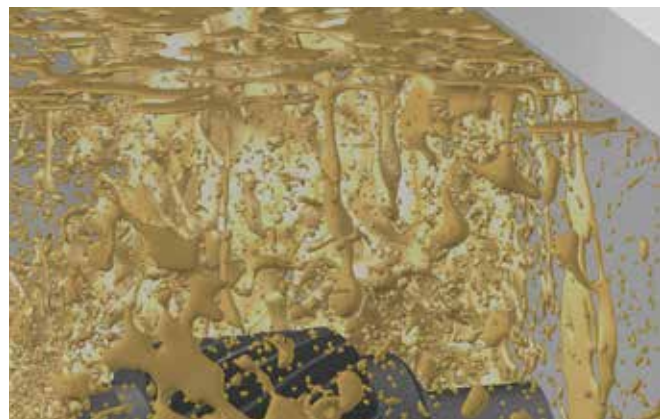


Fig. 7. Lubricant dripping from the middle of the top wall.

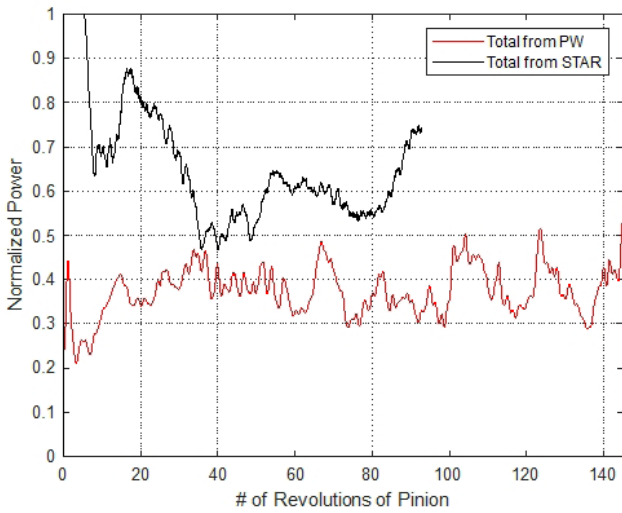


Fig. 8. Comparison of churning loss between Particleworks (PW) (1.87M particles) and STARCCM+ (STAR).

In Particleworks, the 0.95M- and 1.87M-particle simulations predicted globally similar flow behaviour in terms of churning power loss and local flow dynamics. The difference between the average values of total churning loss predicted by the two simulations was 3.4%. The lower particle-count simulation apparently provided the same level of resolution in terms of the averaged churning power loss.

Thus, the averaged churning loss is not sensitive to the two particle settings used in our simulations. It is also worth noting that while the power loss for both runs followed the same trend, the use of

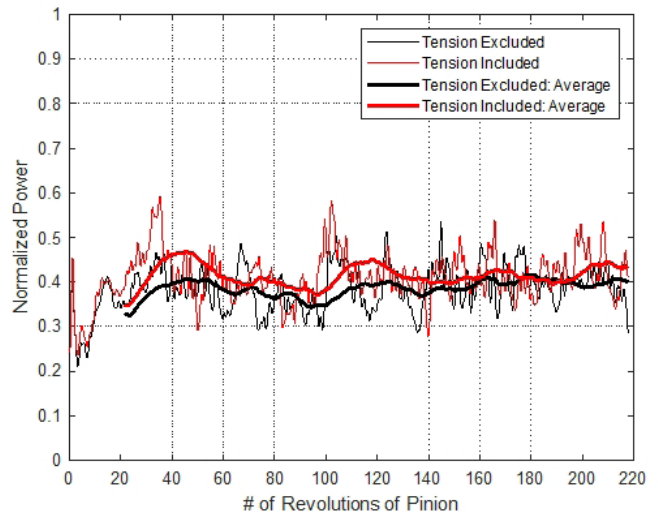


Fig. 9. Effect of surface tension on power loss per gear based on 1.87M-particle simulation results.

more particles seemed to suppress pressure-induced oscillations in the power-loss curve. The pressure-smoothing functionality is available but was not activated in the simulations.

The power loss due to gearbox oil churn obtained using both models is shown in Fig. 8. The churning loss calculated using the particle-based method fluctuates around the averaged value given above, indicating that the simulated flow could reach a state of statistical quiescence. Particleworks predicted that the ring gear churning contributes 86.2% of the total loss, compared to 79.1% in the STAR-CCM+ results. The simulation results of the two



CFD methods show that the ring gear contributes the most to the churning power loss.

For the particle-based method, the effect of surface tension modelling was further evaluated. The lubricating oil has a surface tension coefficient of 0.025N/m and a contact angle of 60°. The effect of surface tension on the churning power loss of the gears was examined separately and plotted in Fig. 9.

The loss pattern is similar with and without surface tension modelling. Oscillation characteristics are observed in the particle-based simulation results shown above, which seem to mask the general trend of transient changes in churning losses. A moving average with a time window of 0.2s was applied to the total churn loss to better observe the trends.

The results show that surface tension has no significant effect on the overall loss trend. Based on a window of 100 revolutions (from 120 to 220 revolutions, a smooth statistical flow was obtained), the average value excluding surface tension was 0.395, which is 4.88% lower than when surface tension was included. The Particleworks results without surface tension modelling were used for the comparison with the STAR-CCM+ simulation results in the Results section.

References

- [1] A.S. Kolekar, A.V. Olver, A.E. Sworski, and F.E. Lockwood, "Windage and Churning Effects in Dipped Lubrication", *Journal of Tribology*, 136, no. 2, 2014: 021801.
- [2] P.M.T. Marques, C.M.C.G. Fernandes, R. Martins, and J.H.O. Seabra, "Power Losses at Low Speed in a Gearbox Lubricated with Wind Turbine Gear Oils with Special Focus on Churning Losses", *Tribology International*, 62, 2013, pp. 186–197.
- [3] S. Seetharaman and A. Kahraman, "Load-independent Spin Power Losses of a Spur Gear Pair: Model Formulation", *Journal of Tribology*, 131, no. 2, 2009: 022201.
- [4] S. Seetharaman, A. Kahraman, M.D. Moorhead, and T.T. Petry-Johnson, "Oil Churning Power Losses of a Gear Pair: Experiments and Model Validation", *Journal of Tribology*, 131, no. 2, 2009: 022202.
- [5] C. Gorla, F. Concli, K. Stahl, B.R. Höhn et al, "CFD Simulations of Splash Losses of a Gearbox", *Advances in Tribology 2012*, 2012, pp. 1–10.
- [6] C. Changenet and P. Velez, "A Model for the Prediction of Churning Losses in Geared Transmissions — Preliminary Results", *Journal of Mechanical Design*, 129, no. 1, 2007, pp. 128–133.
- [7] F. Concli, C.T. Schaefer, and C. Bohnert, "Innovative Meshing Strategies for Bearing Lubrication Simulations", *Lubricants*, 8, no. 46, 2020, pp. 1–14.
- [8] H. Liu, T. Jurkschat, T. Lohner, and K. Stahl, "Determination of Oil Distribution and Churning Power Loss of Gearboxes by Finite Volume CFD Method", *Tribology International*, 109, 2017, pp. 346–354.
- [9] H. Liu, T. Jurkschat, T. Lohner, and K. Stahl, "Detailed Investigations on the Oil Flow in Dip-Lubricated Gearboxes by the Finite Volume CFD Method", *Lubricants*, 6, no. 2, 2018, pp. 47.
- [10] T. Noda, K. Shibusaki, S. Miyata, and M. Taniguchi, "X-Ray CT Imaging of Grease Behavior in Ball Bearing and Numerical Validation of Multi-Phase Flows Simulation", *Japanese Society of Tribologists*, 15, no. 1, 2020, pp. 36–44.
- [11] M. Sasson, S. Chai, G. Beck, Y. Jin et al, "A Comparison between Smoothed-Particle Hydrodynamics and RANS Volume of Fluid Method in Modelling Slamming", *Journal of Ocean Engineering and Science*, 1, 2016, pp. 119–128.
- [12] S. Koshizuka and Y. Oka, "Moving-Particle Semi-Implicit Method for Fragmentation of Incompressible Fluid", *Nuclear Science and Engineering*, 123, no. 3, 1996: 282420.
- [13] M. Galbiati, "Oil Splashing, Lubrication and Churning Losses Prediction by Moving Particle Simulation", presented at the NAFEMS World Conference 2017, June 2017.
- [14] F. Concli, "Numerical Modelling of the Churning Power Losses of Gears: An Innovative 3D Computational Tool Suitable for Planetary Gearbox Simulation", *Tribology International*, 103, 2013, pp. 58–68.
- [15] L. Martinelli, M. Hole, D. Pesenti, and M. Galbiati, "Thermal Optimisation of e-Drives Using Moving Particle Semi-Implicit (MPS) Method", *EnginSoft Newsletter*, Year 15, no. 3, pp. 27–33.
- [16] T. Iino, S. Matsumura, H. Houjoh, and T. Hacıya, "Calculation of the Behavior of Oil Churning and its Loss in a Gear Box by a Moving Particle Method: The First Result of Both Calculation and Experiment", *Power Transmissions*, D. Qin and Y. Shao (Eds) (London: Taylor & Francis Group, 2017), ISBN:978-1-138-03267-5.
- [17] M. Haga and T. Kasahara, "Simulation of Oil Separating Behavior for Engine Breather System", *Honda R&D Technical Review*, 26, no. 2, 2014, pp. 98–106.
- [18] P. Norman and K. Howard, "Evaluating Statistical Error in Unsteady Automotive Computational Fluid Dynamics Simulations", *SAE Technical Paper*, 2020-01-0692, 2020, <doi.org/10.4271/2020-01-0692>.
- [19] H. Tennekes and J.L. Lumley, *A First Course in Turbulence* (Cambridge, MA: MIT Press, 1972), pp. 197–221, ISBN:978-0-262-20019-6.
- [20] <www.plm.automation.siemens.com/global/en/products/simcenter/STARCCM.html>, accessed.
- [21] T.H. Shih, W.W. Liou, A. Shabbir, Z. Yang et al, "A New k-ε Eddy Viscosity Model for High Reynolds Number Turbulent Flows", *Computers & Fluids*, 24, 1995, pp. 227–238.
- [22] Y. Chikazawa, S. Koshizuka, and Y. Oka, "A Particle Method for Elastic and Visco-Plastic Structures and Fluid-Structure Interactions", *Computational Mechanics*, 27, 2001 pp. 97–106.

CFD is widely used in the automotive industry, and simulation time and optimization of CFD modelling remain a significant challenge. The results presented illustrate the difference in computational efficiency between two CFD software programs that are used to simulate gearbox lubrication.

While finite-volume methods have a longer history, particle-based methods have proven their value in capturing flow behaviour, enabling faster simulation of transient free-surface flows such as those in oil lubrication.

Acknowledgments

This work was supported in part by the CAViDS Consortium at Western Michigan University. Thanks to Carlos Wink of Eaton Corp., and Andrea Lucci, Mark Williams, and Dakota Dawson of Dana Inc. for hardware and application software support. Technical assistance was provided by Zach Smith and Dr. Brant Ross of EnginSoft USA.

For more information:

James Crist - EnginSoft USA
j.crist@enginsoft.com



Analysis of the thermo-fluid dynamics of a paint shop's hot water distribution network

by Luca Zanellato, Matteo Caldaroni
SimulHub

This article describes an analysis of the performance of a hot water distribution piping network consisting of a main boiler and various utilities inside an automotive paint shop based in France. The simulation is performed using Flownex, a CFD (computational fluid dynamics) software with concentrated parameters.

A paint shop is powered by several energy sources (hot and cold water, natural gas, electricity, and compressed air) that serve to drive the applications of surface treatments to the car body from the pre-treatment phases to the actual painting. The energy is delivered to different components (process tanks, air supply units, oven heating units) via a complex network of pipes. This study

focuses on the hot water distribution system (Fig. 1).

Using a dedicated tool like Flownex offers several advantages:

- It reduces the need for assumptions and interpretation by operators;
- It enables the building of a simple and efficient model to analyse the performance of complex systems;
- It allows boundary conditions to be modified and gives immediate feedback on results.

The main objectives of the analysis are to:

- Verify the calculations of the global pressure drop that were made during the design phase of the system;

- Calculate the temperature distribution within the circuit and the global return temperature;
- Define an initial state of the system conditions (to regulate the valves and pumps).

System description

The piping network starts from the main boiler and connects eleven utilities by means of a closed ring (Fig. 2). The main distribution pipe first passes through and feeds the hot pre-treatment stages (three utilities) and then divides into two parallel branches that have five and three air supply units respectively. At the end of the circuit the water flow is divided again: part of it is led to the boiler; the rest passes through a heat exchanger to recover heat from an incinerator.

The boiler for this project was supplied by the customer. The water is provided at fixed temperature conditions. The utilities and other components of the circuit, on the other hand, are controlled by a thermoregulation skid with a three-way valve that allows the flow rate to be varied according to the heat required (Fig. 3).

Boundary conditions and simulation scenarios

Flownex makes it possible to recreate the actual distribution network using predefined

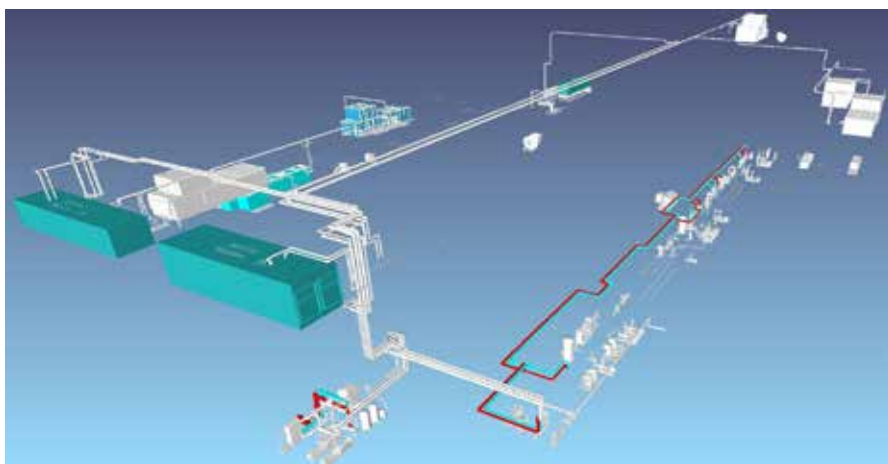
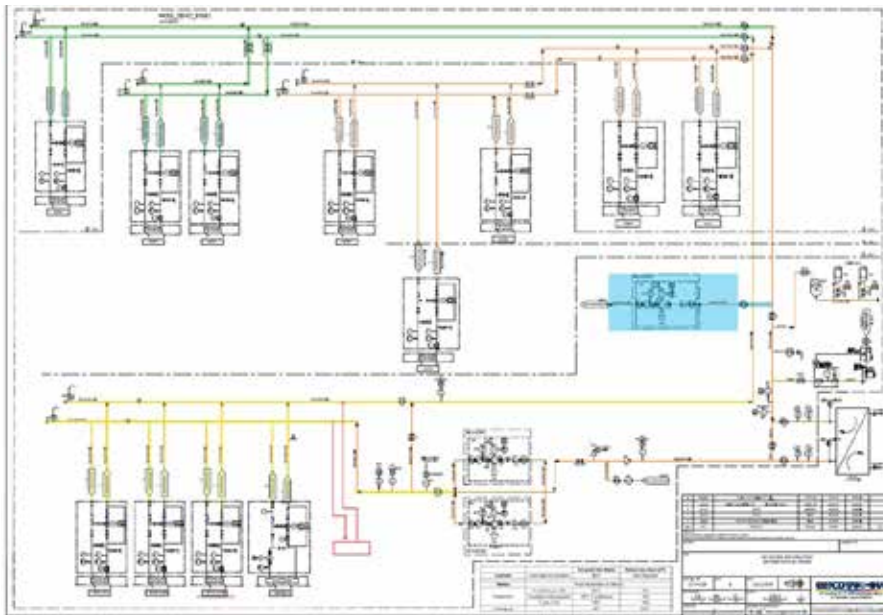


Fig. 1. Hot water distribution network.



start-up (heating of the tanks) and when operating at full capacity.

In the system being studied these variations are sufficiently slow to allow the phenomenon to be approached from a steady state. Since the parameters are so easily edited operation can be tested in three main simulation scenarios:

- The start-up phase;
- Operation at full load in summer conditions;
- Operation at full load in winter conditions.

The complete list of parameters is shown in Table 1.

Results

The temperature and pressure distributions for steady-state operation in summer conditions are shown in Figs. 5 and 6.

To balance the flow rates on both branches of the air supply units and achieve the desired flow rates, it was necessary to adjust the regulation valve to impose an adequate pressure drop. Regulating the valve increases the pressure drop across the entire circuit with a consequent variation in the pump behaviour. This results in a decrease in the total flow rate within the pipe network while maintaining an acceptable value for each user (Fig. 7).

Fig. 2. Piping and instrumentation diagram.

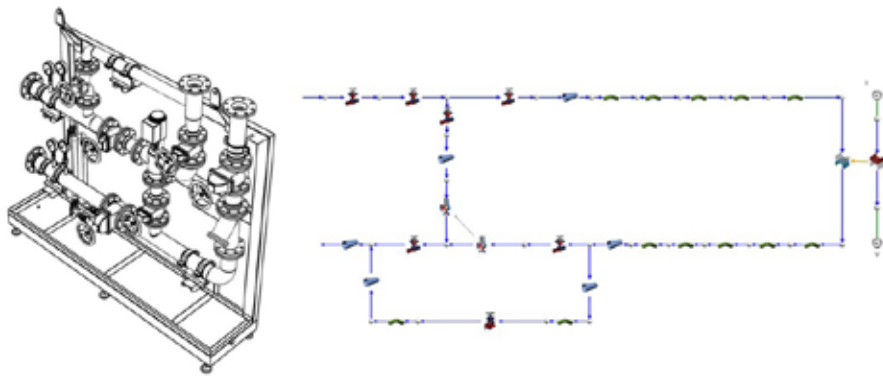


Fig. 3. The thermoregulation skid (left) and its model in Flownex (right).

components and customized elements. The behaviour of each component is modelled through different geometry and performance parameters.

The one-dimensional modelling of concentrated parameters reduces the number of inputs required without sacrificing the fidelity of the simulation model.

Most of the information can be found in the manufacturer's data sheets for each component. The operating curves of the valves and pumps can be specified using dedicated tables in the software database if they are not available in the integrated library (Fig. 4).

To define the heat exchangers, it is necessary to set the geometric and performance characteristics and the boundary conditions of the process side (second side). The operating conditions of the exchangers are not constant over time:

- Fresh-air supply units must offer variable heat output depending on the conditions of the external environment, which are not constant;
- Pre-treatment utilities have very different thermal requirements during

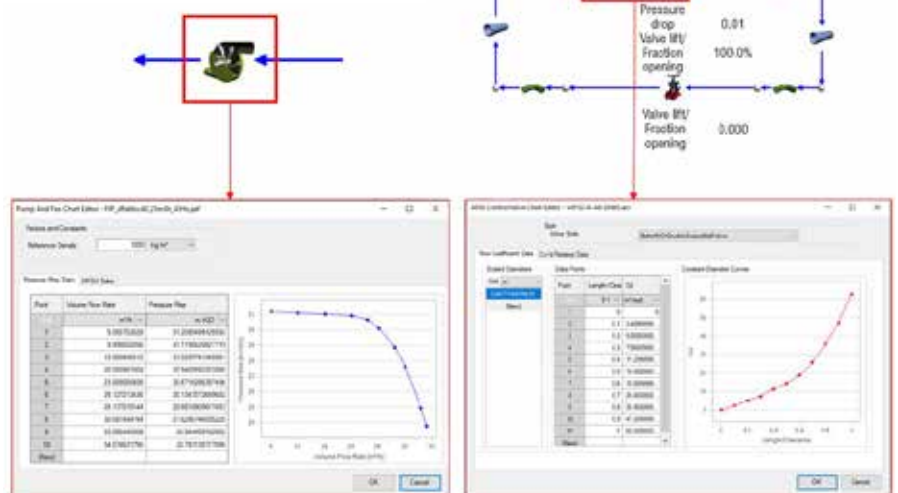


Fig. 4. Pump and valve curves.

Component	Boundary Conditions
Piping	Length
	Diameter
	Roughness
	Curve
	Fittings
	Elevation
Valve	Type
	Diameter
	Pressure drop curve
Pump	Hydraulic efficiency
	Flow rate vs head curve
Heat Exchanger	Type
	Pressure-loss coefficient
	Heat-transfer coefficient

Table 1. Boundary conditions.

The overall pressure drop and the resulting flow rate are in line with the project requirements and confirm the calculations made during the design of the plant components. The contractual temperature constraint on the return line was verified under critical operating conditions (summer).

Conclusions

Traditional spreadsheets cannot manage the whole system and lead to excessive approximations and greater possibilities of error. Flownex enabled the complete system to be studied under various operating conditions using a one-dimensional model with concentrated parameters. The analysis conducted made it possible to calculate:

- The global pressure drop across the system, validating the calculations of the design phase;
- The regulation levels for the system's pumps and valves to obtain the desired flow rate;
- The overall return temperature in critical conditions.

Flownex software can easily manage the complexity typical of engineering plants and will also be used in other areas of the automotive paint shop.

For more information:

Luca Zanellato - Simulation Expert
info@simulhub.com

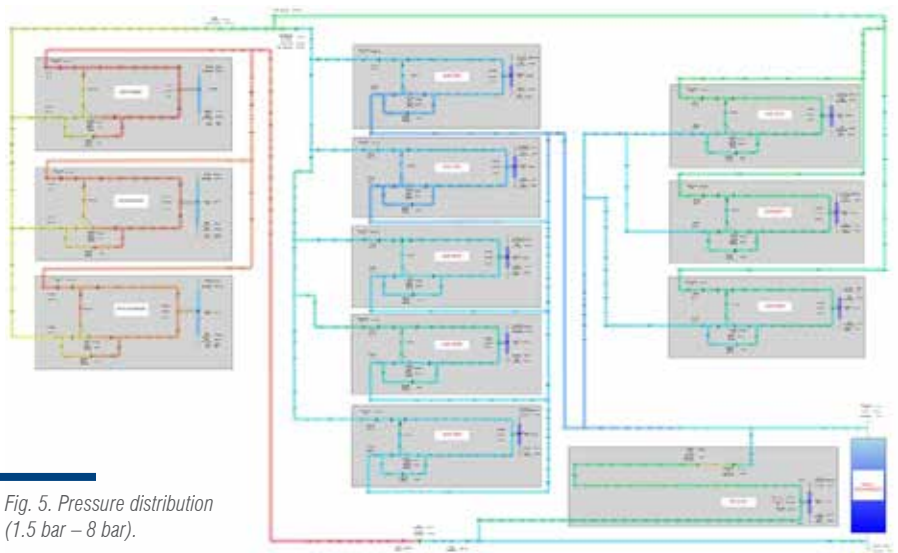


Fig. 5. Pressure distribution (1.5 bar – 8 bar).

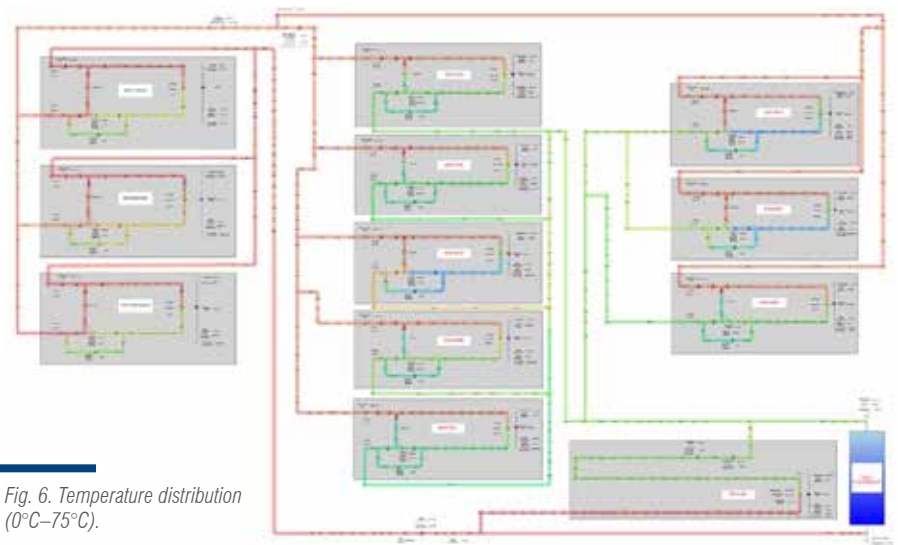


Fig. 6. Temperature distribution (0°C–75°C).

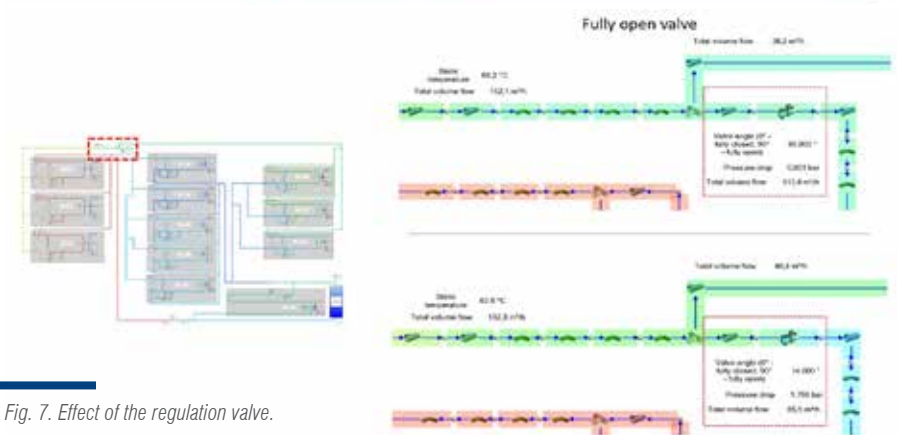


Fig. 7. Effect of the regulation valve.

About SimulHub

SimulHub is a business unit of GeicoTaikisha that plans, executes and analyses engineering simulations using highly professional software with the objective of predicting, preventing and optimising the behaviour of production equipment and products throughout the production process. Thanks to a young and highly experienced team of engineers, SimulHub offers computational fluid dynamics (CFD), discrete event (DES) and one-dimensional (1D) simulations accompanied with a valuable expertise that comes from a very competitive and innovative market such as the automotive industry. SimulHub places the customer at the centre of its existence, making it needs its own, creating tailor-made sustainable solutions.



Digital image correlation (DIC) for vibration analysis

by Floriane Soulas
EikoSim

Digital image correlation (DIC) is well-known for static applications but, under the right circumstances, it is equally applicable to vibration testing: here is an industrial example from Safran.

As part of its development of increasingly high-performance aircraft actuators, Safran Landing Systems (SLS) must ensure the components' integrity during commissioning. The test discussed in this article relates to so-called "actuator vibration" tests (Fig. 1).



Fig. 1. Test setup with the actuator and the cameras positioned above the vibrating pot.

We conducted vibration tests on a hydromechanical actuator using stereo-image correlation monitoring. During these tests we performed real-time monitoring of the actuator's response to the applied load, as recommended by the associated standard. The objective was to use stereo-correlation to quantify the displacements caused by the vibrating pot to ensure the performance of the structure and guarantee passenger safety. We performed vibration tests on the pressurized cylinder on two axes

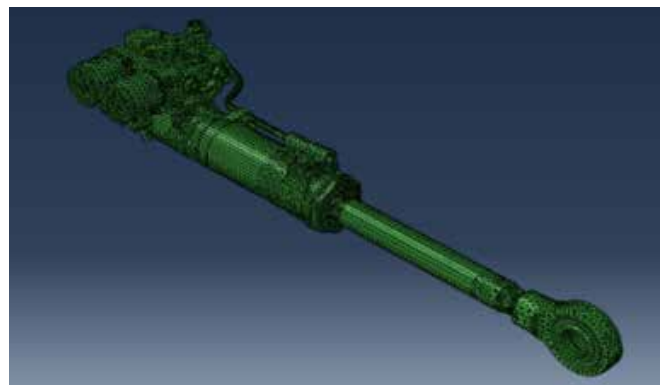


Fig. 2. Finite element mesh of the full cylinder.

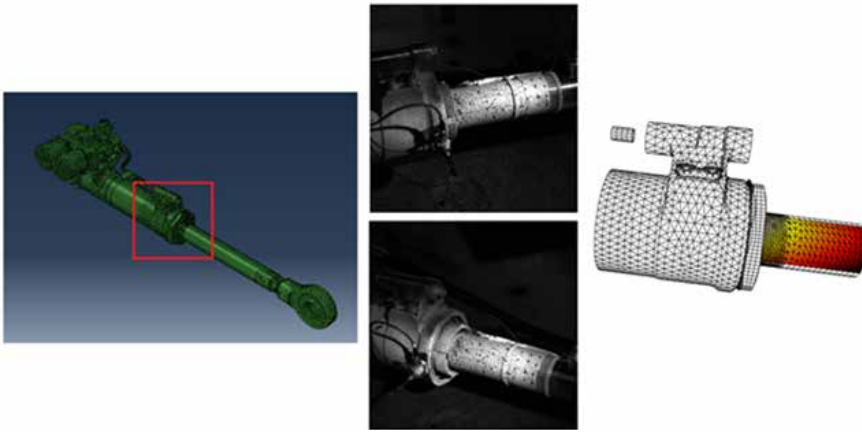


Fig. 3. Mesh reduction according to the field of view of the two cameras.

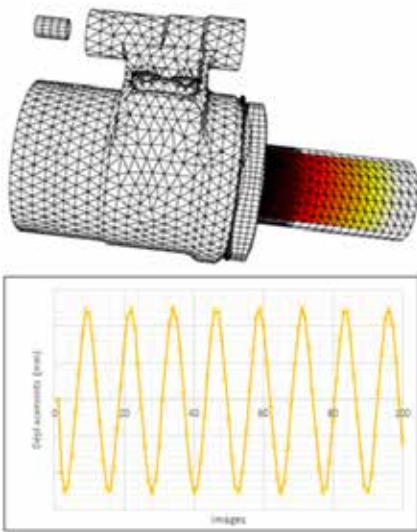


Fig. 4. Measured displacement field projected onto the FE mesh and displacement measured at the point corresponding to the maximum value of the arrow.

(axis 1 and axis 2) and for two resonance modes (frequencies f_1 and f_2) respectively in order to measure the maximum deflection of the structure, and to ensure the validity of the corresponding numerical model. Such tests are costly and the levels recommended by the validation standards are severe and can damage the structures under test when they are brought to failure.

Vibration monitoring by stereo-DIC measurement

As shown in Fig. 1, we positioned a pair of high-speed cameras (1000fps, 2048×2048 pixels) in front of the actuator (Fig. 1). Using EikoTwin DIC, the measurement can now be performed directly on the simulation's finite element (FE) model and compared to the simulation results. Since the FE model of the structure is extremely complex and

refined, we trimmed it down to a lighter version centred on the area of interest. The maximum expected deflection is located on top of the main cylinder (in red in Fig. 2). All displacement measurements were extracted from this point corresponding to the maximum deflection.

Thus, a reduced study area (Fig. 3) was determined and this was the area used for analysis and comparison during the study.

The vibration tests being very long (several tens of minutes) and the high-speed cameras only being able to record a few seconds at a time, we made three recordings for each axis and each clean mode – at the beginning, middle and end of the vibration, respectively.

During the test, we noted that the eigenmode frequencies had slipped and were different from those predicted by the simulation.

This may impact the displacement amplitudes obtained and therefore the test/calculation comparison that should take this parameter into account.

Measurement results

The image processing software projects the measured displacements directly onto the FE model provided by SLS, as shown in Fig. 4. The sinusoidal curve extracted at the point corresponding to the maximum eigenmode deflection (see Fig. 2) is well captured by the image correlation system. The measurement showed that the displacement fields obtained from the DIC during the vibration of the actuator are homogeneous and consistent with the predictions of the numerical model.

Furthermore, by displaying the measurements directly on the FE model, we can retrieve the value of the displacements at a given node for all images. Thus it is possible to retrieve the maximum value of the arrow at the position predicted by the simulation and to check whether the simulation predicted the correct value and position.

The results in measured and simulated displacements at the point of interest (see Fig. 2) are collected in Tables 1 and 2, for axes 1 and 2 respectively. We can see that, at the time of the first image capture (i.e. Start), the displacements obtained are close to those obtained by simulation.

The frequency and amplitude show a decrease during the test (image captured “in the middle”) followed by an increase in amplitude at the end of the vibration cycle, which is found for both axes.

In this test, image correlation did not only show displacement measurements. In fact, the measurements revealed some unexpected behaviour during the

Axis 1 (mm) for f_1	Expected : 4.24mm (for f_1)	
Start ($f = f_1$)	Middle ($f < f_1$)	End ($f < f_1$)
4.00	2.57	3.77

Table 1: Time average of displacements obtained for axis 1 at vibration frequency f_1 , in mm.

Axis 2 (mm) for f_2	Expected : 3.73mm (for f_2)	
Start ($f < f_2$)	Middle ($f < f_2$)	End ($f < f_2$)
3.7	3.0	3.3

Table 2: Time average of displacements obtained for axis 2 at vibration frequency f_2 , in mm.

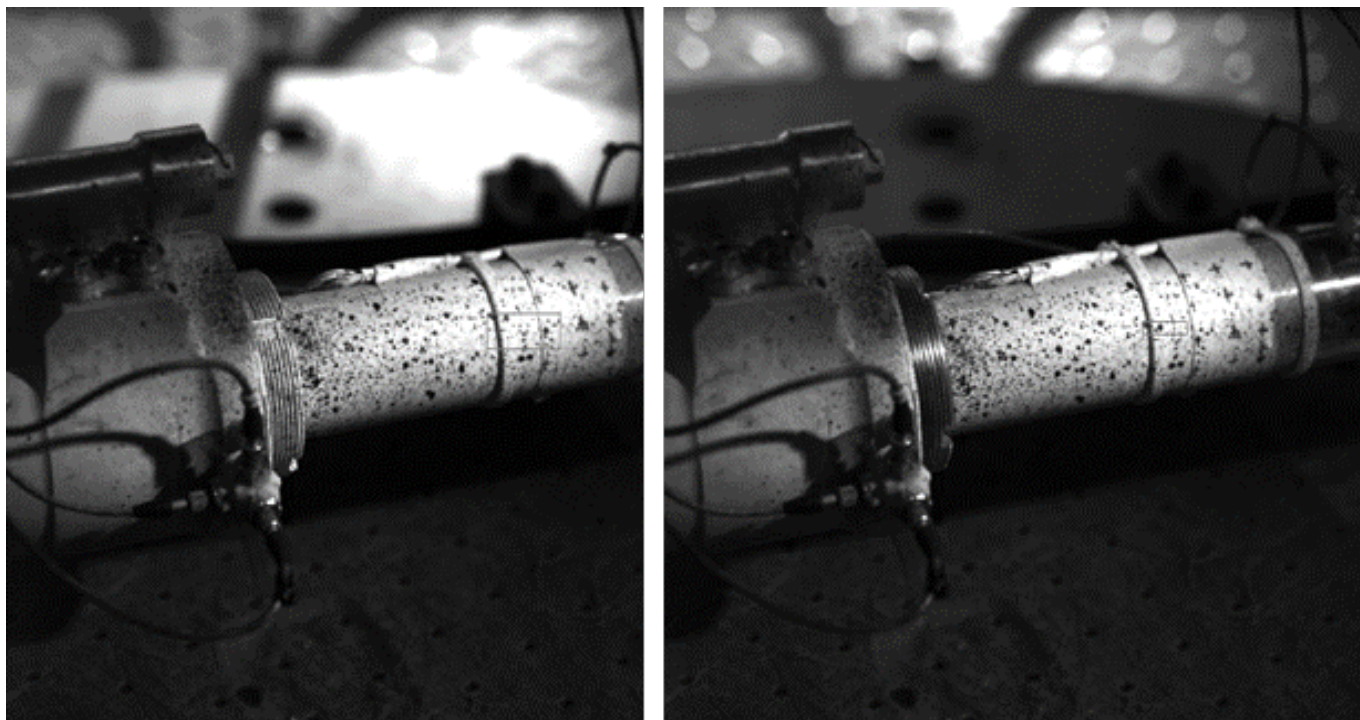


Fig. 5. Illustration of the cylinder's rotation during vibration.

acquisition of the eigenmodes. It showed a rotation of part of the actuator that had not been predicted by the numerical model, as shown in Fig. 5. This behaviour could have several origins but was not visible to the naked eye when the structure was vibrated.

The images captured by the high-speed cameras highlighted this rotation of the structure and thus provided important qualitative information about cylinder's assembly, which could have gone unnoticed even after tests.

Despite the large displacement amplitudes experienced by the structure during its vibration, the high-speed DIC cameras were able to capture the full kinematics of the structure's eigenmodes.

Subsequently, the processing of these images with the EikoTwin-DIC software enabled the measurements to be expressed directly on the FE mesh of the part.

These tests allowed the SLS team to observe not only the displacement but also the overall behaviour of the actuator during loading for the first time. The information collected allowed them to improve their predictive numerical model.

Conclusion

In conclusion, the measurements obtained during the eigenmodes showed the displacement fields to be homogeneous and consistent with the predictions of the numerical simulation.

The test also highlighted some unexpected behaviour. Contrary to what had been predicted by the numerical model, the DIC measurements show that the actuator seems to undergo a rotation of its central cylinder during vibration.

This very fine rotation was captured by the high-speed cameras but could have gone unnoticed, as it was invisible to the naked eye. The evidence of this behaviour provides important information

to test engineers about the assembly of the structure and its behaviour in service.

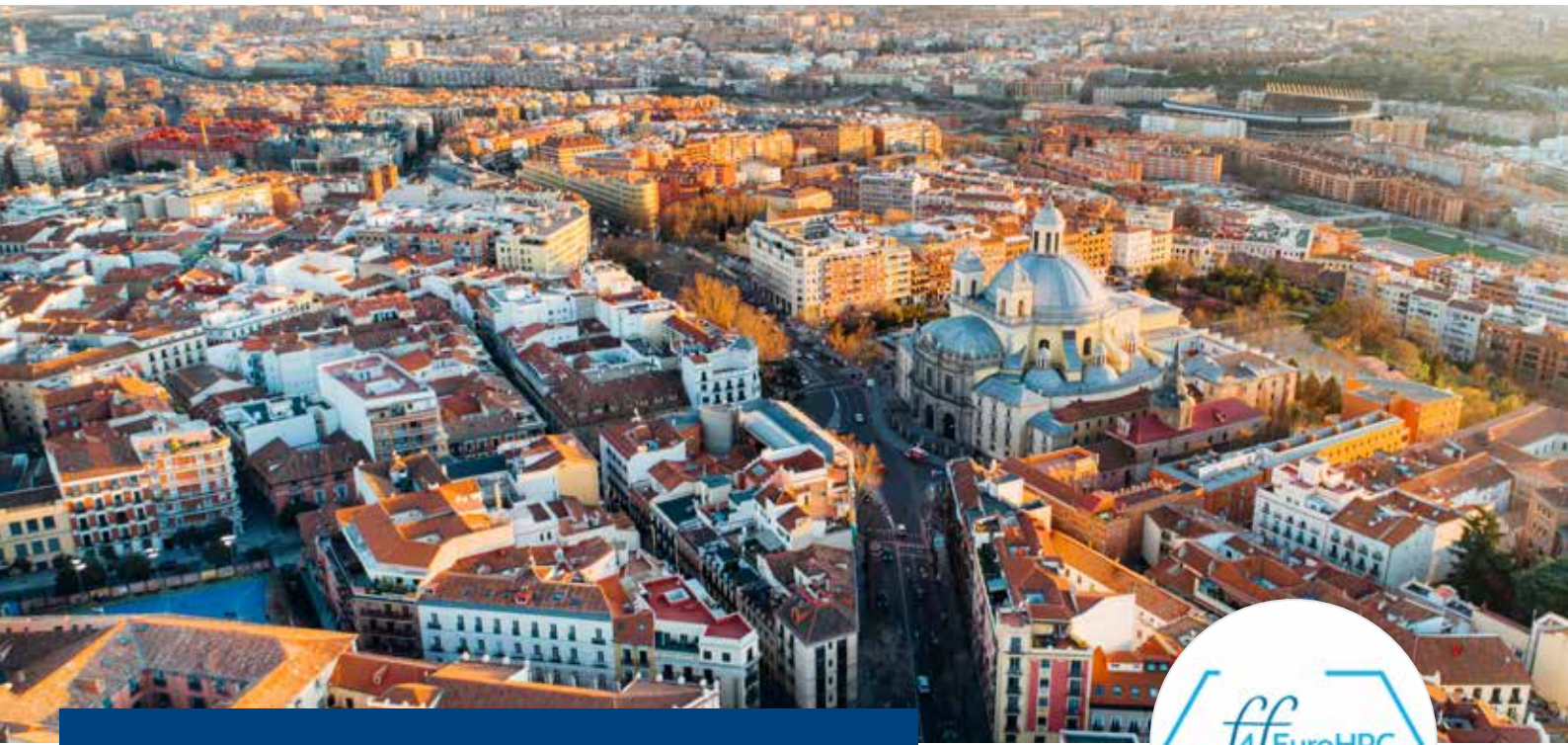
Test data was collected in this area for the first time. These tests are encouraging and provide both qualitative and quantitative results in previously unmeasured areas of study, allowing the company to enhance and optimize its numerical model for future use in validating its hydromechanical actuators.

For more information:

Floriane Soulas - EikoSim
contact@eikosim.com

About EikoSim

EikoSim is a software company that enables users to leverage validated simulation models to support design decisions. The company supports managers of engineers in charge of structural simulations. It assists its customers to explain discrepancies between tests and models so that they can respond more quickly to program requests and reduce delivery times to the end customer. The EikoTwin software solution applies image analysis and simulation model management to improve both simulations and development cycles.



FF4EuroHPC continues inspiring SMEs to unleash their innovation potential with cutting-edge technologies

by Jaime Bustillo¹, Francisco Ramirez-Javeg¹, Samuel Gomez², Joan Calafell², and Oriol Lehmkuhl²

1. Bettair Cities, Travessia Industrial, Barcelona, Spain - 2. Barcelona Supercomputing Centre, Barcelona, Spain

Air pollution is the single largest environmental health risk in Europe and a major cause of premature death and disease. Urban air quality is influenced by complex atmospheric dynamics, urban geometry, land use, and traffic patterns, all leading to very different distributions of pollutants at microscales.

While some air pollution is windborne from outside cities, most urban air quality issues are hyper-local i.e. at street level and within metres of their source. Consequently, any highly accurate air quality mapping needs to use a very dense network of sensors to measure pollution in real-time (which is very expensive) and/or high computational resources to process the data and model the distribution of pollutants with high spatial and temporal resolution.

The challenge: developing air quality models in the most efficient manner. The aim of this experiment was to reduce the computational cost of air quality simulations in urban environments and to give to the company, Bettair Cities, access to affordable and accurate real-time air quality modelling tools.

The use of air quality modelling is not new to the project, and is promoted by the Forum for Air Quality Modelling (FAIRMODE, Joint Research Centre of the European Commission). FAIRMODE is a European network to exchange experience and expertise on the use of air quality modelling

in the context of the European Ambient Air Quality Directives (AAQDs). FAIRMODE currently recommends making modelling mandatory for air quality planning, exposure calculations, and short-term forecasting. More precisely, the recommendations state that “modelling should be strongly encouraged for monitoring network design, exceedance indicator estimates and near real-time mapping, source apportionment and estimates of long-range transport and to define zones and agglomerations” [1]. In this context, Bettair is making a major R&D effort to develop the best possible air quality models in the most efficient way. The most accurate air quality models rely on high-fidelity computational fluid dynamics (CFD) simulations to predict micrometeorology, and largely determine the total computational cost of modelling. These simulations are generally performed using high-performance computing. To understand the scale of the problem, the following estimation was made: on average it takes 45,000 CPU hours to perform a high-resolution simulation of the wind flows over one square kilometre of urban geometry, and 35 minutes of simulation time using the best available CFD algorithms. Thanks to this project, Bettair Cities can now generate a realistic approximation of these flows in just 20s on an NVIDIA T4 GPU. This approximation is good enough for most air quality modelling use cases, and its cost-effective pricing means that it can be made available to all cities and towns in Europe, regardless of their economic capabilities.

Performing WMLES (wall-modelled large eddy simulation) and CFD simulations

As a first step, data on European urban geometries was compiled from different open-source datasets such as OpenStreetMap or Urban Atlas from Copernicus, the EU's Earth observation programme. This information mainly comprises the footprints of different buildings, their heights, and the locations of street segments. This dataset was used to build 3D models of several one-square-kilometre areas of different European capitals. The different areas available were analysed using machine learning tools that helped to select 30 of them as representative of different types of urban geometries.

These urban geometries formed the input for two types of simulations. First, high-fidelity CFD simulations of different micrometeorology scenarios were performed. During the execution of the project, 90 micrometeorology scenarios corresponding to 30 different urban geometries and three different wind directions were simulated. Once the velocity fields were obtained, five different pollutant dispersion scenarios were simulated for each meteorological condition, totalling 450 different configurations.

For the micrometeorology simulations, high-fidelity CFD methodologies were used to ensure the reliability of the final dataset. In particular, WMLES (wall-modelled large eddy simulation) was used for flow modelling, since an adequate resolution of the turbulent scales is crucial in pollutant dispersion mechanisms. For this purpose, the Barcelona Supercomputing Centre's in-house code, Alya, was used. Alya is a Multiphysics code that numerically solves the Navier-Stokes (N-S) equations numerically in space and time, among other physics. The code was previously used to simulate several atmospheric boundary layer tests showing good results [2]. To maximize computational resources, the pollutant transport and LES simulations were decoupled to allow the simulation of different emission scenarios with only a single momentum

Algorithm	Area	Resolution	Average computing requirements
LES	1km ²	1m	45,000 CPU-h
CNN	1km ²	1m	20s NVIDIA T4 GPU

Table 1. Estimated computing requirements of LES (large eddy simulation) v. the proposed method (convolutional neural network - CNN) and estimated price of the two algorithms.

run, which is by far the most expensive. Therefore, the pollutant dispersion problem was treated as a convection-diffusion problem, which requires significantly less computational effort than solving N-S.

The time-averaged velocity obtained in the wall-modelled and hybrid large-eddy micrometeorology simulations were used as the transport field. Since the transport vector is a time-averaged field, the RANS-type turbulent viscosity was also evaluated and introduced into the convection-diffusion problem to properly account for the turbulent transport that is not represented in the averaged solution. The turbulent viscosity field was determined with the RANS k-w turbulence model and evaluated in the time-averaged velocity field.

The result of these simulations were 30 different urban geometries of 1km² in size, and for each geometry:

- Three CFD simulations of wind flow with three different wind directions with respect to the x-axis at 0, 60 and 120 degrees for a total of 90 simulations.
- Five dispersion simulations on each wind flow simulation. Each dispersion simulation corresponds to a different emission pattern during a typical day, for a total of 450 dispersion simulations.

As a final step, deep neural networks were trained on the results of these simulations at different heights, in this example on patches 256m x 256m in size.

Using these AI models, simulations of new urban geometries can now be performed instantaneously with high accuracy and fewer computational

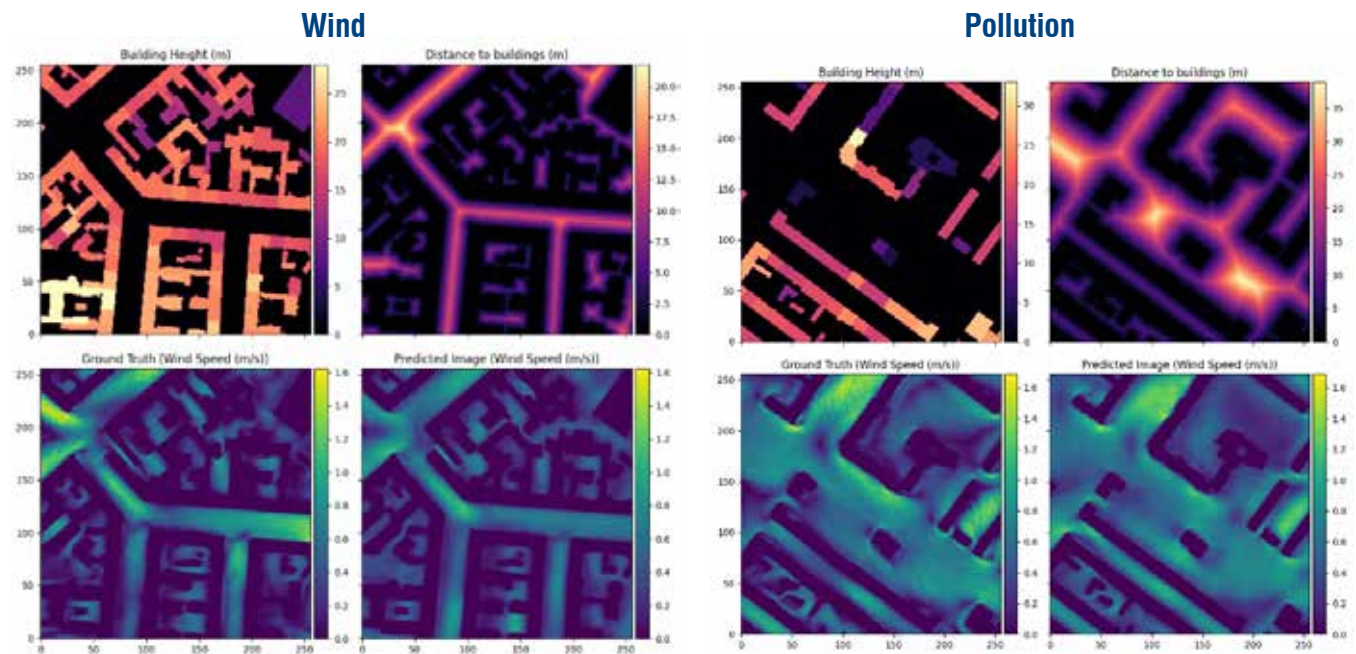


Fig.1. Top: Input to neural network; Top left: Heatmap of building heights; Top right: Heatmap of distance to buildings; Bottom left: Alya simulation results; Bottom right: Emulation results.



Fig. 3. Magnitude of time-averaged wind speed at ground level (1.5m) at Plaza Castilla in Madrid (Kio Towers on the right side of image). West-East mesoscale wind direction.



Fig. 4. Magnitude of time-averaged wind speed at ground level (1.5m) in the Piccadilly Circus area of London. West-East mesoscale wind direction.

resources. These models have been added to Bettair's platform to provide information on air quality and local emissions in real time.

Bettair's new environmental improvement service

Bettair's ultimate goal is to help improve air quality in local communities by providing accurate and actionable information. The company wants to raise awareness and work with stakeholders to create policies and drive initiatives to improve air quality everywhere. As a result of this experiment, Bettair has created a low-cost, energy and computationally efficient AI solution to model air quality in cities with a resolution of up to 1m², in near real-time. This kind of accuracy and resolution is currently beyond the reach of any competitor due to the computational requirements of CFD simulations with scientific software. The cost of the service provided by Bettair is up to 95% lower than competitors' with similar spatial resolution and runs in real-time. Expected revenues this year will be two to three times higher due to the new service and turnover for 2023 will increase by at least a factor of two.

Business Benefits

- Simulation cost is reduced from €1,850 per square kilometre to less than €1 per square kilometre.
- Spatial resolution of real time modelling capabilities is improved from 100m² to 1m².
- Time to setup experiments for new cities is reduced by 80%, from 3 weeks to 4 days.

- Access to new markets: Bettair can offer the service to municipalities and regional governments that cannot afford classical modelling.
- Bettair's turnover for 2023 is expected increase by a factor of at least two.

Thanks to this experiment, Bettair can combine sensor measurements with AI simulations and extract accurate information about local emissions and pollutant concentrations in cities.

This information is then made available on Bettair's platform and allows individuals and communities to take collective action to improve air quality for all. These solutions are already being tested in large cities such as Rome and smaller cities such as El Prat de Llobregat (65,000 inhabitants) in Barcelona.



The FF4EuroHPC project has received funding from the European High-Performance Computing Joint Undertaking (JU) under grant agreement No. 951745. The JU receives support from the European Union's Horizon 2020 research and innovation programme and from Germany, Italy, Slovenia, France, and Spain.

For more information:

Tina Crnigoj Marc, Arctur, FF4EuroHPC Communication lead
ff4eurohpc@hirs.de

References

[1] P. Thunis, S. Janssen, J. Wesseling, A. Piersanti, G. Pirovano, L. Tarrason, F. Martin, S. Lopez-Aparicio, B. Bessagnet, M. Guevara, A. Monteiro, A. Clappier, E. Pisoni, C. Guerreiro, and A. Gonzalez-Ortiz, "Recommendations for the revision of the ambient air quality directives (AAQDs) regarding modelling applications", EUR 31102 EN, Publications Office of the European Union, Luxembourg, 2022, ISBN 978-92-76-53279-8, doi:10.2760/761078, JRC129600.

[2] H. Owen, G. Chrysokentis, M. Avila, D. Mira, G. Houzeaux, R. Borrell, J. C. Cajas and O. Lehmkuhl, "Wall-modeled large-eddy simulation in a finite element framework", International Journal for Numerical Methods in Fluids, n° 92, pp. 20-37, 2020.

The success story presented in this article was developed during the first tranche of FF4EuroHPC Project.

FF4EuroHPC supports the competitiveness of European SMEs by funding business-oriented experiments and promoting the uptake of advanced HPC technologies and services. The experiment is an end-user-relevant case study demonstrating the use of cloud-based HPC (high-performance computing) and its benefits to the value chain (from end-user to HPC-infrastructure provider) for addressing SME business challenges that require the use of HPC and complementary technologies such as HPDA (high performance data analytics) and AI (artificial intelligence). The successful conclusion of the experiment created a success story that can inspire the industrial community.



Multiphysics and multiscale modelling of aeronautical components

by P. Bene¹, R. Dotoli¹, A. Gerardi¹, and A. Russo²

1. CETMA - European Research Centre for Technologies, Brindisi, Italy - 2 MANTA GROUP, Foggia, Italy

The challenge: developing a more effective manufacturing process for aeronautical components

The autoclave moulding process, in which composite layers are placed on a mould according to a lamination sequence and then cured inside an autoclave using vacuum, heat, and pressure, is the main method used in the aerospace industry for manufacturing composites. This process involves both mechanical and chemical phenomena, and a correspondingly large number of variables influence the final result.

Working with innovative materials and geometries leads to an increase in the number of defects and voids in the finished components, which are then rejected. During the curing process, the mechanical stresses in the various materials increase, which can lead to unwanted consequences. For example, during the cooling phase, the different thermal expansion coefficients of the fibre, matrix, and mould materials generate high residual stresses that can lead to defects in the finished composite parts. Given the expense of the autoclave process, it is important to minimize defects in the finished parts.

Currently, a costly trial-and-error approach is used to find the optimal process parameters to produce components with complex shapes, minimizing the risk of voids or geometric distortions. This leads to long development times and high costs.

The MANTA GROUP's goal is a more efficient production process for its products: finding the optimal process parameters by means of multiscale, multiphysics numerical simulations. This significantly reduces the development time and costs required compared to the trial-and-error approach currently used.

Building multiscale numerical models using HPC resources

To optimize the parameters of the autoclave process (e.g. lamination sequence, maximum temperature, curing times, heating times, maximum pressure), it is necessary to simulate the various phenomena that occur during the curing process in order to predict the effects of the parameters on the quality of the components being manufactured.

To this end, two separate multiphysics and multiscale numerical models were set up using HPC resources. In detail, these are 1)



a thermo-mechanical model (on the macro scale) to predict the dimensional variations of the laminates due to residual stresses generated during the autoclave process; and 2) a fluid-structure model (on the micro scale) to simulate the resin flow during the application of pressure. Both numerical models were validated by comparison with experimental test results.

To reduce the computing time, the utilization of HPC resources and the scalability of the simulations were substantially analysed.

Thermo-mechanical model (macroscale)

The aim was to study the dimensional variations of flat and L-shaped profiles due to residual stresses generated during the curing process.

The technological process used to manufacture these profiles was vacuum bagging. To simulate the curing process, a numerical finite element (FE) model was implemented and subsequently validated through experimental tests.

To comprehensively simulate the manufacturing processes of composite materials, various phenomena that occur during the curing process such as thermal flows and curing kinetics were considered because they lead to macroscopic defects.

The curing process was modelled with a thermo-mechanical approach that covers the curing phase and analyses residual stresses. In this phase, heat transfer and curing influence the stresses and, consequently, the deformations of the part. The material is treated as a composite and the temperature and pressure cycles (with their effects on shrinkage and spring-in) are simulated.

Fig. 1 shows the contour plot of the dimensional changes in the flat laminate during the autoclave process. As the temperature rises the composite material's strength and mechanical properties increase as a result of the polymerization of the resin. In addition, the chemical transformation of the resin generates tension stresses due to chemical shrinkage. During the cooling phase, residual stresses increase due to the CTE (coefficient of thermal expansion), and the misalignment of fibres, matrix, and mould materials. Residual stresses cause unwanted dimensional changes during demoulding. The geometric distortions after curing are approximately 0.5mm along the z-axis.

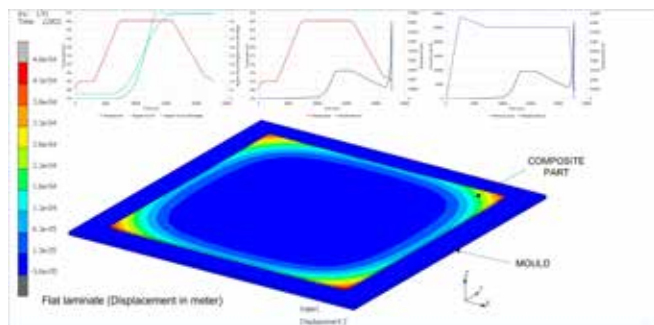


Fig 1. Dimensional changes in a flat laminate due to residual stresses (macroscale).



Fluid-structure model (microscale)

A microscale fluid-structure model was implemented to simulate the effects of pressure. The FE model generated at the microscale enabled simulations to be conducted concerning the effect of resin flow pressure on the defined fibre layup (see Fig.2). The optimum pressure value for the process is close to 0.6MPa (6 bar) and represents an acceptable compromise between tow integrity, void level, compaction of the fabric layers, and the mechanical behaviour of the final composite material.

Analysis of the fluid-structure interaction at the microscale enabled the voids and resin pockets generated during the process and their positions in the RVE (representative volume element) geometry to be studied. In addition, the analysis provided the tow displacement with respect to the initial tissue architecture. By increasing the pressure, the rotation of the tow was acceptable

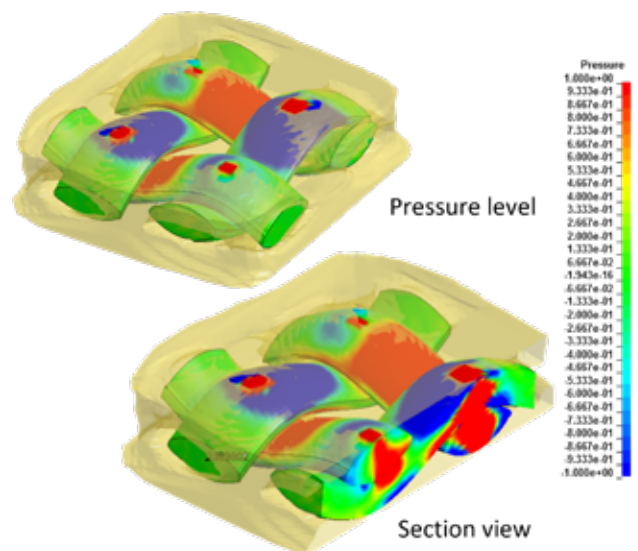


Fig 2. Resin flow through composite layers (microscale) due to pressure loading [percentage].

if the load level did not exceed 6bar. Furthermore, the fabric maintains its orthogonal architecture under greater compaction minimizing the presence of voids.

Using the material properties, lamination sequence, part geometry, and the autoclave cure cycle specification as input parameters, the HPC simulations set up in the first phase proved able to provide the required information on the resulting part distortion and the possible defects in the finished part in a very short time. This HPC-supported simulation workflow now allows the MANTA GROUP to easily find the optimal parameters for the production process in a matter of minutes, thus reducing development time and significantly reducing the number of physical tests required.

Business benefits: reduction of development time and costs and increased competitiveness

- MANTA (end-user) expects to reduce design costs by 50% (saving approximately €100,000 per year), material waste by 70% (saving approximately €60,000 per year), and raw material usage by 15% (saving approximately €150,000 per year).
- CETMA expects the success story to lead to new R&D projects and consultancy services with an increase in turnover of about €50,000 per year.
- CINECA aims to become MANTA's HPC resource provider and estimates the related increase in turnover at €20,000 per year and will leverage the success story to attract new customers estimating a further increase in turnover of the same order.



The success story presented in this article was developed during the first tranche of FF4EuroHPC Project. FF4EuroHPC supports the competitiveness of European SMEs by funding business-oriented experiments and promoting the uptake of advanced HPC technologies and services. The experiment is an end-user-relevant case study demonstrating the use of cloud-based HPC (high-performance computing) and its benefits to the value chain (from end-user to HPC-infrastructure provider) for addressing SME business challenges that require the use of HPC and complementary technologies such as HPDA (high performance data analytics) and AI (artificial intelligence). The successful conclusion of the experiment created a success story that can inspire the industrial community.



Fig 3. Available autoclave used for curing composite parts and prototypes.

HPC-based simulations were used to produce high-quality composite components, reducing development time and costs while increasing competitiveness. As autoclave moulding is likely to remain the main production technology for aerospace structures for at least the next ten years, this significantly strengthens the MANTA GROUP's business position.

Furthermore, the improved know-how of the autoclave process offers MANTA the ability to profitably enter many other sectors besides aerospace (e.g. luxury boats, automotive, sport). This will help the company to attract new customers by offering a complete service from design to component production.



The FF4EuroHPC project has received funding from the European High-Performance Computing Joint Undertaking (JU) under grant agreement No. 951745. The JU receives support from the European Union's Horizon 2020 research and innovation programme and from Germany, Italy, Slovenia, France, and Spain.

For more information:

Tina Crnigoj Marc, Arctur, FF4EuroHPC Communication lead
ff4eurohpc@hirs.de



Decision-support system for smart cities to assess and manage terrorist threats

by Javier González-Villa¹, Arturo Cuesta¹, Gemma Ortiz¹, Marco Spagnolo², Marisa Zanotti², Luke Summers³, Alexander Elms³, Anay Dhaya³, Karel Jedlička⁴, Jan Martolos⁴, Deniz Cetinkaya⁵

1. Universidad de la Cantabria - 2. EnginSoft - 3. Crowd Dynamics - 4. Plan4All - 5. Bournemouth University

Society and terrorism

The dimensions and characteristics of international terrorism are dependent on historical and geographical context, political links, or various factors related to specific terrorist groups and organizations. The social and economic impact it generates means counterterrorist security has become one of the greatest challenges for law enforcement agencies, policy makers, and institutions.

Despite this dependence on differing factors, terrorist attacks are generally intended to cause great harm and create consternation in the population. Urban public spaces are key targets for terrorists because large populations cluster vulnerably in these areas.

The field of urban counterterrorist security for the defence of critical infrastructure and soft targets, more specifically in the context of mass events, has made adequate planning and the preparation of emergency response strategies mandatory. In 2021, the Global Terrorism Database

(GTD) recorded that more than half of the attacks worldwide make use of Improvised Explosive Devices, mass shootings, and arson or incendiary/smoke device attacks. Projecting the evolution of these types of attacks is necessary to develop models to help minimize their consequences.

In addition, 29.4% of the terrorist attacks between 2010 and 2020, were directed against the general population [16] meaning that cities are becoming a significantly important target for terrorists. This paper therefore proposes a decision support system for emergency management that can be used during planning and response to anticipate terrorist threats to help address these issues.

Smart cities as a countermeasure

Smart cities that use current information and communication technologies to increase operational efficiency, share useful information with the population, and improve the security of government services, can be a tool to ensure citizen welfare.

It is mandatory for smart cities to create a safe physical and digital ecosystem for their inhabitants. To this end, it is crucial to fully use all the capabilities already available for enhancing safety and security. These include, for example, anomaly detection, identification and authentication of individuals, threat localization, behavioural profiling, suspect tracking, traffic monitoring, emergency management, and many other capabilities related to awareness, prevention, and response [22].

These capabilities have been studied from different perspectives leading to a wide range of results including the detection of individuals and threats [5], [9]; detection and tracking [2], [8]; recognition-based authentication [4], [7]; or the enhancement of legacy systems deployed by the city by equipping them with intelligence [37], [38].

However, it should be noted that there are hardly any studies [6], [12], proposing the use of a comprehensive decision support system that simultaneously includes emergency management; forecasting the evolution of threats and the impact of the most common terrorist attacks; and real-time decision support. The closest studies in the existing literature focus on the management of common crimes such as vandalism and violence [15], information systems [32], the management of abnormal traffic [17], emergency evacuations [36], and, to a lesser extent, on the prediction of events such as robberies or murders [3], [26]. Consequently, we contend that it is necessary to simultaneously forecast and assess the impact of the most common terrorist attacks, while at the same time managing emergency situations regarding pedestrians and vehicles, evacuations and surveillance, by making use of comprehensive conceptual and computational models to support decision-making.

Theoretical framework for terrorist threat assessment and management

In order to improve terrorist threat assessment and management in smart cities by exploiting smart-city features, we have proposed a theoretical framework based on the initial definition and capabilities of a smart city using a three-layered structure to formalize the proposed model (see Fig. 1).

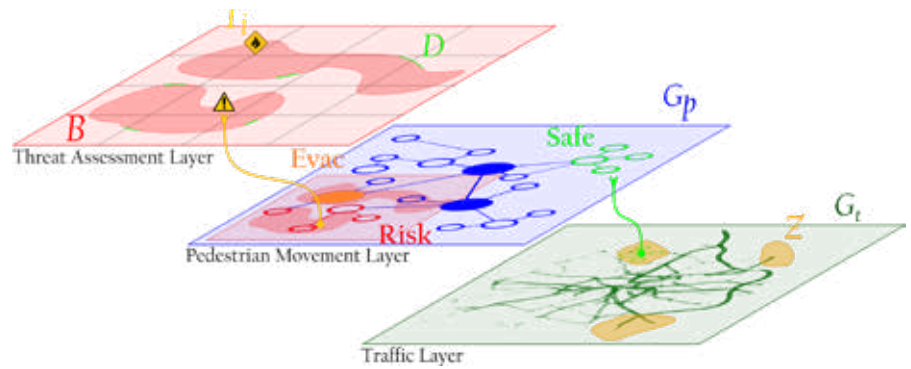


Fig. 1. Layer-based theoretical framework for terrorist threat assessment and management applied to a hypothetical Smart City.

Threat assessment layer

This comprises a set of soft targets such as crowded areas and infrastructure where security monitoring is desirable. (A soft target can be defined as a geographically delimited and bounded area, taking into account its safe zones and obstacles, which is associated with a spatial distribution of people and deployed security devices such as checkpoints, cameras, or patrols. Therefore, the threats monitored in these zones are defined as sets of locations and categories, for example fire, smoke device, explosive device, or firearm.) This layer assesses the threats and potential impacts/consequences of three types of attacks by generating results summarized as a set of geographic locations linked to counter-terrorism security information that allows lower layers to increase their level of intelligence to enable more accurate modelling results.

1. Arson and smoke bomb: A fire dynamics simulator [24] is used for the most likely locations of these types of attacks by simulating various scenarios in which the actual combustion parameters (different loads of wind and fire) are changed. The results generated provide artificial measurements such as visibility and fractional effective dose that are then classified and stored in a structured way for later use.
2. Improvised explosive device (IED): based on a threat probability approach [10] this layer divides the geographic area of the simulated scenario into small regions that conform to a fine grid of square cells. A risk function is calculated for each cell within the grid based on factors such as distance to exits, population density and distribution, or distances to deployed resources. After

processing all cells, a matrix of risk values is obtained and combined with the threat level, resulting in a probability map with critical locations for each soft target.

3. Mass shooting attack (MSA): An agent-based model that discretizes the scenario being studied by means of uniformly distributed reference points. These are subsequently displayed as nodes on a direct reachability graph for the purposes of calculating the agent's trajectory. The optimal trajectory from each initial location is calculated using a backtracking approach with the associated cost function based on three key factors: 1) the proximity of a node to an exit/security zone; 2) the spatial availability of that node; and 3) the risk associated with the attacker's location. After these routes have been calculated, the movement and behaviour of the people involved in the scenario are represented using a microsimulation approach that considers the interactions of agents and the repulsive forces between terrorists, people, and the scenario boundaries and obstacles through a social force model [18]. To represent people who are shot, we follow an approach based on the physical dynamics of gunfire [1], in which the probability of being shot is estimated and the number of victims is calculated using a stochastic approach.

Pedestrian movement layer

The topological definition of traversable pedestrian zones is replicated in the form of a graph in which each node is defined by its geographic location and occupant density, as



well as by its current status (passable, impassable, evacuated, safe). Similarly, each boundary represents passable zones and is defined by its people density, origin and destination nodes, and available flow. Using the threat assessment layer results as input for the pedestrian movement layer, the status of each node in the network can be updated, indicating safe nodes; affected impassable nodes; and assigning nodes to be evacuated. In addition, the occupancy densities of the different nodes and boundaries of the network are updated using one of the following approaches, depending on the capabilities of the smart city: 1) estimates based on the history of predicted occupancy; 2) real-time monitoring of occupancy via cameras, Wi-Fi tracking devices, access controls or similar; and 3) random assumptions of occupancy based on predicted distributions.

This graph is used as a reference graph to perform an initial calculation of minimum paths using Dijkstra's algorithm. Its subsequent optimization is performed by considering node availability and using a weighted multiple criteria decision analysis (MCDA) to evaluate conflicting nodes. The MCDA considers the weights associated with the different criteria by defining a function that produces an unweighted, normalized relevant score for each criterion and inverts it to maximize it where necessary. The weights are calibrated for each network using defined scenarios to ensure that the ranking of results is logical, and to improve the efficiency of the optimization model. The criteria considered are: congestion and additional distance cost incurred by re-routing different nodes; and congestion and available flow at surrounding nodes. Then, following an iterative process, we generate a set of candidate networks that resolve these conflicts and apply another MCDA scoring function among them in the same way to choose the optimal network. In this case the criteria considered are the estimated total evacuation time and the sum of the node congestion in the candidate network.

Once the optimal graph is found it becomes the active graph and can be iteratively optimized as model inputs change. This model provides evacuation routes, estimated departure times, and mobility profiles and forecasts the number of people who will go to specific locations in a specific time period by determining and modelling the initial impact on the traffic network.

- **Traffic layer:** This layer provides a real-time traffic forecast on the different sections of road by date and time following a network calibration based either on historical traffic data or data obtained from traffic monitoring sensors installed in the smart city. Similarly, to the pedestrian layer, the traffic network is also represented by a graph in which the vertices represent vehicular traffic landmarks associated with physical locations and the axes represent the reachability associations similar to the pedestrian layer but with density and flow measurements for vehicles instead of people. To generate traffic profiles, this layer considers the different habitual areas of trip origin and destination, which in turn are related by proximity to a node of the traffic network, generating a set of routes and a weighted origin-destination matrix. The calibration process starts from the non-calibrated network represented by the graph that solves the shortest routes considering the availability constraints of the sections of road

and updates the origin-destination matrix using route-based algorithms [19] and bush-based B [13]. Thereafter, following an iterative process to adapt the origin-destination matrix based on the gradient approach [31] with some adjustments for large traffic models [21], the model optimizes the set of trajectories and the origin-destination matrix based on real traffic data, paying attention to discrepancies between the model and reality. The applied methodologies can, therefore, be summarized in two models for specific purposes.

- **Trip distribution model:** the classical gravity model is used for the trip distribution model. The distribution model estimates the number of trips between two zones by considering the number of trips originating from the source zone to the destination zone and the equilibrium coefficients that are determined by the iterative proportional adjustment procedure. The most important part of this distribution process lies in the deterrence function that considers the cost (travel time) between the zones. The forms of the deterrence function are described in [28].
- **The traffic assignment model** is used to address the traffic assignment problem (TAP). The definition of TAP is based on Wardrop's first principle. This principle states that for all paths used from the source node to the destination node the travel time must be equal, and this travel time must be minimal [35]. All pairs must fulfil this condition. Mathematically, TAP can be defined as a variational inequality (VI) per [30] and [11] where the set of feasible flows associated with the origin-destination matrix is considered. To solve this problem, Jayakrishnan's trajectory-based algorithm [19] is combined with Dial's bush-based algorithm B [13] with certain improvements by Nie [25] and the fully parallelized implementation of algorithm B [29]. Algorithm B decomposes the problem into bushes. A bush is the acyclic subgraph of the main graph relating to the source area. A bush contains only the flow from the source zone to all other target zones. Each bush is balanced by shifting the flow from the minimum path to the maximum path. The minimum and maximum paths are topologically ordered in the acyclic bushing. In terms of the source-destination matrix calibration algorithm, the Spiess method [31] is implemented with some adjustments. This method uses the steepest descent with a long step to minimize the object function. Some adjustments are described in [21].

From theory to practice

To test this theoretical framework, a decision support system was implemented according to the architecture presented in Fig. 2 to help security managers in the planning and response phases by taking advantage of some of the resources and devices already installed in smart cities. Examples of these resources and devices include cameras, Wi-Fi monitoring devices, access control sensors, and so on. These devices can help estimate the number of people in specific locations while, for example, traffic monitoring systems make real-time simulation of abnormal traffic flows more reliable.

The architecture follows a producer-consumer approach using a centralized platform of distributed data flows (Apache Kafka)

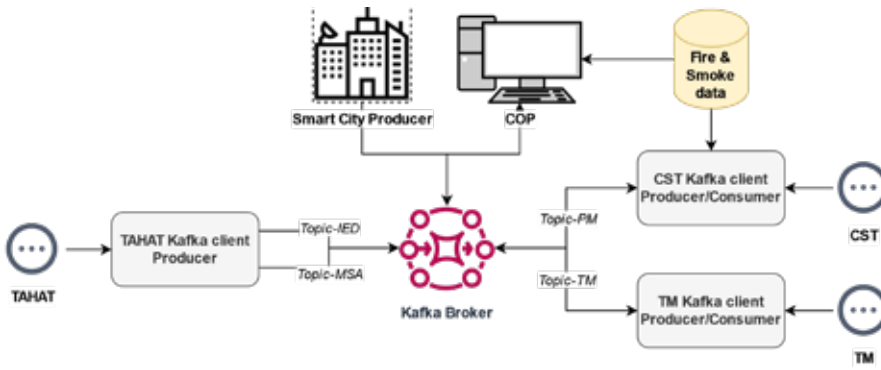


Fig. 2. Overview diagram of architecture. Terrorist attack hazard analysis toolkit (TAHAT), crowd simulation toolkit (CST) and traffic modeller (TM) modules.

Fig. 3. Diagram of the Doosan Arena drill case study. 1) Doosan Arena stadium (green); 2) Boundary of drill area (yellow); 3) Car parks near drill area (blue); and Drill location (red).

to exchange information between layers. In turn, each layer is implemented as an independent module with a graphical user interface (GUI) for configuration and an application programming interface (API) that provides an on-demand service to the rest of the layers, except for fire and smoke simulations that have to be pre-simulated due to the computational cost and then stored locally for later use in specific scenarios, if necessary. Various development technologies were used to implement the individual modules, the main ones being:

- Microsoft .NET Framework 4.6.1: calculation of the terrorist attack simulation and scenario management using the Mapsui, BruTile and SkiaSharp libraries.
- Fire dynamics simulator: ad-hoc modelling of critical soft targets and fire-risk infrastructure.
- Unity: creation of the pedestrian evacuation network with respect to real landmarks, providing geospatial references.

- HSLayer framework: implementation of traffic layer elements including geographical information systems (GIS) functionalities.
- Apache Kafka: information exchange between modules.

Once a usable implementation became available, the system had to be validated by means of a case study. The case study was designed using data provided by Správa Informačních Technologii Města Plzně, p.o., a partner in the S4AllCities project.

It was tested in a terrorist attack drill that took place in the Doosan Arena stadium in the city of Pilsen in the Czech Republic and was organized and conducted by the Czech police (see Figs. 3 and 4). A detailed description of the stadium and its surroundings, along with the city of Pilsen itself and the chronology of the drill were provided, including information such as:

- A 3D model of the Doosan Arena obtained by Lidar and RGB scanning using DJI Zenmuse L1 and DJI Zenmuse P1 cameras.
- Initial locations and specifications of a possible smoke bomb (Antari Z 3000 II fog machine).
- One year of traffic data providing a dataset of 250 million observations from 627 sensors embedded in the road, with a 90-second time granularity traffic model calibrated from traffic data [20].
- A 2D map of the areas surrounding the stadium with the expected attendance (11,700 spectators + 3,300 people), transit locations, typically deployed security resources, car parks, and other minor details.

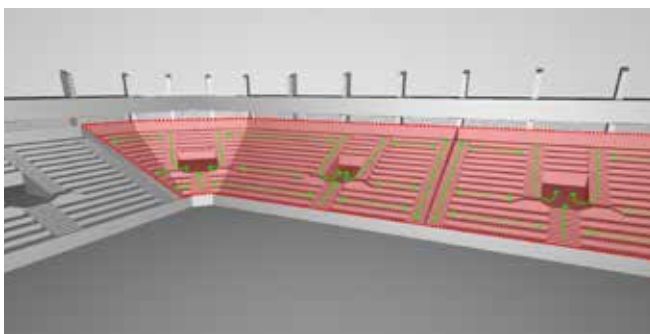


Fig. 4. 3D model of the stadium interiors showing the drill area, with drill boundaries and available evacuation routes.

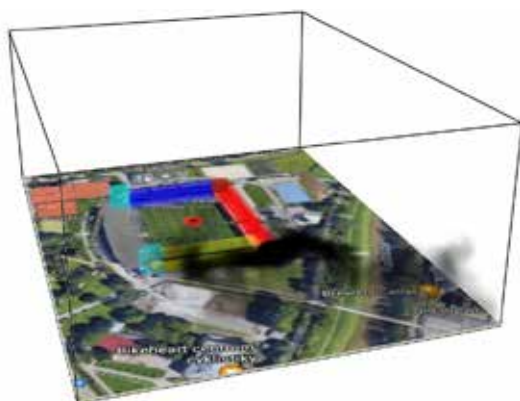


Fig. 5. Smoke propagation in the GUI of the fire dynamics simulator (FDS) simulation.

Regarding the structure of the drill, several exercises were conducted combining explosive devices with firearms (pistol and rifle) and a variable number of shooters (1-2). Each iteration was organized in three rounds: 1) placement in the grandstands of volunteers acting as victims (600 people); 2) initiation of the mock attack; and 3) police intervention and evacuation. In this last phase the system was activated to provide information to first responders on the potential number of victims and dangerous areas and, in the case of an incendiary or explosive device, the spread and impact of the resulting fire. The current status of the evacuation process and anticipated developments are also provided, together with the projected abnormal traffic flows and their impact on the city's traffic network.

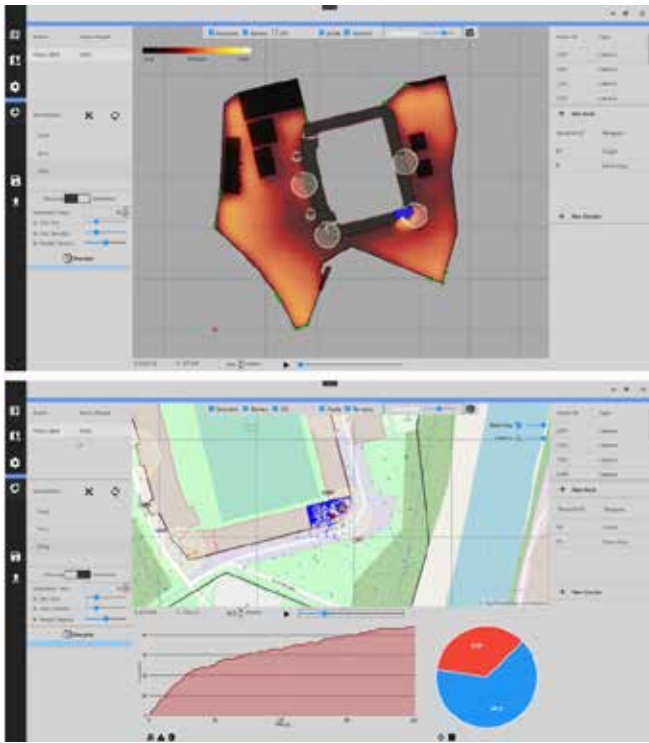


Fig. 6. Simulation results presented via GUIs for threat assessment and impact analysis of IEDs and MSAs.



Fig. 7. Pedestrian evacuation management GUI showing agents leaving the stadium and heading towards car parks across the city.

It should be noted that the scope of the simulations is not limited only to the simulation area presented in Fig. 5. Instead almost the entire city centre is included in the evacuation and traffic simulations, as can be seen in Fig. 7. and Fig. 10.

The results of the on-site implementation and the real-time operation of the system are provided sequentially according to the details and structure of the drill and following the logical course of the emergency event.

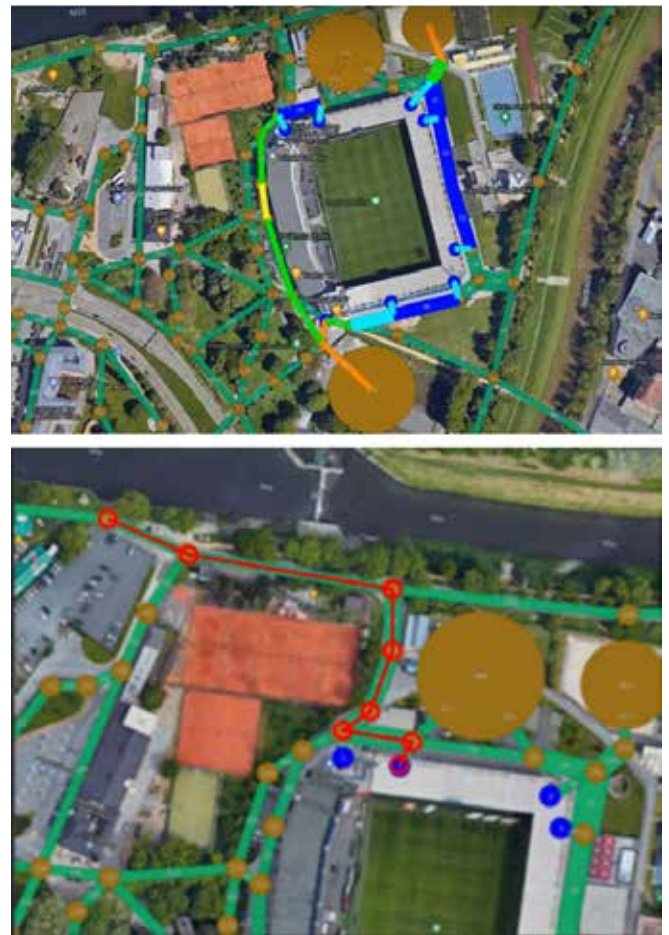


Fig. 8. Crowd density levels on routes surrounding the stadium (top) and the first responders route (red line) towards stadium (bottom).

As mentioned previously, the case of the "smoke bomb" explosive device combined with a mass shooting attack was simulated using a sound effect and smoke machine located below the grandstands for the bomb, together with two volunteers acting as shooters who were located at the top of the grandstands. For this case, the system provided various types of results, starting with the retrieval of the output of the FDS analysis of the smoke propagation (virtual smoke machine set on the Antari Z 3000 II fog machine, wind direction NW); followed by the simulation of the impact of the threat and the attack where the system operator is shown both the evolution of the different incidents and the data associated with the artificial scenario measurements (probability of IED, fractional effective dose (FED), visibility, and casualties). As can be seen in Figs. 5 and 6, the results present the visible spread of the smoke and the potential IED firing positions by means of a probability heat map. These results also reveal that, in the real event of such an attack a total number of 44 casualties could be assumed in a worst-case scenario, considering an attack perpetrated by two shooters and assuming it takes two minutes for the intervention forces to reach the emergency site.

After this initial phase of the attack, the evacuation phase would begin sequentially and automatically due to the panic created. For this case, using the complete model from the stadium to the car parks to simulate the evacuation of the stadium and surrounding areas to the car parks would normally take 58 minutes of simulation time, but the proposed



Fig. 9. GIS data representing the traffic network, car parks, and drill area to be unified with pedestrian evacuation.

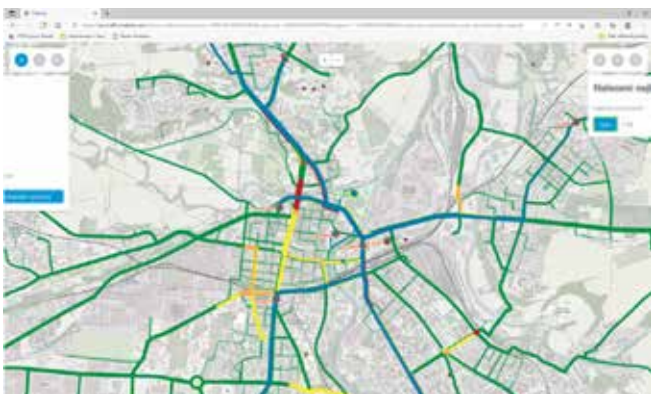


Fig. 10. Traffic network status simulation GUI showing abnormal traffic.

solution completed it in only a few seconds of real time. The simulation was followed by an evacuation of 600 volunteers who followed the routes suggested by the model; they were able to evacuate the stadium grandstand in eight minutes.

The crowd simulation component was used in several ways during the Pilsen scenario. A small-scale simulation of 600 agents was conducted to represent the same conditions as the simulation undertaken in the field, in which the 600 volunteers were able to follow the routes to exit the stadium grandstands sent by the component. An evacuation of the entire stadium was also simulated to demonstrate the component's ability to simulate large-scale models. In both scenarios, the density of evacuating crowds was calculated with the Fruin level-of-service scale, which calculates the density of crowds as they leave the stadium and disperse across the city by assigning a colour scale based on the concentration of people per square meter per minute. The component integrates with the traffic modelling component by considering the results of the traffic model and the expected waits at intersections and road junctions, and then provides input to the traffic model regarding arrival patterns at the car parks surrounding the stadium.

Thereafter, the intervention phase would be initiated by the arrival on the scene of the intervention methods during which the evacuation model provides the principal safe-access routes to the incident site, considering the progression of the threats. The systems allow both

incidents and the evolving crowd situation, including the concentrations of people evacuating the stadium, to be defined or modified manually (see Fig. 8). In all cases, the component is able to simulate faster than real time and provide safe and optimized routes in a very short time. The component runs continuously in the background, allowing the system operator to request the most up-to-date evacuation or first aid routes as they are needed, and allowing these to be disseminated to those on the ground for the most effective response to an incident.

The last simulation given by the system according to the logical evolution of the event would be the emergency's impact on the traffic network of the city of Pilsen (see Fig. 9). Based on the pedestrian evacuation data of the large-scale scenario that considered the full stadium, the impact of abnormal vehicle traffic flows on the city's traffic network was simulated. The number of spectators and the time of their arrival at their respective vehicles were taken from the results of the previous simulation (the spectators' evacuation from the stadium). Vehicles were directed by the traffic model to specific streets in Pilsen, and this traffic was added to the normal traffic. Congested intersections that could be controlled by the crisis scenarios were identified. Concurrently, the fastest routes for the vehicles of the integrated rescue system were identified. These pedestrian evacuation profiles would increase the traffic in the first hour by approximately 700 vehicles in the northern traffic section and 900 vehicles in the southern section, creating a high density of vehicles in both directions, as shown in Fig. 10.

How we got here and what lies ahead

Emerging technologies being used in smart cities, together with innovative computer simulation tools and methodologies being applied to threat analysis and citizen security represent a breakthrough in the fight against terrorism. This paper described the design of a methodological framework with three layers (threat, pedestrians, and traffic) and the implementation of a decision support system to enable private operators, law enforcement agencies, and local authorities to effectively protect soft targets in a smart city. This system provides support for both threat assessment and emergency management of pedestrian evacuation emergencies and their impact on the metropolitan traffic network. This paper also presented a case study based on data from a simulation exercise in the city of Pilsen in the Czech Republic, where the system was installed and the correct functioning of the different layers of the system was evaluated in situ during the simulation exercise. This case study better illustrated the advantages and features of the implemented system, including its analysis of the main terrorist threats; the comprehensive management of evacuations; and monitoring for decision making regarding the state of the traffic network.

The limitations of the proposed system can be resolved in subsequent developments. For one thing the system does not cover all types of dangers within a city and scenarios should be defined in advance so that data for calibration and modelling purposes can be obtained. More specifically, current reports [14] suggest that future trends in terrorism will evolve towards low cost attacks (knife attacks or ramming with vehicles), or combined attacks (cascading attacks or sabotage of critical infrastructure). On the other hand one of the benefits of this



theoretical framework is that it can be applied to other fields. For instance, the possible direct interaction of terrorist threats with the traffic network can be explored, which could lead to the development of riot control measures during urban planning, among many other fields of application. In our view, these limitations are not obstacles but open up future lines of research that will lead to the development of ever more comprehensive safety and security systems.

Aknowledgment

S4Allcities project has received funding from the European Union's H2020 research and innovation programme under grant agreement No. 883522

For more information:

Javier Gonzalez Villa

Universidad de Cantabria

javier.gonzalezvilla@unican.es

References

- [1] O. Abreu, A. Cuesta, A. Balboa, and D. Alvear, "On the use of stochastic simulations to explore the impact of human parameters on mass public shooting attacks". *Safety Science*, 120, pp. 941–949, 2019
- [2] V. Anees, and G. Kumar, "Direction estimation of crowd flow in surveillance videos", presented at IEEE Region 10 Symposium (TENSYP), 2017, pp. 1–5.
- [3] A. Araujo, N. Cacho, A. Thome, A. Medeiros, and J. Borges, "A predictive policing application to support patrol planning in smart cities", presented at the International smart cities conference (ISC2), 2017, pp. 1–6.
- [4] P. B. Balla and K. Jadhao, "IoT based facial recognition security system", presented at the international conference on smart city and emerging technology (ICSCET), 2018, pp. 1–4.
- [5] P. Bellini, D. Cenni, P. Nesi and I. Paoli, "Wi-Fi based city users' behaviour analysis for smart city", *Journal of Visual Languages & Computing*, 42, pp. 31–45, 2017.
- [6] A. Bonatsos, L. Middleton, P. Melas, and Z. Sabeur, "Crime open data aggregation and management for the design of safer spaces in urban environments", presented at the International Symposium on Environmental Software Systems, 2013, pp. 311–320.
- [7] A. Boukerche, A. Siddiqui, and A. Mammeri, "Automated vehicle detection and classification: Models, methods, and techniques", *ACM Computing Surveys (CSUR)*, 50(5), pp. 1–39, 2017.
- [8] M. R. Brust, G. Danoy, P. Bouvry, D. Gashi, H. Pathak, and M. P. Gonçalves, "Defending against intrusion of malicious uavs with networked uav defense swarms", presented at the IEEE 42nd conference on local computer networks workshops (LCN workshops), 2017, pp. 103–111.
- [9] S. Chackravathy, S. Schmitt, and L. Yang, "Intelligent crime anomaly detection in smart cities using deep learning", presented at the IEEE 4th International Conference on Collaboration and Internet Computing (CIC), 2018, pp. 399–404.
- [10] A. Cuesta, O. Abreu, A. Balboa, and D. Alvear, "A new approach to protect soft-targets from terrorist attacks", *Safety Science*, 120, pp. 877–885, 2019.
- [11] S. Dafermos, "Traffic equilibrium and variational inequalities", *Transportation Science*, 14(1), pp. 42–54, 1980.
- [12] M. Dbouk, H. Mcheick, and I. Sbeity, "CityPro: an integrated city-protection collaborative platform", *Procedia Computer Science*, 37, pp 72–79, 2014.
- [13] R. B. Dial, "A path-based user-equilibrium traffic assignment algorithm that obviates path storage and enumeration", *Transportation Research Part B: Methodological*, 40(10), pp. 917–936, 2006.
- [14] EUROPOL, "European Union Terrorism Situation and Trend Report" EUROPOL, 2021.
- [15] J. Fernández, L. Calavia, C. Baladrón, J. M. Aguiar, B. Carro, A. Sánchez-Esguevillas, ... and Z. Smilansky, "An intelligent surveillance platform for large metropolitan areas with dense sensor deployment," *Sensors*, 13(6), pp. 7414–7442, 2013.
- [16] GTD (Global Terrorism Database). (2021). Accessed at www.start.umd.edu/gtd/
- [17] D. Hartama, H. Mawengkang, M. Zarlis, R. Sembiring, M. Furqan, D. Abdullah, and R. Rahim, "A research framework of disaster traffic management to Smart City", presented at Second International Conference on Informatics and Computing (ICIC), 2017, pp. 1–5.
- [18] D. Helbing and P. Molnár, "Social force model for pedestrian dynamics", *Physical Review E*, 51(5), pp. 4282, 1995.
- [19] R. Jayakrishnan, W. T. Tsai, J. N. Prashker and S. Rajadhyaksha, "A faster path-based algorithm for traffic assignment", trid.trb.org/view/388970, 1994.
- [20] K. Jedlicka, D. Beran, J. Martolos, F. Kolovský, M. Kepka, T. Mildorf, and J. Šháněl, "Traffic modelling for the smart city of Pilsen," 2020.
- [21] F. Kolovský, J. Ježek and I. Kolingerová, "The Origin-Destination matrix estimation for large transportation models in an uncongested network", presented at the International Conference on Mathematical Applications, 2018, pp. 17–22.
- [22] J. Laufs, H. Borrión, and B. Bradford, "Security and the smart city: A systematic review", *Sustainable cities and society*, 55, pp. 102023, 2020.
- [23] R.H. Martin, "Soft targets are easy terror targets: increased frequency of attacks, practical preparation, and prevention", *Forensic Research & Criminology International Journal*, 3(2), pp. 1–7, 2016.
- [24] K. McGrattan, S. Hostikka, R. McDermott, J. Floyd, M. Vanella, C. Weinschenk and K. Overholt, "Fire Dynamics Simulator User's Guide", National Institute of Standards and Technology, 2017.
- [25] Y. Nie, "A class of bush-based algorithms for the traffic assignment problem", *Transportation Research Part B: Methodological*, 44(1), pp. 73–89, 2010.
- [26] M. Noor, W. Nawawi, and A. Ghazali, "Supporting decision making in situational crime prevention using fuzzy association rule", presented at International Conference on Computer, Control, Informatics and Its Applications (IC3INA), 2013, pp. 225–229.
- [27] J. Ortúzar, and L. G. Willumsen, *Modelling transport*, John Wiley & Sons, 2011.
- [28] T. Potužák, and F. Kolovský, "Parallelization of the B Static Traffic Assignment Algorithm", *Ain Shams Engineering Journal*, 13(2), pp. 101576, 2022.
- [29] M. J. Smith, "The existence, uniqueness and stability of traffic equilibria", *Transportation Research Part B: Methodological*, 13(4), pp. 295–304, 1979.
- [30] H. Spiess, "A gradient approach for the OD matrix adjustment problem", *A*, 1, 1990.
- [31] Y. V. Truntsevsky, I. Lukiny, A. Sumachev and A. Kopytova, "A smart city is a safe city: the current status of street crime and its victim prevention using a digital application", presented at MATEC Web of Conferences, 2018, 170, pp. 01067.
- [32] J. S. Tuman, *Communicating terror: The rhetorical dimensions of terrorism*, Sage Publications, 2009.
- [33] E. Turban, *Decision support and expert systems: Management support systems*, Prentice-Hall, Inc., 1995
- [34] J. Wardrop, "Road paper. some theoretical aspects of road traffic research", *Proceedings of the Institution of Civil Engineers*, 1(3), 1952, pp. 325–362.
- [35] W. Zhang, V. Terrier, X. Fei, A. Markov, S. Duncan, M. Balchanos, ... and E. Whitaker, "Agent-based modeling of a stadium evacuation in a smart city", presented at Winter Simulation Conference (WSC), 2018, pp. 2803–2814.
- [36] W. Zhou, D. Saha and S. Rangarajan, "A system architecture to aggregate video surveillance data in Smart Cities", presented at IEEE Global Communications Conference (GLOBECOM), 2015, pp. 1–7.
- [37] A. Zingoni, M. Diani and G. Corsini, "A flexible algorithm for detecting challenging moving objects in real-time within IR video sequences", *Remote Sensing*, 9(11), pp. 1128, 2017.



Multiscale.Sim

Identifying unknown material properties using reverse engineering by combining materials databases and artificial intelligence

by Koji Yamamoto
CYBERNET SYSTEMS

Material constants are one of the most important factors for determining the accuracy of analysis results and are essential for designers to make confident material decisions. For materials with non-uniform microstructures, such as fibre-reinforced composites, failure is initiated by many factors. Typical examples are delamination between layers, fibres, and matrices; fibre breakage; and crack initiation and propagation within the resin. Unfortunately, it is usually very difficult to measure these properties directly by physical testing because the fractures often occur at the microscale level. Delamination strength can be measured by double cantilever beam testing or end-notch bending beam testing. This is the largest scale problem and is easy to characterize directly by experiment.

But what about failure modes between the fibre and the matrix? One way to resolve this is through pull-out testing. This involves using a robotic arm to pull out a single fibre embedded in a droplet of resin. However, there are two problems with this test: one is that tangential stresses dominate at material interfaces and so the normal strength cannot be measured;

the other problem is that the resin used in the experiment has a different moulding history to the actual FRP (fibre-reinforced plastic). There is no guarantee that the interfacial strength obtained in the tests can be directly applied to FRP problems.

To accurately determine the information about the internal microstructure, it is important to use the actual FRP as the test specimen. Therefore, in this paper, in order to establish a highly accurate method of predicting the static strength of FRP, we first studied the factors that strongly influence the strength through sensitivity analysis. In addition, we present an example of the inverse identification of those factors (i.e. material constants) by reverse engineering methods that combine big data and artificial intelligence (AI). Both analyses require the preparation of large amounts of data on material behaviour under various test conditions. This data was obtained by virtual material testing using Multiscale.Sim, add-on tool for Ansys software [1]. Note that the examples presented in this article are synopses of articles co-authored with collaborators. See references [2] and [3] for the detailed analytical methods and a description of the results.

Sensitivity assessment of the strength of composite materials

There are many factors that affect the strength of composite materials, but the degree of influence varies from factor to factor. Prior to the inverse identification analysis, the sensitivity of each factor to strength is evaluated by virtual materials testing. A surrogate model with a response surface was constructed from the analysis results for various sample conditions. Monte Carlo

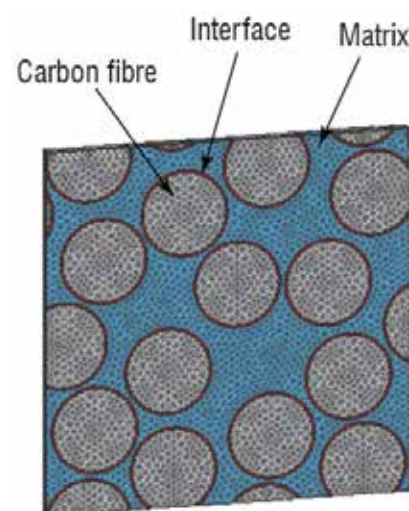


Fig. 1. FE (finite element) model of RVE (representative volume element) with random fibre distributions.

Variation factors	Shape	Mean	Standard deviation
Young's modulus of resin[MPa]	Normal dist.	4207.80	404.7
Poisson's ratio of resin[-]	Normal dist.	0.38	0.013
Volume fraction of fibre[%]	Normal dist.	56.30	1.74

Variation factors	Shape	Mean	Shape parameter
Strength of resin[MPa]	Weibull dist.	55.7	16.6
Strength of material interface[MPa]	Weibull dist.	95.7	9.0

Table 1. Statistics of variation factors.

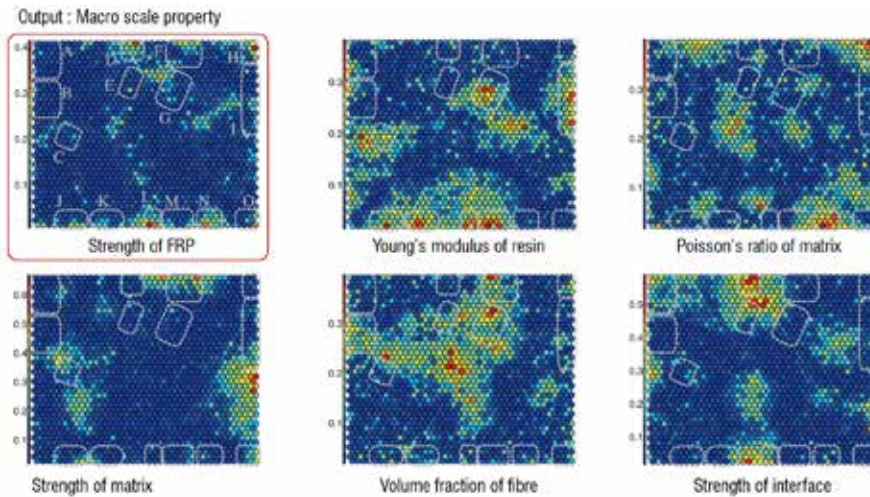


Fig. 2. Self-organizing maps of variation indices of Monte Carlo simulation results.

simulations were used to predict response to various macro rigidities and static strengths, which were then extracted from the data to identify key variables affecting static strength.

Fig. 1 and Table 1 provide an overview of the microstructural models and parameters with quantified material properties and variability, respectively. A surrogate model was created based on the results of the sample analysis conducted using partial factorial design with the L36 orthogonal array.

The sensitivity of the analytical results was studied by applying the variability shown in Table 1 to the surrogate model.

As shown in Fig. 2, we created a self-organizing map (SOM) to visualize the relationship between the large number of inputs and outputs in two dimensions. These results confirm that the Young's modulus and the Poisson's ratio of the resin, and the variations in fibre and resin strength correlate with changes in macro strength, and less so with fibre volumetric content and resin strength.

Identifying material properties for strength in microstructures

The SOM analysis showed that accurate input regarding interfacial strength is critical for predicting the static strength of composite materials. Although there are many models to describe interfacial delamination, in this study we used a type of bilinear approximation of the Cohesive Zone Model (CZM), as shown in Fig. 3. For each of the two modes in which delamination occurs, the contact stiffness increases as the distance between the contact surfaces and the amount of slip increases. There are four material constants: the threshold for the onset of delamination at the material interface and the amount of space in

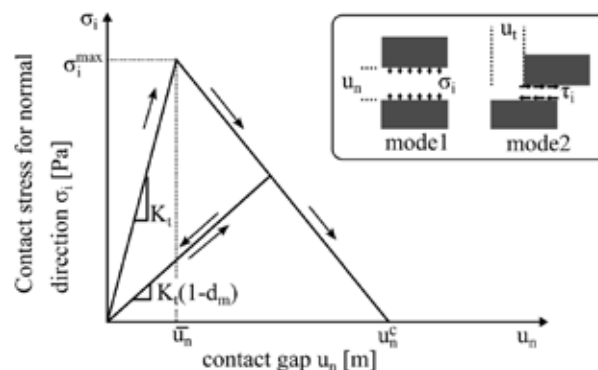


Fig. 3. Concept of the bi-linear approximation of the cohesive zone model.

which contact stiffness completely disappears for the two delamination modes.

As shown in Fig. 4, we propose a combination of experimental and analytical approaches to identify these material constants. The analysis consists of three phases. The first is a learning phase for the AI in which a large set of input parameters related to the unknowns of the microstructure, and the output parameters representing the response of the macroscopic materials are generated by virtual material tests. Here, the unknown quantities are the fibre volume content, the matrix strength, and the interface strength. In addition, tests on real materials are also performed under the same conditions as the virtual material tests. This undoubtedly reveals the true essence of the real FRP material. Therefore, in the second phase, the test results of the real materials are transmitted to the output of a well-trained AI and unknown input parameters are proposed to obtain the output. Finally, the virtual material tests are carried out again using the properties identified. This is compared with the results of the real material tests to validate the series of analytical approaches.

The material constants identified and the stress-strain curves obtained consequently are shown in Table 2 and Fig. 5. Young's modulus and the fracture strength properties of the FRP are also shown in Table 3. In order to measure the influence of the two modes of interfacial delamination, material tests were conducted off-axis with the fibre orientation tilted away from the loading direction. As the fibre orientation approaches an angle parallel to the loading axis, interfacial de-bonding due to the tangential component dominates (the only exception is at 0° where fracture due to fibre breakage dominates). The analysis reproduces the experimental results well for all test orientations.

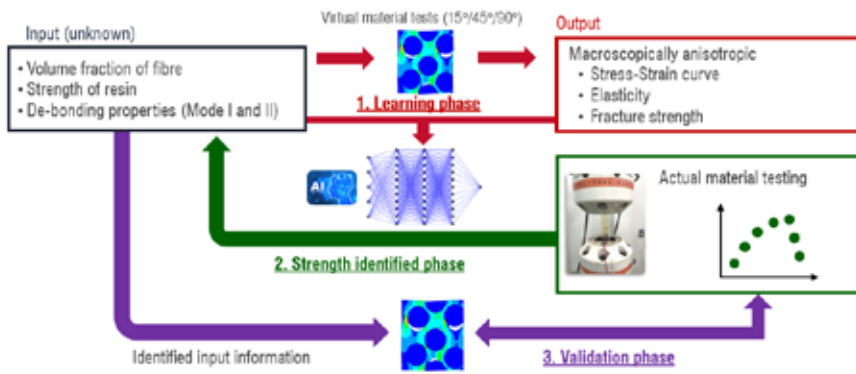


Fig. 4. Workflow to identify material constants by inverse analysis.

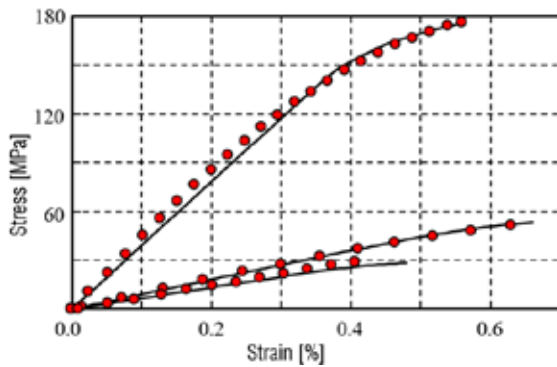


Fig. 5. Stress-strain curve obtained from virtual material testing using material constants identified.

Parameter	Output by inverse analysis
Strength of matrix	90.8 [MPa]
De-bonding threshold (Normal dir.)	63.4[MPa]
De-bonding threshold (Tangential dir.)	72.1[MPa]

Table 2. Material constants identified.

Conclusion

In this article, two analyses were performed to establish a highly accurate method for predicting the static strength of composite materials using virtual material testing, and the results are presented.

- Virtual material tests were conducted using various material parameters related to microstructure to quantify the factors affecting the strength of composite materials. SOM analyses show that the strength of composites containing unidirectional reinforcement is relatively strongly affected by the strength of the material interface and the

Young's modulus and Poisson's ratio of the resin.

- A large amount of material test data was used to train the AI to identify those factors through inverse analysis. The results agreed well with the measured values.

Virtual material testing is very useful for generating the large amount of material test data required for inverse identification analysis. Not only can the tests be done in a short time, but they are also easy to conduct under any conditions. The diversity of input conditions increases the generalizability of the AI. In the

	$\theta = 15^\circ$		$\theta = 45^\circ$		$\theta = 90^\circ$	
	E_c [GPa]	σ_c^t [MPa]	E_c [GPa]	σ_c^t [MPa]	E_c [GPa]	σ_c^t [MPa]
Actual tests	44.2	176.5	9.44	51.7	7.33	29.9
Virtual tests	39.2	174.8	9.10	53.2	6.67	28.3
Error [%]	11.3	0.963	3.60	2.90	0.00	5.35

Table 3. Comparison of experimental and analytical intensities. (θ : fibre orientation, E_c : Young's modulus as composites, σ_c^t : Strength as composites).

About CYBERNET SYSTEMS

CYBERNET SYSTEMS, an Ansys software reseller and solution provider for the past 35 years, provides various analysis solutions based on techniques that have been developed over time. CYBERNET has also been recognized as an Elite Channel Partner and a Solution Partner (Software) by Ansys.

For further information, visit: www.cybernet.co.jp/ansys/product/lineup/multiscale/en/ or email: cmas@cybernet.co.jp

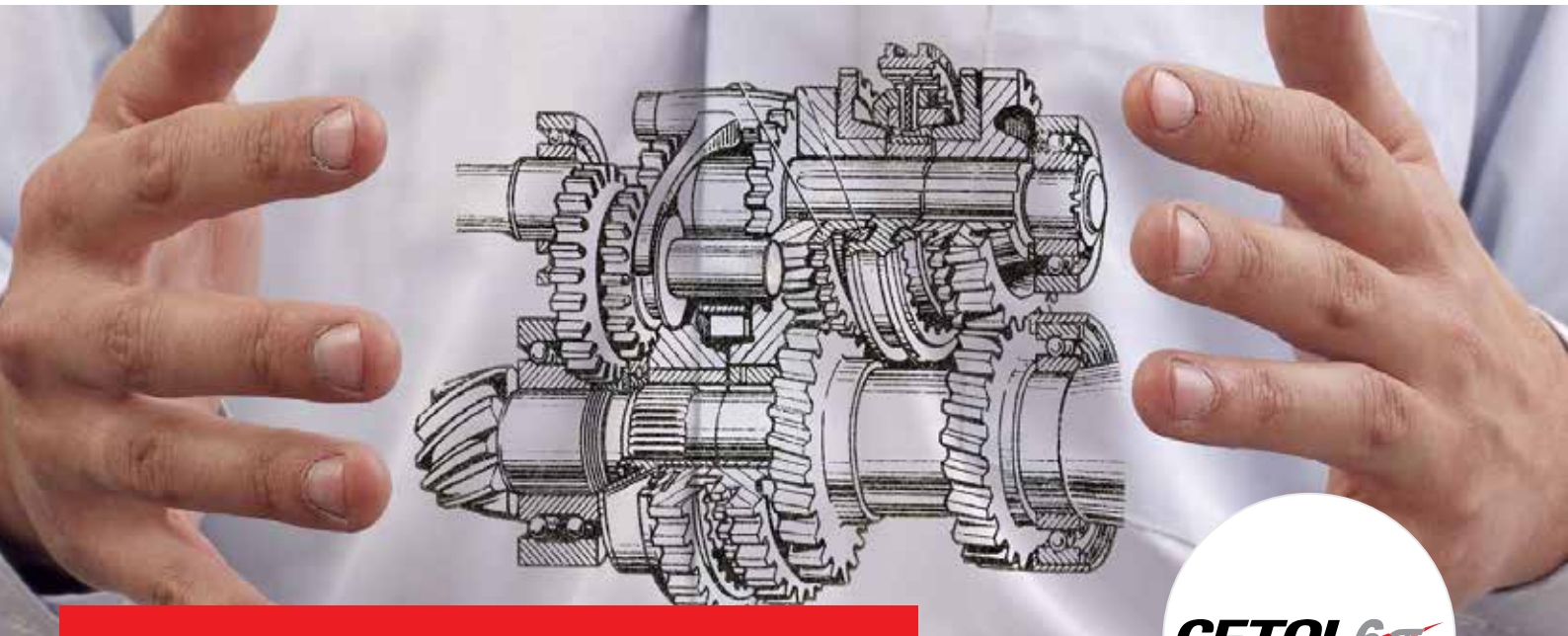
present analysis, the matrix was assumed to have elastic properties, but in principle, non-linearities such as elasto-plasticity and viscoelasticity can be accommodated. Moreover, since microstructure is not limited to FRP, it is possible to predict the material properties of various microstructures that are difficult to measure in practice.

For more information:

Francesco Lori - EnginSoft
f.lori@enginsoft.com

References

- www.cybernet.co.jp/ansys/product/lineup/multiscale/en/multiscale/
- Y. Ishibashi et al, "Suppression method of static strength variations of CFRP with data mining techniques", (Japanese), 23rd proceedings of Japan Society for Computational Engineering and Science, 2018
- R. Takami et al, "Evaluation of Interface Adhesion Strength of Unidirectional CFRP using Numerical Material Test and Neural Network", (Japanese), Japan Society for Composite Materials, Vol. 48, 2022



Understanding tolerance stacking: Using CETOL 6σ to improve production quality

by Kwangsu Kim
Tae Sung S&E

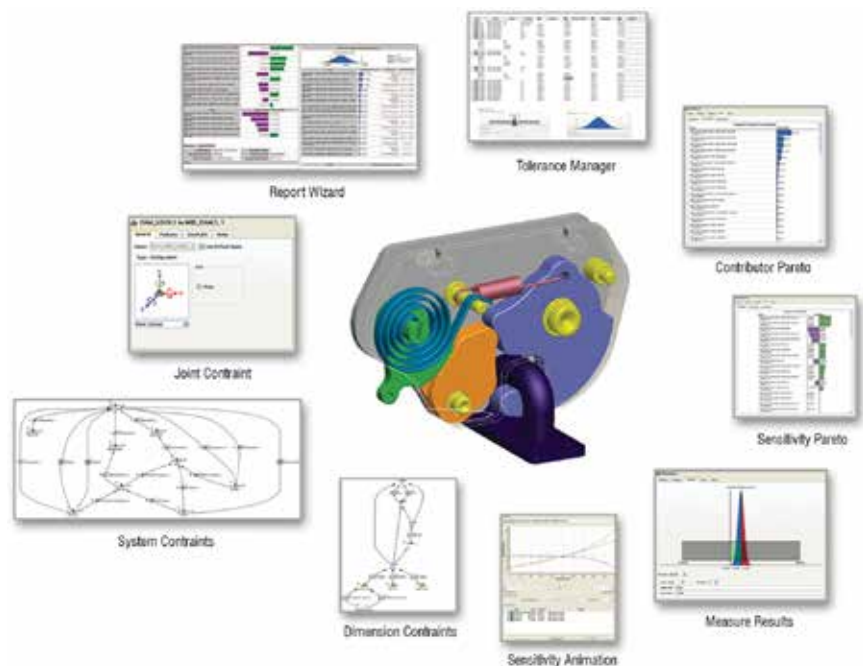
Creating high-quality products starts with the design process where tools such as CAE (computer-aided engineering), SQC (statistical quality control), and SPC (statistical process control) are used to improve the quality of production output. Once a product has been manufactured, its appearance and function are inspected and its measurements reviewed to ensure that they meet the standards of the drawings at which point a pass/fail decision is made.

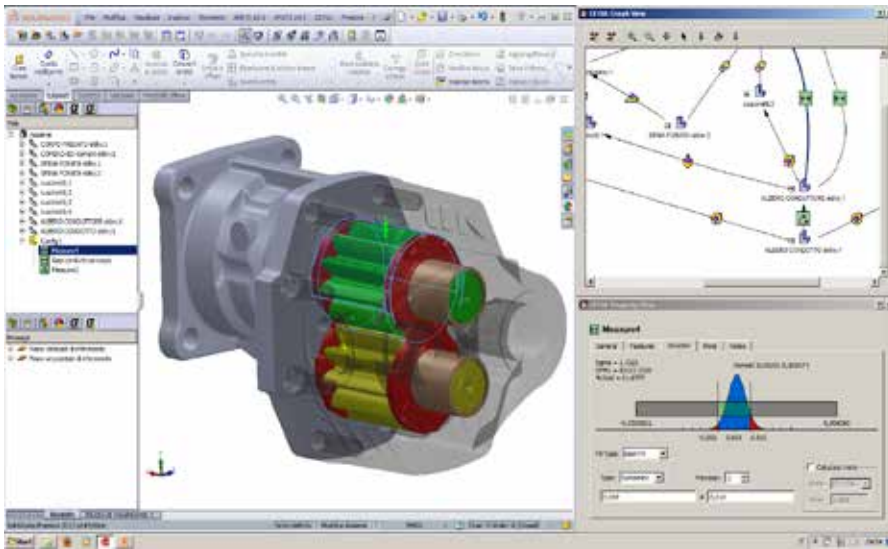
Typically, designers create drawings by considering the order and method of processing, the dimensions and tolerances, as well as the desired performance, assembly process, function, and purpose of the part. Based on the above information, they consider and apply the appropriate Dimension Chain and Tolerance ranges. Eventually, once the parts with variations are collected and assembled, the assembly can either be executed normally or not.

To review the correct assembly, a simple model can easily calculate the minimum/maximum intervals.

However, while the cumulative tolerance can easily be calculated, it is not always easy to apply directly to the model in the field. Many aspects have to be considered when applying the cumulative tolerance to a product, namely:

- Which tolerances have the greatest impact on assembly?
- How should the tolerance(s) be adjusted?
- How can the dimensions be adjusted?
- What is the range that can be processed?
- What happens if the design changes?
- Can 1D calculation results be applied to real 3D models?





Key characteristics (KC) and cumulative tolerance

In addition, it is essential to understand the relationship between the key characteristics when calculating the cumulative tolerance. Technical drawings contain a lot of production and assembly information which is not all necessary for calculating the cumulative tolerance.

The term KC [1], widely used in academic circles, refers to “the product, sub assembly, part, and process features that significantly impact the final cost, performance, or safety of a product when the key characteristics vary from nominal” [1].

The calculation of cumulative tolerance analyses for 1D and 2D models is relatively simple. However, most models in the field are 3D for which it is almost impossible to calculate the tolerance analysis manually, so it is necessary to use specialized software, such as CETOL 6σ.

Furthermore, it is not possible to assemble products that are 100% accurate because of deviations in the distribution of product quality during the manufacturing process.

By calculating the cumulative tolerance considering the actual production quality, one can set a suitable tolerance value for the real product rather than a simple theoretical value, with the ultimate goal being to improve quality and reduce costs.

3D cumulative tolerance analysis with CETOL 6σ

CETOL 6σ is feature-rich software that uses the elements of the 3D CAD drawings directly. A relationship model can be easily created simply by selecting elements from the CAD model with the mouse.

As previously explained, the product’s technical drawings contain a lot of information such as processing details, assembly information, inspection features,

etc., the KC relationship is constructed and calculated during the cumulative tolerance calculations.

When creating a 3D cumulative tolerance analysis model, the following aspects can be considered for review:

- Order of actual assembly
- Mechanical degrees of freedom
- Quality data

In general, it is advisable to proceed in order, although one can proceed flexibly by changing the order of the two tasks, depending on the model construction method and the engineer’s skill level.

- Objectives (measurements)
- Assembly modeling
- Part Modeling
- Model validation

CETOL 6σ includes the GD&T (geometric dimensioning and tolerancing) standard and if this is not met, the software displays warning messages concerning the errors and omissions in the drawing. This allows the drawing to be inspected and improved, which is essential because the technical drawings can provide valuable supporting material for legal disputes in the event of a problem.

Tolerance analysis is therefore essential in the product development process for improving quality and increasing trust in the company’s products.

Leveraging the results of CETOL 6σ

When the target quality (tolerance range) is applied to the point under review, CETOL 6σ calculates the WC (worst case) result and the dispersion result.

Furthermore, CETOL 6σ also displays the sensitivity and contribution results. The dimensions and tolerances can then be reviewed to improve the product quality.

Sensitivity is used to review the direction and magnitude of the resulting variance when this information is available. Contribution represents the influence (%) of each element when the prerequisite factor used in the

About TSNE

Since its establishment in 1988, TSNE has specialized in CAE, providing engineering programs and services to Korean customers. Tae Sung S&E (TSNE) aims to be the “One Stop Total CAE Solution Provider” (OSTS) both in domestic and global markets. The company leverages its large base of business capabilities and its team of CAE experts to provide services to customers in various industries (aerospace, automotive, civil engineering, biomedical, shipbuilding, electrical and electronics, energy, defence, chemical industries, etc.) and is expanding its business scope to research innovative technologies and apply them in the field. It strives to become a global engineering company and increase its potential as a sustainable engineering company.

Tae Sung S&E partners all engineers who endeavour to solve challenges. Tae Sung S&E will work with you to achieve “NO PROBLEM, BE HAPPY”.

construction of the tolerance analysis model is 100%. Efficiency can be increased by only including those elements that have a large influence without performing a full inspection of the product.

Using the CETOL 6 σ results as a guide, you can review the cost reductions that would result from mitigating those tolerances with a low impact on product quality, which cannot be easily performed in the field.

CETOL 6 σ is highlighted on all screens (tree, graph, properties, CAD windows) when a result factor is selected. This is useful from the user's point of view as the model

configuration status or enhancement work can be easily seen and used.

Conclusion

Quality issues frequently occur in the field as a result of assembly performance which often causes product functionality problems.

This can create cost and delivery issues, and simply reducing the tolerance size on items does not necessarily improve the product quality or reduce costs.

3D tolerance analysis can improve product quality by examining these issues at near-realistic values.

Tolerance analysis is essential for product development. If you have not yet performed 3D tolerance analysis on the products you develop and produce, it is worth trying.

References

1. Tolerance Analysis: Key Characteristics Identification by Sensitivity Methods", 15th CIRP Conference on Computer Aided Tolerancing, CIRP CAT 2018, pp. 33–38

For more information:

Kwangsung Kim - TAE SUNG S&E, Inc.

kskim@tsne.co.kr

What is new in CETOL 6 σ ver. 11.3.1

by Enrico Boesso
EnginSoft

Many different and fascinating features have been added in the latest versions of CETOL 6 σ , software that allows anyone to perform complex 3D tolerance analyses using statistical variables.

Some new features aim to improve the usability of the software and to make it more user friendly:

Auxiliary features

Users often need geometry for their CETOL 6 σ models (e.g. a plane) that does not exist in the CAD model. In previous releases, this required defining the necessary geometry in the CAD model, a procedure that could sometimes be frustrating.

It is now possible to define simple geometry/auxiliary features in CETOL 6 σ without having

to modify the CAD model. Auxiliary point, auxiliary line, auxiliary plane, auxiliary cylinder, and auxiliary width are all supported.

Auxiliary features can be used as references for measurements, joints, and dimensions just like standard features. In this way it is not necessary to exit the CETOL 6 σ environment if a new geometry is required to complete the tolerance analysis calculation model.

Managing ignored messages

Large models often have a long list of messages in the Advisor. After reviewing an information or warning message, you can choose to ignore it from the message context menu to place it in the 'ignored' message list. You can choose "Don't ignore" to return any ignored message to the normal message list

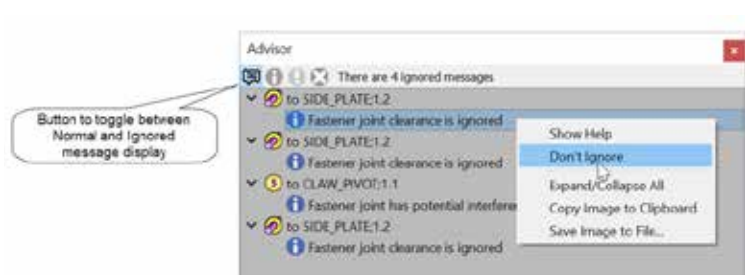
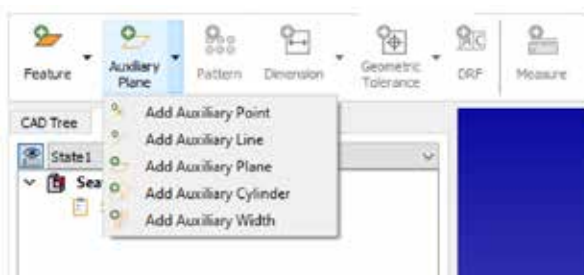
Reporting improvements

Some minor improvements have been made to the report style sheets. In addition, symbolic tolerance strings are written in the XML of the report. These strings can be included in reports and rendered with the GD&T font Y14.5-2018 (public domain).

Improved Analyzer user interface

The user interface of Analyzer has been modernized:

- A command ribbon has replaced the toolbar.
- Menus have been simplified and reorganized.
- The window layout is improved and more flexible.
- Properties views are consistent with the Modeler user interface.



Other new features speed up the modeling process and maximize the reliability of the output measurements:

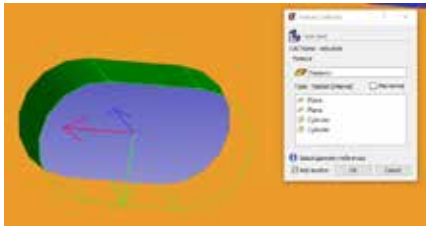
Import CATIA assembly constraints

CATIA assembly constraints can now be imported into the CETOL 6σ model. Options are available to automatically import assembly constraints when adding a component to the model. This option has been available (and much appreciated) for some time in other CAD platforms such as PTC/Creo and Dassault/SOLIDWORKS but is now also available to CATIA users. Users do not have to replicate the definition of mating conditions between parts, which saves considerable time during CETOL 6σ modeling.

Feature Collector improvements

The Feature Collector includes the following enhancements:

- Displays information about the parent part for the selected geometry.
- Continuous Add Feature mode.
- Message indicating what to select.



These enhancements allow users to quickly and easily define complex feature types recursively.

Cross-sectional views

It is possible to define and save cross-sectional views of the CAD model and reuse them later when required.

Floating Joint improvements

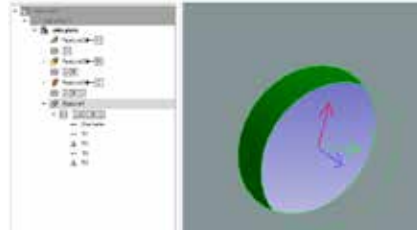
- A single constraint representing float and a better presentation of the float constraint properties showing the joint reference features and their tolerance properties.
- More accurate worst-case analysis for floating joints (i.e. circular, rather than square, worst-case area for flotation between a pin and a hole).

Separate contributions for float are shown for feature variation and joint clearance. Previously all contributions were attributed to the float variables.

There are also some new features to enable the software to behave more closely to GD&T rules:

Improvements to profile tolerance constraints

The implementation of profile tolerance when applied to features of size (FOS) is more closely aligned with the way profile tolerance is described in the ASME and ISO GPS tolerancing standards.



When applying a profile tolerance to Sphere, Cylinder, Cone, Torus, or Arc feature types, the size dimensions are constrained by the profile tolerance, if applicable.

In previous versions of CETOL 6σ, separate independent size dimensions were required for these features. When opening an older model in CETOL 6σ ver. 11.1.0 or later, a message is displayed showing all features affected by this change.

The “Variation Rule Editor” includes a “Tolerance Zone Allocation Controls” option that allows you to specify how the tolerance zone of the profile is allocated between the size variation and the position/orientation variation. Improvements have also been made to the way limits and distributions are calculated for variables constrained by profile tolerances, resulting in more accurate measurement analyses.

Common Parallel axis references

Common parallel axis references (e.g. B-C) referring to cylindrical or conical features are now supported.

Enhancements to Patterns

There have been a number of improvements related to patterns:

- Coaxial Cylinder Pattern – CETOL 6σ ver. 11.0.0 introduced support for parallel (but not coaxial) cylinder or cone patterns. You can now also add coaxial cylinder patterns.
- Topological constraints to pattern members – A topological constraint can

now be defined from an arc feature to a corresponding pattern member (e.g. a cylinder or cone feature).

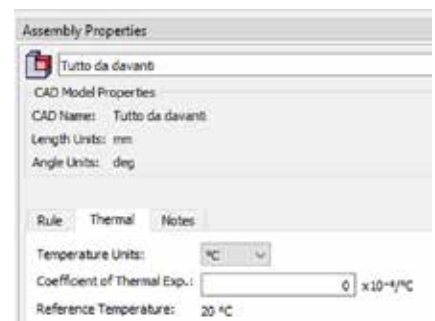
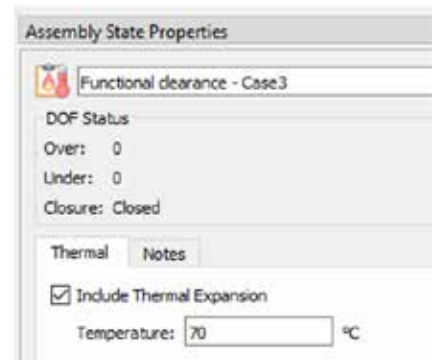
- Context menu for pattern operations – Many common pattern operations are now available in the context menu of the model tree.
- Pattern member as a datum feature – It is now possible to designate a pattern member as a reference characteristic.

Last but not least, the most important feature to take into account the effect of temperature variations on tolerances chains:

Thermal Expansion

You can now include the effects of thermal expansion in your model:

- Assembly state properties include a Thermal tab where you can indicate the temperature at which to evaluate the assembly.
- Part and Assembly properties include a Thermal tab where you can specify the coefficient of thermal expansion (CTE).



For more information:

Enrico Boesso - EnginSoft
e.boesso@enginsoft.com

**Ansys**

CERTIFIED ELITE CHANNEL PARTNER

Teaching AI “brains” using digital twins with Microsoft Project Bonsai

Engineers are increasingly using artificial intelligence (AI) to automate processes and make decisions faster and more effectively than humans can. But while engineers are experts in their area of specialization, most of them are not data scientists and they don't have the time to learn data science and write the complex code that AI modules require.

Microsoft Project Bonsai helps engineers create AI-powered automation without using data science by graphically connecting software modules that have already been programmed to perform certain AI functions. A complete set of connected functions that can perform a task is called a “brain.” A brain is a standalone, portable software module that can be used as part of an open loop to advise a human operator on the best decision to make, or it can replace the human, making decisions and carrying them out by itself when configured in closed-loop mode.

Microsoft is working with Ansys Twin Builder software to create digital twins of equipment or processes to be automated using AI. Digital twins can generate the large amounts of data needed to train AI brains much more quickly and less expensively than using physical machines for data generation.

Machine teaching v machine learning

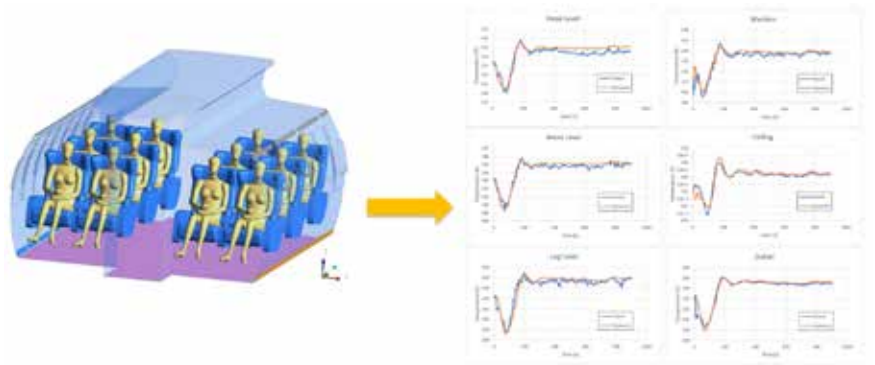
As automated processes become more complex, the method of training an AI brain is changing too. When the goal was simply image or text recognition, flooding the AI brain with tons of labelled data so it could pick out patterns worked fine. This is the basis of machine learning (ML).

But when AI is being relied upon to control a complex, multistep process on an industrial scale, ML is not as effective. The variety of inputs from numerous sensors of different types simply overwhelm the brain.

So Microsoft engineers developed the concept of machine teaching (MT), which relies more on the human approach to learning. Just as a maths teacher does not start teaching young students calculus before they have mastered the concepts of arithmetic, engineers cannot expect an AI brain to understand how an electric turbine works before it learns about rotation.

“Imagine you're starting with the hardest problem where the chances of finding a solution are almost nil,” says Cyrill Glockner, a principal program manager at Microsoft. “The AI brain will never find a way to do that. But it can slowly work its way up to it by following a combination of exploitation and exploration, taking advantage of what it has

already learned and looking across the data environment to ensure that it finds an optimal solution to the problem. In practice human experts first break the process down into smaller tasks. They then give the AI brain a few simple problems so it can begin learning how to use its algorithms to solve these easy challenges. Thereafter they combine small tasks the brain has already seen into larger ones until it can automatically control large, complex systems.

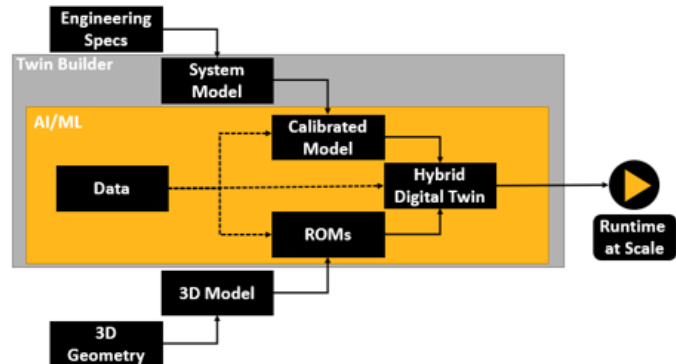


“We basically reduce the mathematical space that the AI brain has to look at by limiting it to certain parameters and ranges,” Glockner says. “Then we increase the range over time. The brain only has to deal with the new delta, and it already has some methods that it found in the earlier, smaller range that can be applied to the larger ones as well.”

The role of digital twins

As explained above, while it is important to start with small tasks and limited amounts of data when initially training a brain using MT, once the brain is well-trained large amounts of data are required to fully optimize its operations.

Typically, this involves generating huge amounts of data by running a physical process over and over. This data can then be fed into the brain to fine-tune its operation on the complete machine or process it was designed to automate. But generating so much data from physical processes is time-consuming and expensive. Also, if a condition occurs only once every trillion times — a “corner case” — and is not encountered during the training runs, the brain will not



have seen it before and will not know how to react if the situation occurs later.

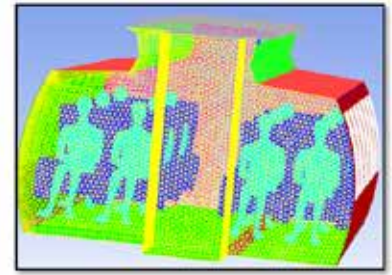
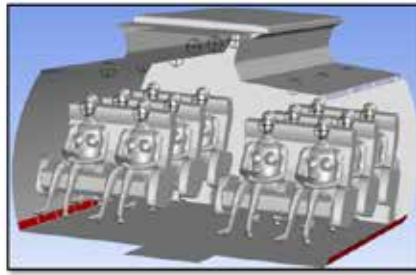
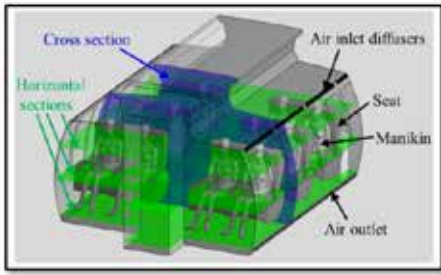
Working with Ansys Twin Builder, Microsoft Project Bonsai overcomes these limitations by running hundreds of virtual models of the machine or application simultaneously and feeding the data generated by these digital twins directly into the brain to optimize it. Using large numbers of virtual models instead of fewer physical ones reduces the time and cost of training a brain. It also enables engineers to introduce corner cases, which might be potentially dangerous or damaging to a physical machine, in the virtual environment so the brain has seen all possible scenarios before it is put into operation.

From digital twin to machine learning: how it works

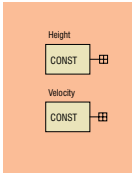
Engineers start by using Twin Builder to create a multiphysics system-level model by combining different modelling techniques such as OD/1D modelling and reduced-order modelling (ROM) from higher fidelity simulation results. These higher fidelity models provide the greatest simulation accuracy but also take a long time and lots of computational resources to run. A ROM is smaller and less computationally intensive than the original model, but runs much faster while sacrificing very little of the accuracy of the physics involved in the simulations. Twin Builder models the overall system using component libraries (pumps, valves, actuators, sensors, etc.) and ROMs for components requiring accurate predictions that typically cannot be achieved with OD/1D modelling (for example a complete field prediction of physical variables), which enables optimization and validation of component choices with the system response. The physics-based digital twin model can be further improved by incorporating knowledge from asset data, for example for model calibration or augmentation, which leads to a hybrid digital twin.

The final models can be exported and deployed in the form of a Twin Runtime

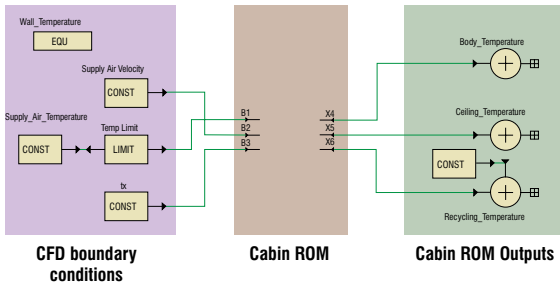
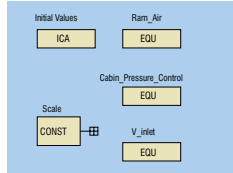




Mission Profile



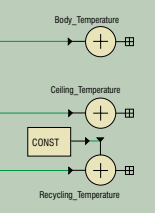
Outside air conditions



CFD boundary conditions

Cabin ROM

Cabin ROM Outputs



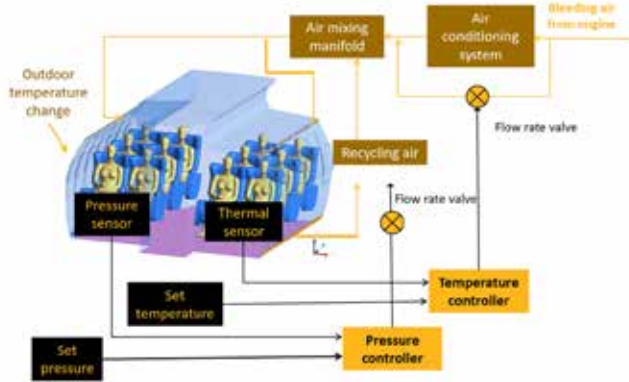
Example of an aircraft cabin pressure control system

A cabin pressure control system (CPCS) is one way to demonstrate digital twin technology and its integration with Bonsai. A CPCS is an avionics system designed to minimize the rate of change of cabin pressure. Its purpose is to ensure the safety of the airframe and passengers while maximizing comfort for aircrew and passengers during all phases of flight. It represents part of the overall energy consumption of the aircraft and therefore requires complex controls.

In Bonsai, engineers can build the AI brain by graphically selecting and connecting functional blocks of control code that take cabin temperatures and pressures at various points in the cabin as inputs and issue active commands (e.g. “turn down air conditioning”) as outputs.

In Twin Builder, the air conditioning subsystem can be modelled using 0D/1D components in Modelica, and a high-fidelity representation of the aircraft cabin can be modelled with a 3D computational fluid dynamics (CFD) model in Ansys Fluent. A ROM is created from this 3D model and connected to the system model in Twin Builder. This provides accurate virtual sensors distributed spatially in the cabin to monitor pressure and temperature.

Once the model is assembled and validated in Twin Builder, engineers can generate a portable, plug-and-play Twin Runtime application. Through the simple Python API it can be ported to a digital twin workflow and used to train a Bonsai brain to create a controller. In this case the digital twin will make predictions of the virtual sensors and, based on that, the AI controller will act on the air conditioning system to maintain the targeted pressure and temperature.



module. “We can directly integrate Twin Runtimes into Microsoft Bonsai,” says Christophe Petre, manager product specialist for digital twins at Ansys. “Twin Runtimes come with a very simple API that can be used in different programming languages like a Python application and that tells the users how to manipulate the digital twins by transmitting inputs, simulating the models, and retrieving the outputs seamlessly.”

Once the API is integrated with Bonsai, engineers can determine whether a virtual change to any operating condition improves the behaviour of the equipment or process that they want to control. They can also access new information, like virtual sensor data (something that you cannot measure physically but that you can predict with the model); explore “what if” scenarios; or run simulations to see how the asset is aging to predict when maintenance will be required.

For more information, visit:

www.ansys.com/blog/teaching-ai-brains-using-digital-twins-with-microsoft

SPACE - Scalable Parallel Astrophysical Codes for Exascale – launches in Turin



In January 2023 the European High Performance Computing Joint Undertaking (EuroHPC JU) launched ten Centres of Excellence (CoEs) to develop and scale up existing computing codes towards exascale performance over the next four years. The SPACE (Scalable Parallel Astrophysical Codes for Exascale) European Centre of Excellence, which officially started on 1 January 2023, held its kick-off meeting at the Università di Torino (University of Turin) on 13 and 14 March under the guidance of Prof. Andrea Mignone, the project coordinator.

In astrophysics and cosmology (A&C), HPC (high performance computing)-based numerical simulations are invaluable instruments to support scientific discovery. Given the complexities of the problems, they represent essential tools for modelling, interpreting, and understanding the physical processes behind the observed sky.

Advances in computational power promise a wealth of groundbreaking, new scientific discoveries by making ever greater numerical simulations feasible provided that equally advanced tools are created to exploit these computational resources.

Future exascale computing systems are expected to have extremely complex, heterogeneous architectures. The currently used numerical simulation codes are not

suitable for use on these systems since they were not purposely designed for them and therefore cannot effectively take advantage of the superior processing capabilities promised. SPACE's main goal, therefore, is to enable current astrophysical and cosmological codes to be used on the pre-exascale HPC architectures funded by the EuroHPC JU and made available at the end of 2022, as well as on future architectures by re-designing or adapting the existing computational tools for this next-generation hardware.

It will bring together scientists, community code developers, HPC experts, hardware manufacturers, and software developers in co-design activities to re-engineer eight of the most widely used European A&C HPC codes into new products that can efficiently exploit future computing architectures.

These eight A&C HPC codes represent 70% of the HPC A&C simulations and were selected after an extensive analysis of their features and capabilities. They will initially be prepared to adequately exploit the pre-exascale systems with a view to their transition to exascale systems and beyond. At the same time, SPACE will work to advance workflows and data processing based on machine learning and visualization applications and to enhance their exascale capabilities.

Furthermore, the SPACE Centre of Excellence (CoE) will promote the adoption of general and community standards for data products based on FAIR principles, and the interoperability of data and applications based on the technology standards and best practices of the International Virtual Observatory Alliance (IVOA).

SPACE will also implement the selected applications and foster their use by means of a specific outreach and training programme aimed at creating a broad and skilled talent pool in Europe to boost the use of high performance and high throughput solutions in academia in order to pave the way for the transition to exascale technologies and beyond.

You can meet SPACE delegates at the following upcoming events:

- **2023 Swiss Conference and HPCXXL User Group** – Lugano, Switzerland, 03–06 April 2023
- **RAMSES user meeting** – Oxford, UK, 19–21 April 2023.
- **ISC High Performance Computing** – Hamburg, Germany, 21–25 May 2023
- **Teratec Forum** – Paris, France, 31 May– 1 June 2023

For more information:

Marisa Zanotti - EnginSoft
m.zanotti@enginsoft.com



EuroHPC
Joint Undertaking

Centres of Excellence for HPC Applications – Horizon-EuroHPC-JU-2021-COE-01

Funded by the European Union. This work has received funding from the European High Performance Computing Joint Undertaking (JU) and Belgium, Czech Republic, France, Germany, Greece, Italy, Norway, and Spain under grant agreement No 101093441

www.space-coe.eu
info@space-coe.eu



CINECA

KU LEUVEN

IT4I



E4
COMPUTER
ENGINEERING

ENGINSOFT

Atos



**2023, June 7-8
Bergamo, Italy**



Particleworks experience

**The benefits, advantages
and how-tos
of going meshless**

**Register now!
It's free!**

particleworks-europe.com/experience